

NASA/SP-2013-605



# **An Analysis and a Historical Review of the Apollo Program Lunar Module Touchdown Dynamics**

*George A. Zupp, PhD  
Engineering Directorate, Retired  
Structural Engineering Division  
NASA Johnson Space Center, Houston, TX 77058*

---

January 2013

## NASA STI Program ... in Profile

Since its founding, NASA has been dedicated to the advancement of aeronautics and space science. The NASA scientific and technical information (STI) program plays a key part in helping NASA maintain this important role.

The NASA STI program operates under the auspices of the Agency Chief Information Officer. It collects, organizes, provides for archiving, and disseminates NASA's STI. The NASA STI program provides access to the NASA Aeronautics and Space Database and its public interface, the NASA Technical Report Server, thus providing one of the largest collections of aeronautical and space science STI in the world. Results are published in both non-NASA channels and by NASA in the NASA STI Report Series, which includes the following report types:

- **TECHNICAL PUBLICATION.** Reports of completed research or a major significant phase of research that present the results of NASA Programs and include extensive data or theoretical analysis. Includes compilations of significant scientific and technical data and information deemed to be of continuing reference value. NASA counterpart of peer-reviewed formal professional papers but has less stringent limitations on manuscript length and extent of graphic presentations.
- **TECHNICAL MEMORANDUM.** Scientific and technical findings that are preliminary or of specialized interest, e.g., quick release reports, working papers, and bibliographies that contain minimal annotation. Does not contain extensive analysis.
- **CONTRACTOR REPORT.** Scientific and technical findings by NASA-sponsored contractors and grantees.
- **CONFERENCE PUBLICATION.** Collected papers from scientific and technical conferences, symposia, seminars, or other meetings sponsored or co-sponsored by NASA.
- **SPECIAL PUBLICATION.** Scientific, technical, or historical information from NASA programs, projects, and missions, often concerned with subjects having substantial public interest.
- **TECHNICAL TRANSLATION.** English-language translations of foreign scientific and technical material pertinent to NASA's mission.

Specialized services also include organizing and publishing research results, distributing specialized research announcements and feeds, providing help desk and personal search support, and enabling data exchange services.

For more information about the NASA STI program, see the following:

- Access the NASA STI program home page at <http://www.sti.nasa.gov>
- E-mail your question via the Internet to [help@sti.nasa.gov](mailto:help@sti.nasa.gov)
- Fax your question to the NASA STI Help Desk at 443-757-5803
- Phone the NASA STI Help Desk at 443-757-5802
- Write to:  
NASA STI Help Desk  
NASA Center for AeroSpace Information  
7115 Standard Drive  
Hanover, MD 21076-1320

NASA/SP-2013-605



# **An Analysis and a Historical Review of the Apollo Program Lunar Module Touchdown Dynamics**

*George A. Zupp, PhD  
Engineering Directorate, Retired  
Structural Engineering Division  
NASA Johnson Space Center, Houston, TX 77058*

---

January 2013

Available from:

NASA Center for AeroSpace Information  
7115 Standard Drive  
Hanover, MD 21076-1320  
301-621-0390

National Technical Information Service  
5285 Port Royal Road  
Springfield, VA 22161  
703-605-6000

This report is also available in electronic form at <http://ston.jsc.nasa.gov/collections/TRS>

# Table of Contents

List of Figures .....	ii
List of Tables .....	v
Acknowledgments.....	vi
Summary .....	1
1.0 Introduction.....	1
2.0 Landing Dynamic Analysis.....	3
3.0 Drop Testing of Subscale and Full-scale Lunar Module Models .....	5
4.0 The Lunar Module .....	6
5.0 Critical Design Cases.....	10
6.0 Analysis of the Apollo 11 Lunar Module Landing Dynamics and Lunar Surface Mechanical Properties.....	11
7.0 The Apollo Lunar Module Landings .....	13
7.1 Apollo 11 Lunar Landing.....	13
7.1.1 <i>Summary: Apollo 11 Lunar Module Landing</i> .....	22
7.2 Apollo 12 Lunar Landing.....	23
7.2.1 <i>Summary: Apollo 12 Lunar Module Landing</i> .....	31
7.3 Apollo 13 Lunar Landing (Aborted) .....	31
7.4 Apollo 14 Lunar Landing.....	31
7.4.1 <i>Summary: Apollo 14 Lunar Module Landing</i> .....	43
7.5 Apollo 15 Lunar Landing.....	43
7.5.1 <i>Summary: Apollo 15 Lunar Module Landing</i> .....	52
7.6 Apollo 16 Lunar Landing.....	52
7.6.1 <i>Summary: Apollo 16 Lunar Module Landing</i> .....	58
7.7 Apollo 17 Lunar Landing.....	58
7.7.1 <i>Summary: Apollo 17 Lunar Module Landing</i> .....	63
8.0 Author's Annotation – Apollo 16 and 17 Landings .....	63
9.0 Conclusions.....	64
10.0 References.....	66
Appendix A: Apollo 11 Lunar Module Touchdown Dynamics .....	67
Appendix B: Lunar Soil Mechanical Properties Model.....	75
Appendix C: Apollo 11 Lunar Module Mass Properties at Touchdown .....	81
Appendix D: Apollo 11 Lunar Module Landing Gear Load Stroke Characteristics .....	82
Appendix E: Apollo 11 Lunar Module Descent Engine Thrust Tail-off Characteristics .....	84

## List of Figures

Figure 1. Inverted Tripod design.....	3
Figure 2. Cantilever design .....	4
Figure 3. Body coordinate system of Lunar Module with noted key dimensions for the Cantilever landing gear configuration. ....	7
Figure 4. Final Lunar Module configuration that landed on the moon, and the attachment location of the four Cantilever-type landing gears to the descent stage. ....	8
Figure 5. Lunar Module landing touchdown velocity envelope and landing gear energy absorption performance. ....	10
Figure 6. Apollo 11 Lunar Module pitch rate as a function of time. ....	14
Figure 7. Apollo 11 Lunar Module roll rate as a function of time. ....	14
Figure 8. Apollo 11 Lunar Module yaw rate as a function of time. ....	15
Figure 9. Composite of Apollo 11 Lunar Module rotational rates during the touchdown maneuver.....	16
Figure 10. ( <i>NASA Photograph AS11-40-5915</i> ) Overall view of Apollo 11 Lunar Module resting on lunar surface. ....	17
Figure 11. ( <i>NASA Photograph AS11-40-5864</i> ) Closeup view of Apollo 11 Lunar Module descent engine nozzle bell and the +Z landing gear. ....	18
Figure 12. ( <i>NASA Photograph AS11-40-5858</i> ) Apollo 11 Lunar Module +Y landing gear and footpad, looking from the area of the +Z footpad location toward the +Y footpad. ....	19
Figure 13. ( <i>NASA Photograph AS11-40-5925</i> ) Closeup view of Apollo 11 Lunar Module -Z footpad and the +Y footpad, located in the top center of the photograph, and looking down a line connecting the -Z footpad and the +Y footpad. ....	20
Figure 14. ( <i>NASA Photograph AS11-40-5865</i> ) Apollo 11 Lunar Module -Y landing gear and footpad, located in approximately the upper center of the photograph. ....	21
Figure 15. ( <i>NASA Photograph AS11-40-5850</i> ) Apollo 11 Lunar Module -Y landing gear and footpad, looking at the -Y footpad from the area of the +Z landing gear. ....	22
Figure 16. Apollo 12 Lunar Module pitch rate as a function of time. ....	24
Figure 17. Apollo 12 Lunar Module roll rate as a function of time. ....	24
Figure 18. Apollo 12 Lunar Module yaw rate as a function of time. ....	25
Figure 19. ( <i>NASA Photograph AS12-46-6749</i> ) Overall view of Apollo 12 Lunar Module resting on the lunar surface. ....	26
Figure 20. ( <i>NASA Photograph AS12-46-6905</i> ) The +Y landing gear and footpad.....	27
Figure 21. ( <i>NASA Photograph AS12-46-6904</i> ) Apollo 12 +Y landing gear and footpad. Also shown: an imprint of the astronaut's space suit boot.....	28
Figure 22. ( <i>NASA Photograph AS12-46-6900</i> ) Apollo 12 -Y landing gear and footpad. ....	29

Figure 23. (NASA Photograph AS12-46-6901) Close-in view of Apollo 12 -Y footpad..	30
Figure 24. Apollo 14 Lunar Module pitch rate as a function of time.	32
Figure 25. Apollo 14 Lunar Module roll rate as a function of time.	33
Figure 26. Apollo 14 Lunar Module yaw rate as a function of time.	33
Figure 27. (NASA Photograph AS14-66-09278) View of -Z landing gear and footpad, located to right side of Lunar Module.	34
Figure 28. (NASA Photograph AS14-66-09254) View of -Z landing gear, located in left side of photograph; and the +Y landing gear, located in lower-right side.	35
Figure 29. (NASA Photograph AS14-66-09255) View of +Y landing gear, located in lower center of photograph; and the +Z landing gear, located in Lunar Module shadow to the right.	36
Figure 30. (NASA Photograph AS14-66-09234) View of +Y footpad showing footpad penetration and some soil buildup in the direction of motion.	37
Figure 31. (NASA Photograph AS14-66-09235) View of +Y footpad showing contact probe and trailing edge the footpad.	38
Figure 32. (NASA Photograph AS14-66-09269) View of -Y footpad showing initial contact footpad pattern and subsequent footpad translation.	39
Figure 33. (NASA Photograph AS14-66-09270) View of -Y footpad showing lunar soil buildup on footpad in the direction of the footpad translational motion.	40
Figure 34. (NASA Photograph AS14-66-09264) View of -Z footpad showing footpad penetration and some soil buildup in the direction of initial footpad motion.	41
Figure 35. (NASA Photograph AS14-66-09265) View of -Z footpad showing the contact probe.	42
Figure 36. Apollo 15 Lunar Module descent engine buckled nozzle.	44
Figure 37. Apollo 15 Lunar Module pitch rate as a function of time.	45
Figure 38. Apollo 15 Lunar Module roll rate as a function of time.	45
Figure 39. Apollo 15 Lunar Module yaw rate as a function of time.	46
Figure 40. Apollo 15 Lunar Module composite body rates as a function of time.	46
Figure 41. (NASA Photograph AS15-86-11600) The +Y, +Z quadrant of Apollo 15 Lunar Module resting on lunar surface.	47
Figure 42. (NASA Photograph AS15-87-11818) The +Y, -Z quadrant of Lunar Module resting on lunar surface.	48
Figure 43. (NASA Photograph AS15-87-11839) The -Y, -Z quadrant of Lunar Module resting on lunar surface.	49
Figure 44. (NASA Photograph AS15-82-11601) Lunar Module and Lunar Rover Vehicle resting on lunar surface.	50
Figure 45. (NASA Photograph AS15-82-11534) Apollo 15 astronaut boot print.	51

Figure 46. (NASA Photograph AS16-107-17437) Apollo 16 Lunar Module and Lunar Rover Vehicle resting on lunar surface. ....	53
Figure 47. (NASA Photograph AS16-107-17435) View of Apollo 16 Lunar Module showing the descent engine nozzle clearance between nozzle exit plane and lunar surface. ....	54
Figure 48. (NASA Photograph AS16-107-17441) The -Y footpad and landing gear strut. ....	55
Figure 49. (NASA Photograph AS16-107-17442) The -Y landing gear struts and footpad. ....	56
Figure 50. (NASA Photograph AS16-107-17451) View of lunar rock and an astronaut boot print in the lunar soil. ....	57
Figure 51. (NASA Photograph AS17-134-20511) Lunar Module resting on lunar surface. ....	59
Figure 52. (NASA Photograph AS17-134-20382) Lunar Module resting on lunar surface. ....	60
Figure 53. (NASA Photograph AS17-134-20388) The -Z landing gear struts and footpad. ....	61
Figure 54. (NASA Photograph AS17-134-20432) Astronaut's boot print in lunar soil. ....	62
Figure 55. Apollo Lunar Module landing velocities with respect to the touchdown velocity envelope (or Doghouse). ....	65
<hr/>	
Figure 1A. Comparison between the measured and predicted pitch rate during Apollo 11 Lunar Module touchdown maneuver. ....	69
Figure 2A. Comparison between the measured and predicted roll rate during Apollo 11 Lunar Module touchdown maneuver. ....	70
Figure 3A. Comparison between the measured and predicted yaw rate during Apollo 11 Lunar Module touchdown maneuver. ....	71
<hr/>	
Figure 1B. (NASA Photograph AS11-40-5920) The +Y footpad looking down the +Y Lunar Module body axis. ....	75
Figure 2B. (NASA Photograph AS11-40-5917) The +Y footpad showing approximately 2/3 of the contact probe embedded into the lunar soil and situated about parallel to the surface. ....	76
Figure 3B. (NASA Photograph AS11-40-5926) The -Z landing gear footpad. ....	77
Figure 4B. (NASA Photograph AS11-40-5878) Astronaut's boot print, indicating sufficient bearing strength to support human mobility on lunar surface. ....	78
<hr/>	
Figure 1D. Primary strut load-stroke curve. ....	82
Figure 2D. Secondary strut load-stroke in compression. ....	83
Figure 3D. Secondary strut tension load-stroke curve. ....	83
<hr/>	
Figure 1E. Descent engine thrust time history starting with initial Lunar Module landing gear footpad contact and terminating 0.225 seconds later. ....	84

## List of Tables

Table 1. Summary of Apollo Lunar Module Landing Conditions .....	65
<hr/>	
Table 1A. Lunar Module Landing Orientation, Pitch, Roll, and Yaw .....	68
Table 2A. Lunar Module Touchdown Rotational Rates .....	68
Table 3A. Apollo 11 Lunar Module Touchdown Velocities Expressed in the Inertial Coordinate System. ....	68
Table 4A. Comparison Between the Measured and Predicted Maximum Lunar Module Landing Gear Strut Strokes for Apollo 11 Landing. ....	72
Table 5A. Lunar Soil Mechanical Properties and Dispersions at Apollo 11 Lunar Module Landing Site as Determined by the Iterative Process from the Lunar Module Landing Simulations. ....	73
<hr/>	
Table 1C. Lunar Module Mass Properties at the Time of Footpad Contact with Lunar Surface. ....	81

## **Acknowledgments**

The author wishes to express his indebtedness to Dr. John A. Schliesing and Dr. Harold H. Doiron of the Johnson Space Center/Engineering Directorate for their many hours of consultation we spent in discussing technical issues associated with this paper, and to Sylvia Turner Zupp, my wife, for her patience and encouragement over the years.

Also to Mr. William H. Taylor, Johnson Space Center Film Repository, for his effort in locating the Apollo photographs presented in this paper, and Ms. Christa George, Scientific and Technical Information Center, for her effort in locating the Apollo post-flight mission reports.

The author also wishes to express his appreciation for the efforts of Ms. Susan Breeden, editor, for her constructive suggestions and recommendations.

# Summary

The primary objective of this paper is to present an analysis and a historical review of the Apollo Lunar Module landing dynamics from the standpoint of touchdown dynamic stability, landing system energy absorption performance, and evaluation of the first-order terms of lunar soil mechanical properties at the Apollo 11 landing site. The first-order terms of lunar surface mechanical properties consisted primarily of the surface bearing strength and sliding friction coefficient. The landing dynamic sequence started at first footpad contact. The flight dynamics data used to assess the Apollo 11 landing system performance and the lunar soil mechanical properties included the body axis pitch, roll, and yaw rate time histories as measured by the on-board guidance computer during the Apollo 11 Lunar Module touchdown maneuver, and the landing gear stroke data derived from post-landing photographs. The conclusions drawn from these studies were that the landing gear system performance was more than adequate from a stability and energy absorption standpoint for all Apollo lunar landings, and the lunar soil parameters were well within the limits of the design assumptions for all Apollo landing sites.

---

## 1.0 Introduction

A major milestone in the human exploration of space occurred on October 4, 1957, when the USSR launched the 183.9-pound Sputnik (English translation: “Satellite”)— the first man-made satellite to be put into Earth orbit. On October 1, 1958, the National Advisory Committee for Aeronautics was reorganized to form the foundation for the National Aeronautics and Space Administration (NASA). In the early 1960s, NASA was commissioned to develop the US space program with the ultimate goal of putting astronauts on the moon and safely returning them to Earth, within the decade.

One of the more important questions in the early 1960s, during the period leading up to the first lunar landing, was: What lunar transportation architecture is “optimum” for getting astronauts to the moon and safely back? Two primary candidates for the lunar transportation architecture emerged: the Earth Orbit Rendezvous, which would make a direct descent to the lunar surface and return to Earth; and the Lunar Orbit Rendezvous, which would allow a Lunar Excursion Module\* to descend to the lunar surface while the return vehicle remained parked in lunar orbit. NASA ultimately selected the Lunar Orbit Rendezvous transportation architecture to accomplish the lunar mission. The Saturn rocket (C-5) would be the primary transportation vehicle.

The Apollo Saturn rocket was made up of four primary stages: the S-I first stage; the S-II second stage; the S-IV third stage; and the fourth stage, which was composed of the Lunar Module, Service Module, and Command Module. The Command Module and Service Module remained mated throughout the mission, except during the final approach to Earth. Typically, the Command Module and Service Module were jointly referred to as the Command and Service Module.

Once in lunar orbit, the Lunar Module—a two-stage spacecraft consisting of a descent stage and an ascent stage—undocked from the Command and Service Module and descended to the lunar surface. After

---

\* The Lunar Module was originally called the Lunar Excursion Module — or LEM. Later, within the 1964 timeframe, NASA decided that "Excursion" was not an appropriate description, and the word was subsequently dropped from the name.

mission completion, the ascent stage returned to lunar orbit, leaving the descent stage on the lunar surface. The ascent stage then docked with the Command and Service Module. Subsequently, the Command and Service Module performed a propulsive maneuver to get out of lunar orbit. The Command and Service Module were separated just prior to Earth entry.

The basic requirement for the Lunar Module was to accommodate a crew of two astronauts and all of the support equipment required for a several-day mission on the lunar surface. The development schedule of the landing gear system demanded the system be designed in the face of multiple uncertainties, including the lunar surface mechanical properties; landing site surface slope, rock size, or boulders; touchdown velocities and angular rates; and the possible visibility degradation due to dust caused by the descent engine plume interaction with the lunar surface.

Other NASA programs—i.e., Ranger Program, Lunar Orbiter Program, and Surveyor Program—operated in parallel with the Apollo Program, and further enhanced NASA's understanding of the lunar surface topography through the use of high-resolution photographs. The primary objective of these programs was to reduce topographic uncertainties. The Surveyor Program included the additional objective of reducing the uncertainty of the lunar soil mechanical properties.

**Ranger Program** was a direct shot at the moon, taking photographs up to the time of impact with the lunar surface. Ranger 7 was the first successful Ranger flight, and was launched in the summer of 1964. The closest photographs taken of the lunar surface were about 1000 feet with a resolution of 3 feet. Photographs of the Mare area indicated the surface was fairly flat and free of hazardous boulders.

**Lunar Orbiter Program** consisted of five lunar orbiters—launched from 1966 to 1967—tasked with the mission of photographing the lunar surface at possible Apollo landing sites. The resolution of the photographs was about 200 feet; some low-altitude photographs had a resolution as high as 5 to 10 feet. The lunar orbits were as low as 28 miles from the lunar surface. Photographic analysis of the lunar surface indicated the existence of many acceptable Apollo landing sites.

**Surveyor Program** was the first US soft lander with close-up photography capability. This program consisted of seven launches starting in May 20, 1966, and running through January 10, 1968. Surveyor II experienced a vernier engine failure; Surveyor IV lost radio contact. Both failures resulted in loss of mission. Surveyors III and VII each carried an on-board soil sampler that allowed for an assessment of the lunar surface bearing strength at these landing sites. Also, the Surveyor data indicated the landing sites were **not** covered by a thick layer of lunar dust.

By 1968, lunar surface properties were well enough defined to ensure that the surface had sufficient bearing strength to support the Lunar Module and astronaut activities. The preliminary landing gear design assumed that the lunar surface bearing capability would be at least 1.0 pounds per square inch (psi) at a penetration depth of no more than 4 inches. It was further assumed that the descent engine plume impinging on the surface might produce a lunar dust cloud that would degrade the astronaut's ability to judge the height of the Lunar Module above the lunar surface during the landing maneuver. To mitigate this concern, NASA engineered a landing gear probe that would detect lunar surface contact during the landing maneuver. Once contact with the lunar surface was made, the landing procedure was to terminate the descent engine thrust and allow the Lunar Module to free fall to the lunar surface.

All of this research and activity by NASA engineers and scientists culminated in another major milestone in space exploration when, on July 20, 1969, the Apollo Lunar Module landed on the moon's surface with astronauts Neil Armstrong and Edwin Aldrin on board. Armstrong descended onto the lunar surface and became the first person to walk on the moon. Aldrin followed shortly thereafter. NASA accomplished a total of six Apollo Lunar Module landings, starting with Apollo 11 in July 1969 and ending with Apollo 17 in December 1972. The Apollo 13 mission was aborted because of an explosion that occurred in the Service Module after the flight had traveled about halfway to the moon. Apollo 13 continued on its lunar journey—passing by the moon without landing—and then safely returned to Earth.

## 2.0 Landing Dynamic Analysis

Accurate prediction of the landing dynamic stability of the spacecraft and associated energy dissipation function of the landing gear system was an issue that NASA had to address during the development phase of the Lunar Module. Early studies considered several landing gear configurations. The primary candidates were the Grumman Corporation (Bethpage, New York) “Inverted Tripod” (Figure 1) and the “Cantilever” (Figure 2) configurations. Each of these configurations was made up of several landing gear legs. Each leg was made up of a primary strut and two secondary struts. Each strut could deform axially under a given load and absorb the touchdown kinetic and potential energies. (A detailed history of the Lunar Module landing gear evolution can be found in Reference 10.) The primary difference between these two configurations was the lower attachment location of the secondary struts. The Tripod configuration attached the secondary struts at the base of the primary strut/footpad location. The Cantilever configuration attached the secondary struts approximately 32 inches above the footpad to the primary strut.

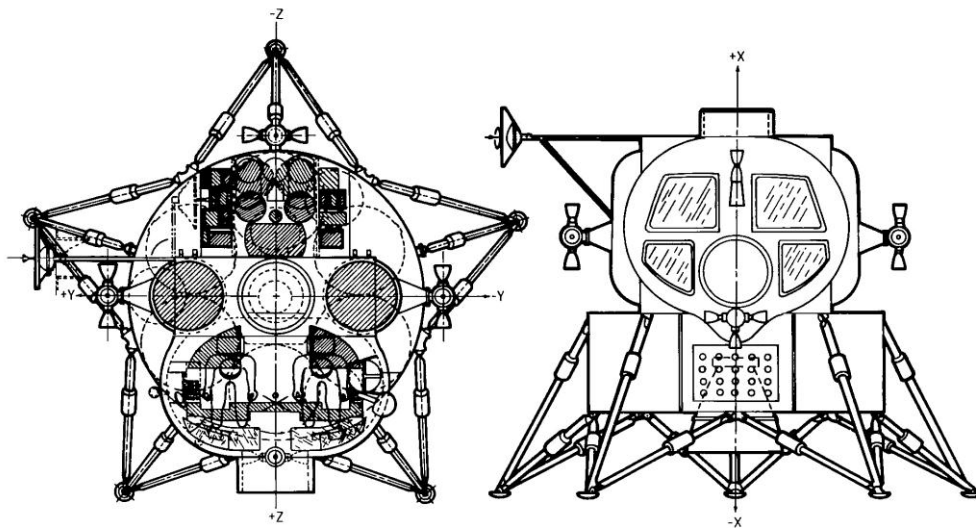


**Figure 1. Inverted Tripod design.** The secondary struts are attached at the landing gear footpads. Of the two configurations, the Cantilever design was chosen because of the better ground clearance.

Several activities taking place around the country further enhanced the program's ability to accurately predict the landing dynamics of a soft landing system. The field of lunar touchdown dynamics included these pioneers: M. Mantus and W. Elkins of the Grumman Corporation; Harold Doiron of the NASA/Manned Spacecraft Center, Houston, Texas; W. C. Walton, B. J. Durling, R. W. Herr, H.W.

Leonard, and U. J. Blanchard of the NASA/Langley Research Center, Hampton, Virginia; and Ray Black of the Bendix Corporation, South Bend, Indiana.

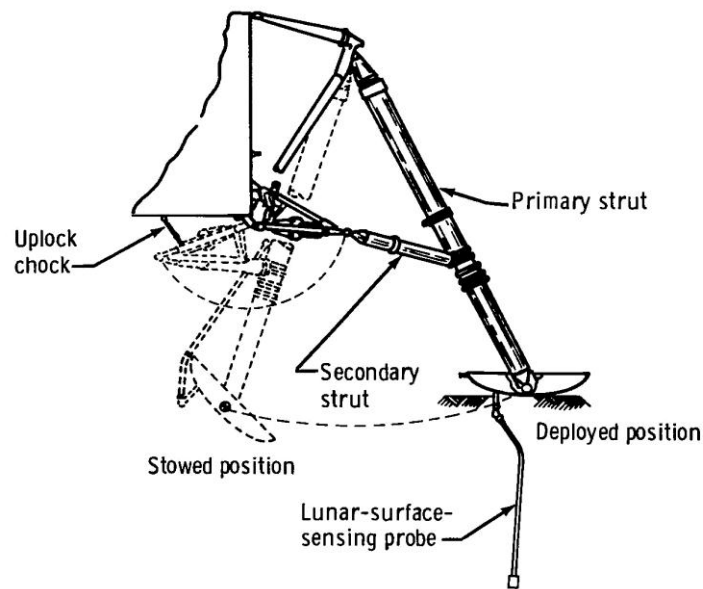


**Figure 2. Cantilever design.** The secondary struts are attached to the primary strut approximately 32 inches above the landing gear footpad.

During the 1963-64 time frame, Langley Research Center developed a computer code for predicting time domain solutions to the touchdown dynamics problem. Their analytical model contained six rigid body degrees of freedom with non-articulating and non-deforming landing gears. The Langley touchdown dynamics code was test verified. The touchdown analysis and test data indicated the minimum landing stability was not always associated with the "minimum overturning radius."<sup>†</sup>

In parallel, Grumman developed a six rigid body degrees of freedom Lunar Module landing simulation with articulation and deformable landing gears with three rigid body degrees of freedom for each landing gear footpad. The Grumman landing dynamics code reflected the company's aircraft experience in landing gear systems analysis. The landing dynamic analytical code developed at the Manned Spacecraft Center was similar to that of the Grumman code.

In the early stages and throughout the program, it was generally assumed that landings on a rigid surface with constrained footpads represented the most severe case for landing gear energy absorption and landing dynamic stability. These assumptions precipitated the following question: "How does landing on a non-rigid surface affect landing gear performance?"

During the 1966 time frame, Bendix Corporation researched the effect of landing on soil surfaces. Extensive work was being done in developing analytical models to reflect the soil dynamic interaction

---

<sup>†</sup> The definition of the "minimum overturning radius" is analogous to the inverted pendulum (i.e., a pendulum that has its center of mass above its pivot point). In the case of the Lunar Module, the minimum overturning radius is a line perpendicular to a line connecting two adjacent footpads and the center of mass.

with Lunar Module landing gear footpads. These soil models were incorporated into the landing dynamics code developed by the Manned Spacecraft Center.

These analyses are presented, in detail, in References 1 through 9.

### 3.0 Drop Testing of Subscale and Full-scale Lunar Module Models

During the 1960s, extensive “drop testing” was conducted using subscale and full-scale models of the Apollo Lunar Module landing gear system. These scaled models replicated the mass and inertia, center of gravity, landing gear articulation, and energy absorption function of the full-scaled landing gear system. A primary objective of this type of testing was to develop experimental data to verify the various analytical models used in predicting the touchdown dynamics and energy absorption capability. Another objective was to demonstrate the successful articulation of the landing gear system. These data were used in the final verification process of both the Grumman and the Manned Spacecraft Center landing dynamic codes for predicting landing gear performance.

Landing dynamic experts reached a consensus, at the time, that the most severe design condition for landing stability and landing gear energy absorption was the landing case where the surface was “rigid” and the landing gear footpads were laterally constrained on surface contact. The one exception was landing gear secondary strut tension stroking with unconstrained footpad motion in the planar direction where the sliding friction coefficient between the footpad and the rigid surface was 0.4. At the time, it was assumed that the lowest value for the effective friction coefficient between the Lunar Module footpad and the lunar surface would be no less than 0.4.

Langley Research Center was one of the first to develop drop test data using a rigid block in which the landing gears were represented by four spikes that would penetrate the surface and constrain the motion of each contact point in the plane of the landing surface. The vertical motion at each contact location was unconstrained. Analysis and test data indicated that planar landings were not the most critical for overturning stability. Engineers at Langley later investigated the landing dynamics of a 1/6 scaled model of the Apollo Lunar Module in which the landing gear configuration was the Inverted Tripod design. This model drop test program and the supporting analytical simulations verified the earlier Langley results of the rigid model drop test program, which again verified that the minimum overturning stability was **not** the path of minimum overturning radius.

Later in the 1967 time frame, Langley performed full-scale drop testing using the Cantilever gear configuration. These tests used a “tilt” table configuration to produce a 1/6g environment for the landing dynamic simulations. The touchdown dynamics of the test article were restricted to planer motion. (Landings that result in planar motion are those in which the trailing pair of landing gear footpads contact the surface simultaneously, followed by the leading pair of footpads making surface contact simultaneously, or a 2-2 landing. Similarly, a 1-2-1-type of landing can result in planar motion.) These full-scale drop tests provided additional data to support the verification of the Manned Spacecraft Center landing dynamics code.

Similarly, in the mid 1960s, Grumman conducted drop tests using a 1/6 scale model of the Cantilever gear configuration in which the dimensions, mass, center of gravity, and inertias were scaled. These drop tests occurred on a rigid surface with a constrained landing gear footpad motion in the plane of the landing

surface, and with unconstrained vertical motion of each footpad off of the landing surface. The emphasis of these drop tests were on model drops that resulted in planar motion.

Grumman also conducted drop tests using a single full-scaled model of the Cantilever configuration. A primary objective of these drop tests was to demonstrate that the articulation of the Cantilever design was successful and that the energy absorption function of the gear could be accurately predicted for both the footpad constraint cases and the footpad sliding cases.

After completion of the Grumman drop testing and the analysis and acceptance of the critical drop test data, the Grumman 1/6 scale model was shipped to the Manned Spacecraft Center where the drop tests continued with an emphasis on non-planar landings. These tests were conducted in the 1966 time frame.<sup>9</sup>

From the early 1960s to 1968, Bendix Corporation conducted scale model drop tests on rigid surfaces, employing several types of landing gear configurations that included both the Grumman Cantilever and the Inverted Tripod designs. In the 1967 time frame, Bendix Corporation performed extensive drop testing on simulated lunar soils. These data provided the basis for developing the footpad/lunar soil interaction analytical model that was eventually incorporated into the Manned Spacecraft Center landing dynamics code. This model was the basis for the simplified soil model used in the analytical prediction of the Apollo 11 Lunar Module landing dynamics.

## **4.0 The Lunar Module**

The Lunar Module critical landing dynamic parameters that governed the landing stability and touchdown energy absorption were the landing gear geometry, landing gear overturning radius, energy absorption characteristics, descent engine thrust decay profile, and mass properties. In addition, the lunar surface slope at the landing site and the lunar soil mechanical properties were critical parameters in the assessment of landing stability and energy absorption performance. However, it was assumed that landing on a rigid surface with constrained footpads was generally the most severe landing design case for the landing gear system.

The basic requirement for the landing gear system was the ability to land on the lunar surface with up to an equivalent slope of 12 degrees, remain in a stable upright attitude post landing, and absorb the touchdown kinetic and potential energies without exceeding the design structural limits of the primary structure. The landing velocity specification was guided in part by Federal Air Regulation-25 and Military Specification 8862. The initial touchdown velocity specification for the Lunar Module was to land on a slope of up to 12 degrees with a sink velocity of up to 10 feet per second and a horizontal velocity of up to  $\pm 5$  feet per second in any direction with respect to the landing slope.

The touchdown velocity envelope was later modified to accommodate a maximum sink speed of 10.0 feet per second with a 0.0 foot per second horizontal velocity. As the sink speed was decreased to 7.0 feet per second, the horizontal velocity was linearly increased to  $\pm 4.0$  feet per second. For sink speeds less than 7.0 feet per second, the maximum allowable horizontal velocity was limited to  $\pm 4.0$  feet per second in any direction with respect to the local surface slope. The touchdown velocity envelope was commonly referred to as the “Doghouse.” (Figure 5.)

The final Lunar Module configuration was a two-stage vehicle composed of an ascent stage and a descent stage. The four symmetrically placed Cantilever landing gears were attached to the descent stage. The radius of the footpad ball joints measured 167 inches.

Figure 3 provides the definition of the Lunar Module body coordinate system with selected critical dimensions.

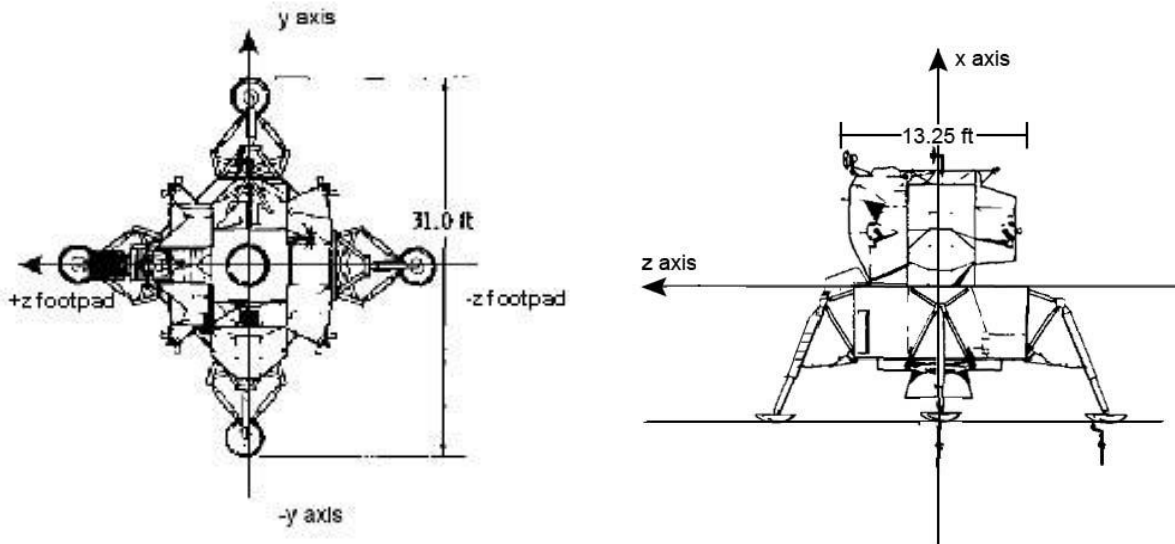


**Figure 3. Body coordinate system of Lunar Module with noted key dimensions for the Cantilever landing gear configuration.**

The crew would be looking forward down the body +Z axis. The body +Y axis would be to the right of the crew. The body +X axis pointed vertically. From the crew's viewpoint, the yaw angle would be a rotation about the X axis, the pitch angle would be a rotation about the Y axis, and the roll angle would be a rotation about the Z axis, all according to the right-hand rule.

The landing gear footpads measured approximately 36 inches in diameter with a contact area of about 1018 in<sup>2</sup> for each footpad. The footpad depth measured about 6 inches. This was equivalent to an average static bearing pressure on each footpad of less than 0.7 psi for the Lunar Module resting on the lunar surface. The radius to the landing gear footpad centers measured 167 inches. The static clearance between the descent engine nozzle exit plane and the landing surface was about 18.5 inches for the Apollo 11, 12, 13, and 14 Lunar Modules. The Apollo 15, 16, and 17 Lunar Modules had an additional 10-inch extension to the descent engine nozzle, thereby reducing the static clearance to about 8.5 inches between the nozzle exit plane and the landing surface. On these flights, the Lunar Module also carried the Lunar Rover Vehicle, which extended the astronauts' mobility range during lunar surface exploration. The Lunar Rover Vehicle weighed about 1200 pounds (Earth) and could carry two astronauts to a range of approximately 20 miles. The rover was powered by four 0.1 horsepower direct-current motors (one for each wheel), and powered by two 36-volt silver-zinc potassium hydroxide non-rechargeable batteries.

The landing system was composed of four landing gear legs symmetrically attached to the descent stage. Each landing gear leg was comprised of three struts—one primary strut and two secondary struts. Each

strut had energy absorption capability in the form of crushable honeycomb cartridges. The secondary struts possessed energy absorption capability in both tension and compression stroking, whereas the primary strut had energy absorption capability in compression stroking only.

Figure 4 offers a sketch of the final design showing the ascent stage and descent stage, as well as the arrangement of the landing gear system. The astronauts were looking in the forward direction over the descent ladder and service platform, and along the +Z body axis.

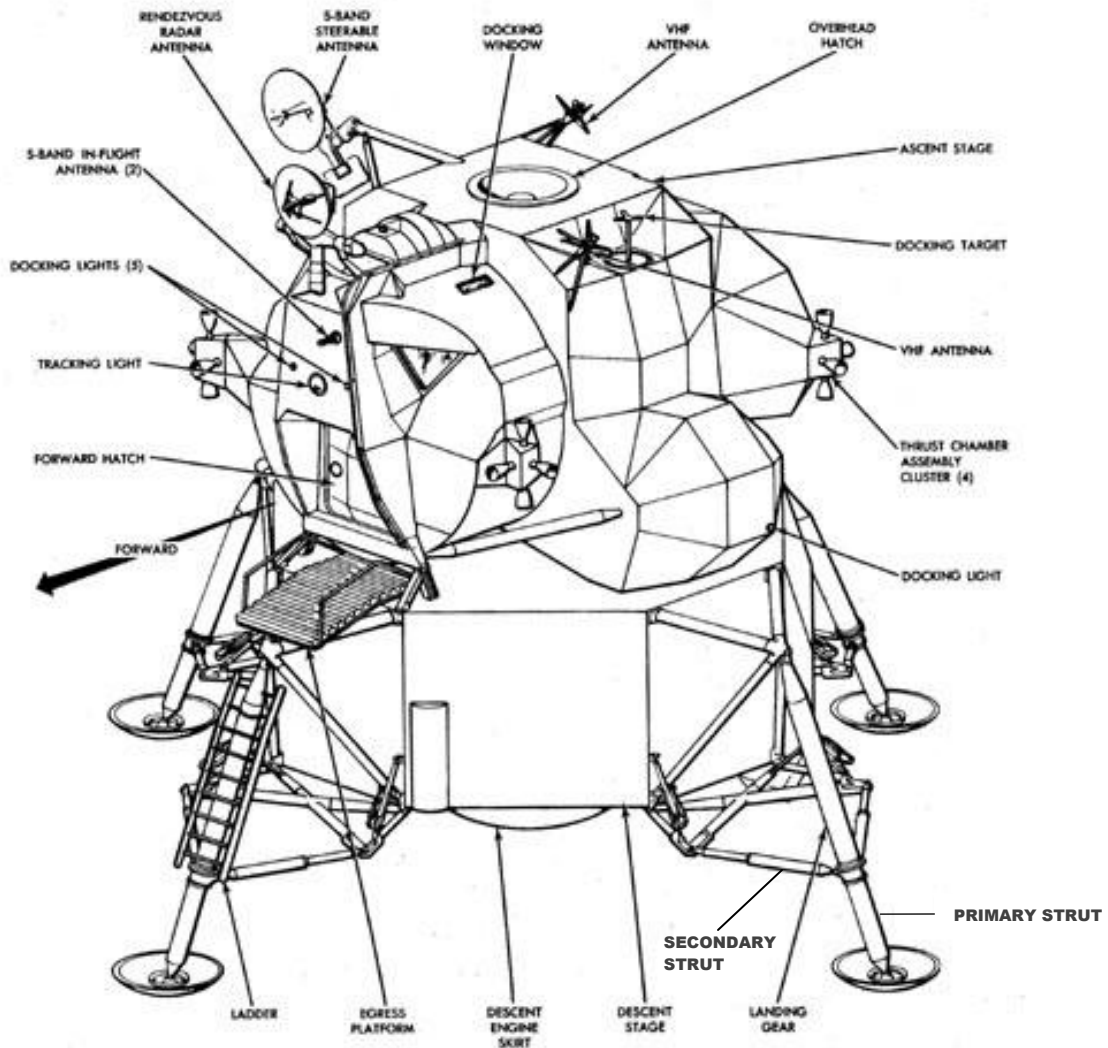
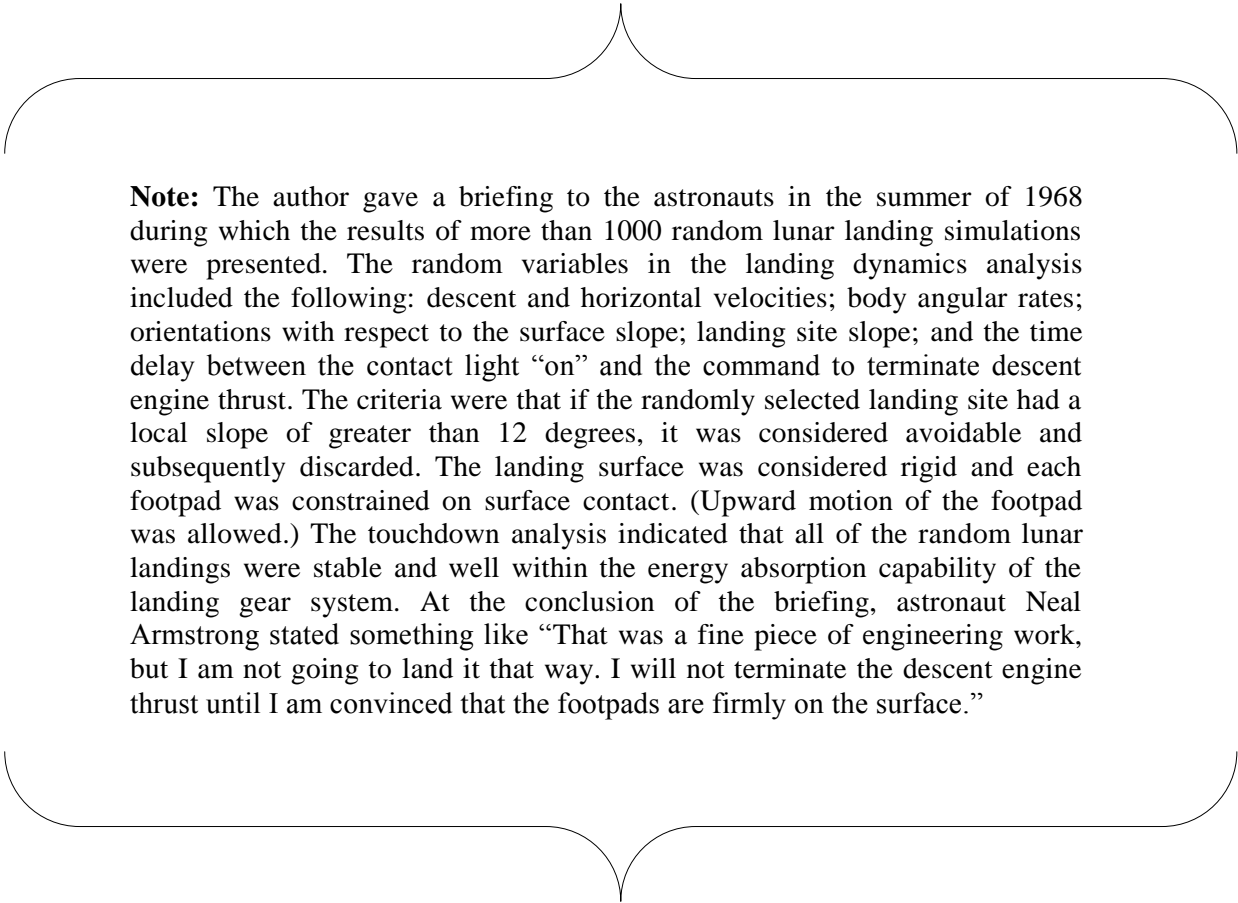


Figure 4. Final Lunar Module configuration that landed on the moon, and the attachment location of the four Cantilever-type landing gears to the descent stage.

A lunar surface probe (not shown) was attached to three landing gear assemblies. The probes, which measured approximately 67 inches in length, were designed to collapse (i.e., buckle) during the touchdown maneuver and not interfere with the articulation of the landing gear, and not produce sufficient landing dynamic forces to affect landing stability. The +Z landing gear (showing the descent ladder and the service platform) did not have a lunar surface probe because a buckled probe may have presented a hazard to the astronauts as they descended down the ladder to the lunar surface. When the lunar probe made contact with the lunar surface, a contact light illuminated in the crew cabin. The landing gear design was based on the assumption that when the contact light was illuminated, the commander would terminate the descent engine thrust and the Lunar Module would subsequently land on the lunar surface.



**Note:** The author gave a briefing to the astronauts in the summer of 1968 during which the results of more than 1000 random lunar landing simulations were presented. The random variables in the landing dynamics analysis included the following: descent and horizontal velocities; body angular rates; orientations with respect to the surface slope; landing site slope; and the time delay between the contact light “on” and the command to terminate descent engine thrust. The criteria were that if the randomly selected landing site had a local slope of greater than 12 degrees, it was considered avoidable and subsequently discarded. The landing surface was considered rigid and each footpad was constrained on surface contact. (Upward motion of the footpad was allowed.) The touchdown analysis indicated that all of the random lunar landings were stable and well within the energy absorption capability of the landing gear system. At the conclusion of the briefing, astronaut Neal Armstrong stated something like “That was a fine piece of engineering work, but I am not going to land it that way. I will not terminate the descent engine thrust until I am convinced that the footpads are firmly on the surface.”

## 5.0 Critical Design Cases

The Lunar Module landing dynamic analysis simulations<sup>1-8</sup> were used to evaluate all landing gear critical cases. These included landing cases that were critical in stability (i.e., the propensity to overturn) and landing cases that were critical in landing gear energy absorption. For the most part, the design conditions were produced by landings on a rigid 12-degree slope with the footpads constrained in the lateral direction on contact.

The final touchdown velocity envelope—i.e., the Doghouse—is shown in Figure 5 with the noted boundaries for landing gear energy absorption and landing stability. The landing gear boundaries were analytically determined using test-verified touchdown dynamic computer codes.

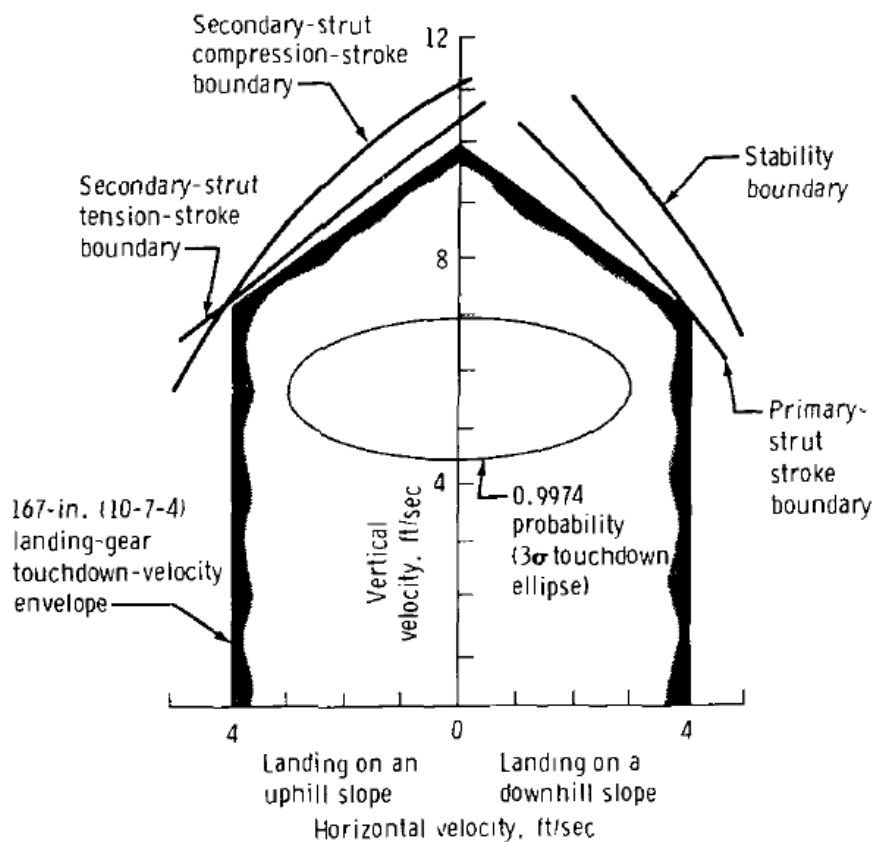


**Figure 5. Lunar Module landing touchdown velocity envelope and landing gear energy absorption performance.<sup>10</sup>**

The minimum landing stability of the Lunar Module was associated with a high center of gravity, which would represent the minimum landing weight. The basic design requirement for the landing gear system was that all critical landing cases fall outside the Doghouse or the design velocity envelope. The landing dynamics stability boundary for all of these critical cases fell outside of the Doghouse. This indicated that all landings inside the Doghouse were stable.

The maximum energy absorption landing cases for the primary landing gear struts were downhill landings. These cases were associated with the maximum landing weight, which would represent the lowest center of gravity. The primary strut energy absorption capability boundary was also outside the Doghouse. This indicated that the primary strut had sufficient energy absorption capability for all landings inside the Doghouse.

The critical energy absorption cases for the secondary struts in compression stroking were landings in the uphill direction. In all critical uphill landing cases, the secondary struts had sufficient energy absorption capability in compression stroking. The secondary compression stroke capability could satisfy all landings inside the Doghouse.

The critical energy absorption cases for the secondary struts in tension stroking were landings in which the footpads were not restrained on surface contact. The critical landing cases were uphill landings on a surface slope of 12 degrees with a surface/footpad friction coefficient of 0.4. The secondary strut energy absorption capability boundary in tension stroking was also outside the Doghouse. This indicated the capability of sufficient energy absorption in secondary strut tension stroking to satisfy all landings within the Doghouse.

The ellipse within the touchdown velocity envelope centered around a vertical touchdown velocity of about 5.5 feet per second, was the  $3\sigma$  [sigma, population Standard Deviation] touchdown velocity envelope based on the random variables of vertical and horizontal velocities and the time delay between the contact light coming on and the command to terminate descent engine thrust. The probability is based on digital simulations on the order of 1000 cases.

In summary, all touchdown conditions resulting in the definition of stability performance boundaries and landing gear energy absorption boundaries were outside the design velocity envelope or the Doghouse, which meant that all landings inside the Doghouse were satisfactory, stable landings, and that the landing gear system absorbed the touchdown energies without exceeding the structural limits. This indicated all landing gear design requirements were satisfied and the landing gear system was certified for flight.

## **6.0 Analysis of the Apollo 11 Lunar Module Landing Dynamics and Lunar Surface Mechanical Properties**

During the early operational period of the Apollo Program, the scientific and engineering communities placed a high priority on defining the lunar surface mechanical properties because of the uncertainties identified early on in the program. Apollo 11 was the first Lunar Module landing to provide precision touchdown dynamic data that could be used in identifying the lunar surface mechanical properties. The landing dynamic data used in the identification process included the pitch, roll, and yaw body rate data recorded during the touchdown maneuver from the on-board computer and the landing gear strut strokes derived from post-landing photographs of the landing gears.

The touchdown correlation analysis for the Apollo 11 Lunar Module landing is presented in Appendix A: Apollo 11 Lunar Module Touchdown Dynamics. The analysis includes the correlations between the predicted and measured Lunar Module body rotational rates, and comparisons between the predicted and measured landing gear strut strokes. The lunar soil mechanical properties were derived from the correlation analysis.

The footpad/soil interaction model used in the correlation analysis was a simplified model of that presented in Reference 6. The simplified model accounted for only the first-order soil/footpad interaction forces, which were primarily the bearing strength and the horizontal friction forces between the footpad and lunar surface.

The touchdown analysis used in deriving the lunar soil mechanical properties was an iterative process. The lunar soil mechanical property parameters were varied in a systematic manner until a best fit was obtained to the Lunar Module body rotational rate data and the landing gear strut stroke data.

The landing dynamic analysis presented in Appendix A indicates that, at the Apollo 11 landing site, the nominal value for lunar surface bearing strength was 1.88 psi per inch depth with an associated nominal sliding friction coefficient between the footpad and the lunar surface of 0.33. The lunar bearing strength was greater than the design requirement for the footpad. The nominal coefficient of friction was slightly less than the design requirement of 0.4, but this did not pose any structural issues for the landing gear system or structure of the Lunar Module.

The landing gear system energy absorption capability was more than adequate to absorb the touchdown kinetic and potential energies. The maximum energy absorption capability of the landing gear system was 162,000 foot-pounds compared to the touchdown kinetic energy of the Apollo 11 Lunar Module of 1960 foot-pounds.

During the Apollo 11 Lunar Module landing, the landing gear primary strut had a negligible amount of stroking. The landing simulation indicated primary strut elastic compression only. No secondary strut compression stroking was predicted or measured. The secondary struts did have tension stroking. The maximum observed secondary strut tension stroke of 4 inches in the +Z landing gear compared to a total tension stroke capability of 16 inches. The predicted tension stroke was 1.8 inches. This is equivalent to a maximum secondary strut tension loading of 500 pounds. All measured and predicted landing gear strut strokes were well within the landing gear capability.

The overall correlation between the measured and predicted Lunar Module body rotational rates were judged to be very good, using the simplified footpad/soil interaction model. The predicted “rocking” motion during the Apollo 11 Lunar Module landing was about 2 degrees, yet the astronauts reported no rocking sensation during the landing maneuver. The correlation between measured and predicted landing gear strut strokes were considered good; both the analysis and the observed strut strokes indicated that the only gear stroking was in tension in the secondary struts. The primary strut strokes were negligible. The analysis also indicated that more than 80 percent of the touchdown energies were absorbed by the lunar soil.

The Apollo 11 Lunar Module landing gear energy absorption and landing stability performance were well within the touchdown dynamic design envelope.

## 7.0 The Apollo Lunar Module Landings

### 7.1 Apollo 11 Lunar Landing

The Apollo 11 lunar landing occurred on July 20, 1969, in the Sea of Tranquility, located at 0°, 40', 26.7" N and 23°, 28', 22.7" E, with astronaut Neil Armstrong as Lunar Module commander, and astronaut Edwin (Buzz) Aldrin as Lunar Module pilot.

During descent to the lunar surface, the automatic guidance system targeted a landing point that was not acceptable. The guidance computer was switched to manual control, and the crew flew the module to a relatively level area bounded by a boulder field and a sizable crater.

Lunar dust—produced by the descent engine plume interacting with the lunar surface—became visible at an altitude of about 100 feet and increased in intensity up until touchdown. However, the presence of dust did **not** seriously impair the required visibility for landing and, as such, was not a threat to landing safety for the Apollo 11 mission. It was noted that the exhaust velocity of the descent engine was on the order of 10,000 feet per second and the orbital velocity for the moon was about 5000 feet per second. The lunar dust, entrained by the descent engine plume, would move over the lunar surface on the order of lunar orbital speed.

No lunar surface erosion was noted due to the engine plume/surface interaction.<sup>13</sup> Initiation of the descent engine shutdown was approximately the time of footpad contact or shortly thereafter.

The landing velocities were well within the design touchdown velocity envelope. The sink speed at the time of first footpad contact was 1.8 feet per second with an associated horizontal velocity of 2.2 feet per second. From the crew point of view, the Lunar Module horizontal velocity vector was about 87 degrees to the left of forward. With reference to Figure 3, the pitch attitude was +0.8 degrees, the roll attitude was -1.4 degrees, and the yaw attitude was +15.3 degrees at the time of first footpad contact.

The pitch, roll, and yaw rate time histories during the touchdown dynamic maneuver are presented in Figures 6, 7, and 8. The pitch rate was a rotation about the body Y axis, the roll rate was a rotation about the body Z axis, and the yaw rate was a rotation about the body X axis consistent with the right-hand rule.

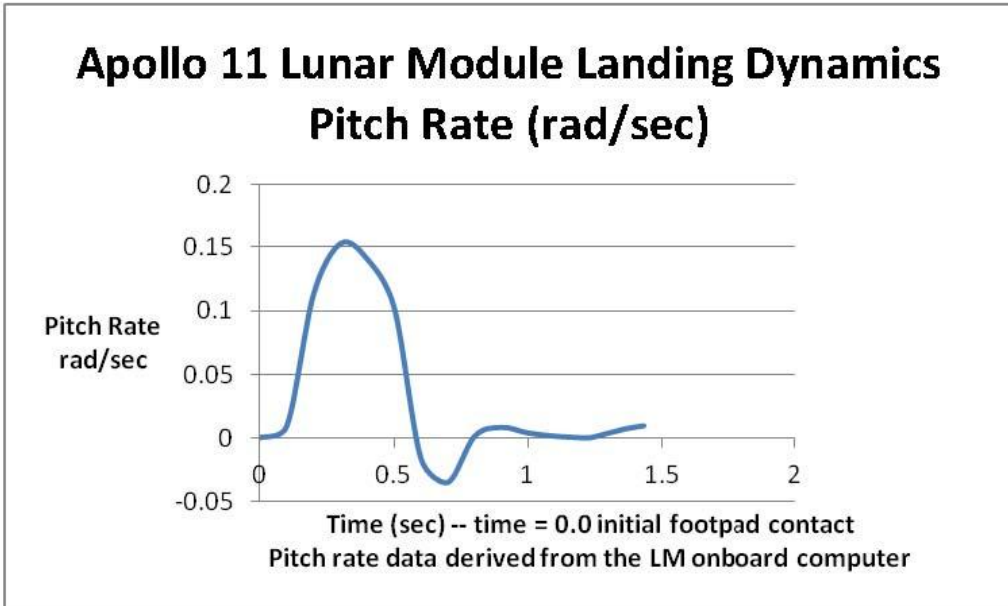


**Figure 6. Apollo 11 Lunar Module pitch rate as a function of time.** The pitch rate data were derived from the on-board guidance computer. (Note: LM = Lunar Module)

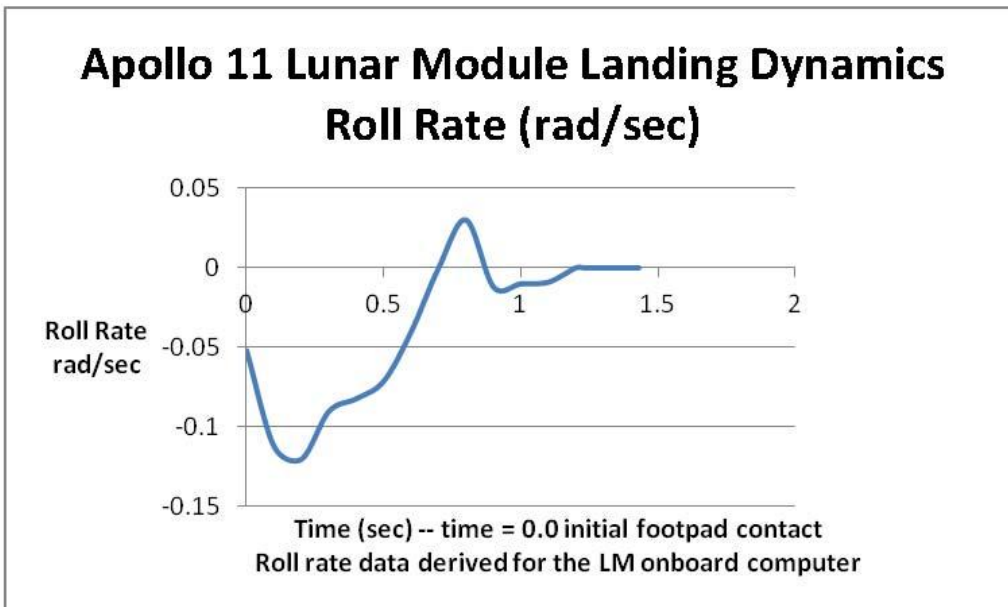


**Figure 7. Apollo 11 Lunar Module roll rate as a function of time.** The roll rate data were derived from the on-board guidance computer. (Note: LM = Lunar Module)

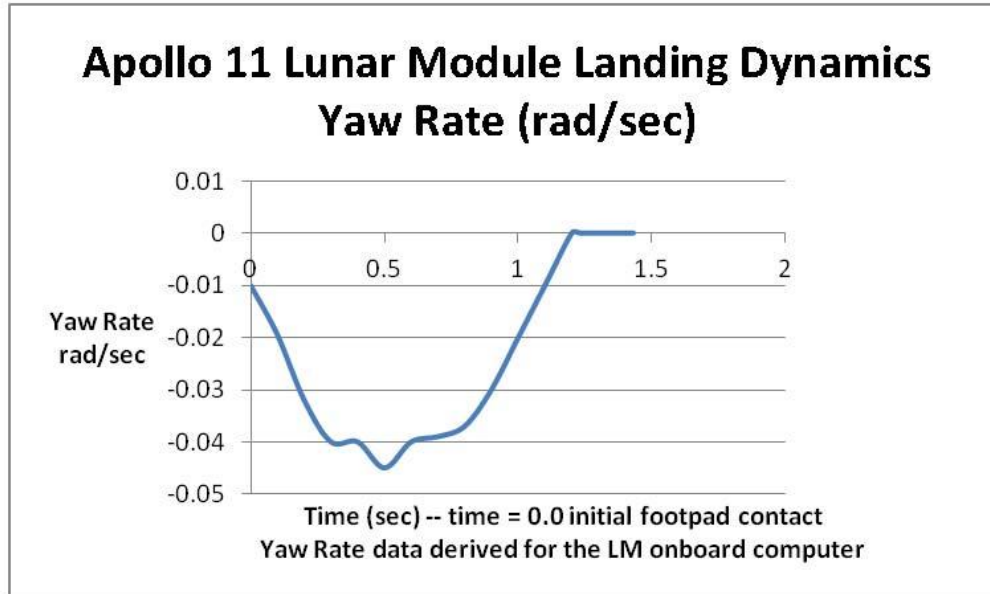


**Figure 8. Apollo 11 Lunar Module yaw rate as a function of time.** The yaw rate data were derived from the on-board guidance computer. (Note: LM = Lunar Module)

With reference to Figures 6, 7, and 8, it is noted that the peak pitch rate was +0.15 radians per second and occurred approximately 0.3 seconds from initial footpad contact during the landing maneuver. Also, the peak roll rate was -0.13 radians per second and occurred at approximately 0.12 seconds, and the peak yaw rate was -0.045 radians per second and occurred at approximately 0.5 seconds. The final at-rest attitudes were +4.4 degrees in pitch, +0.3 degrees in roll, and +13.0 degrees in yaw. The entire Lunar Module touchdown dynamics were arrested in less that 1.5 seconds. From these data, the local landing slope was computed to be 4.5 degrees.

Figure 9 shows the composite of the Apollo 11 Lunar Module body rotational rates as a function of time.

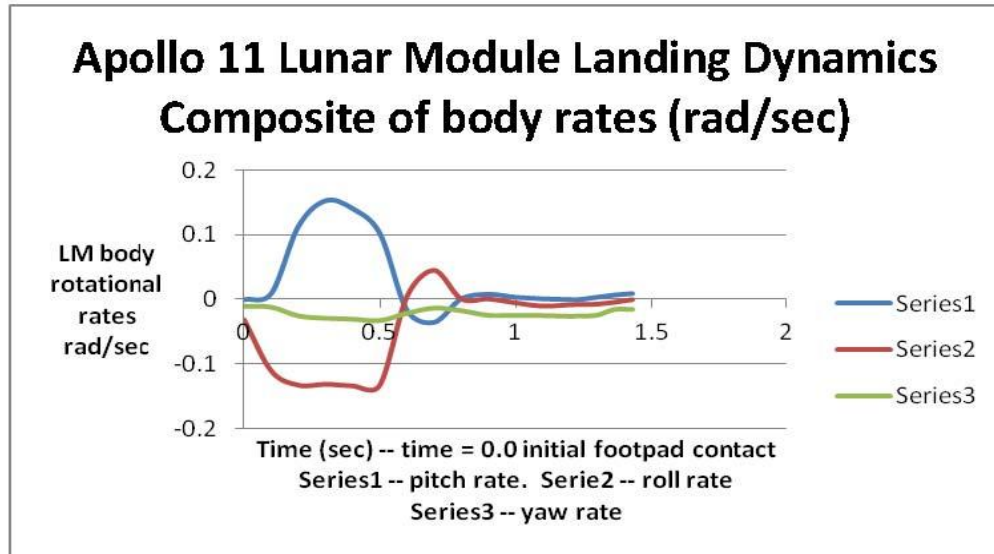


**Figure 9. Composite of Apollo 11 Lunar Module rotational rates during touchdown maneuver.** (Note: LM = Lunar Module)

This graph shows that the predominate rotational motions were in the pitch and roll axes. The yaw rate, by comparison, was very small.

The touchdown dynamic digital simulation of the Apollo 11 indicated that the footpad touchdown sequence was that the +Y footpad made first contact with the lunar surface, followed by the +Z footpad 0.1 second later.

The landing gear energy absorption and landing stability performance were well within the design envelope.

Figure 10 offers a view of the Apollo 11 Lunar Module—the Eagle—resting on the lunar surface.

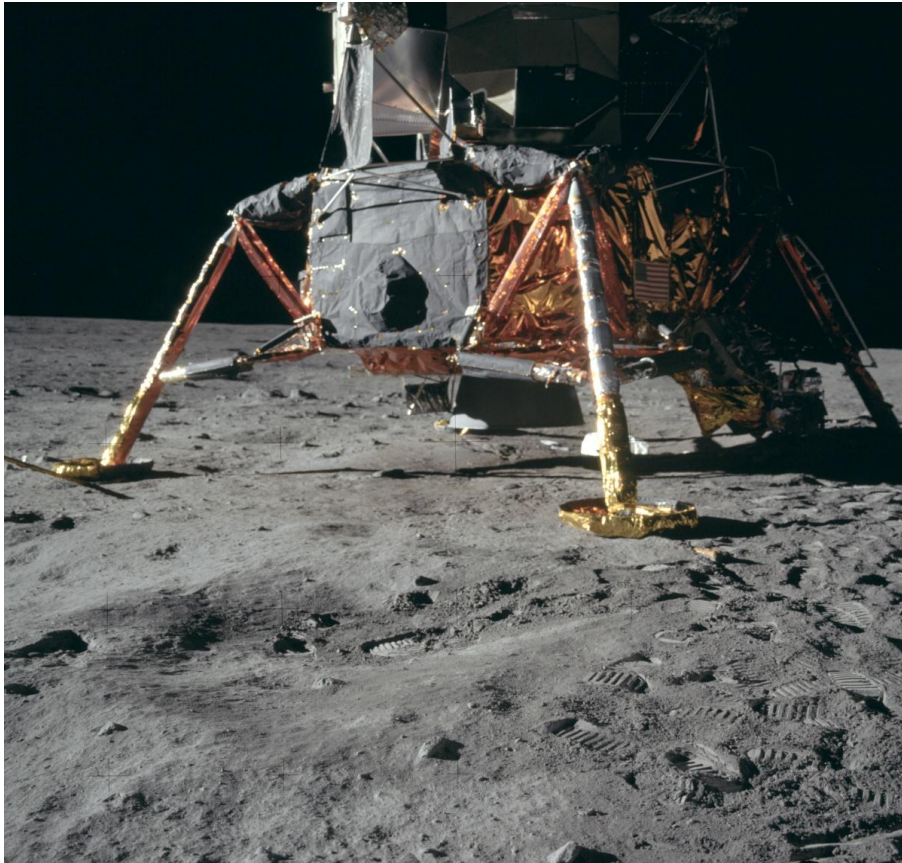


**Figure 10. (NASA Photograph AS11-40-5915) Overall view of Apollo 11 Lunar Module resting on lunar surface.** The local lunar surface slope was computed to be 4.5 degrees with the uphill side in the +Z direction. The sink speed was 1.8 feet per second and the planar velocity was 2.2 feet per second perpendicular to the shadow and in the -Y direction. The +Z landing gear is located to the extreme right within the shadowed area of the Lunar Module.

From the crew cabin windows, the crew members would be looking down the +Z body axis, with the sun to their backs, making the Lunar Module shadow fall along the +Z body axis.

At the time of touchdown, the Lunar Module was basically moving away from the point at which this photograph was taken, or 90 degrees to the local slope. The flight path would have been just over the crater, as seen in the lower left-hand side of the photograph, prior to landing. The landing site was relatively free of large craters and boulders.

The +Z landing gear is located to the extreme right in this photograph. The descent ladder is visible on the +Z landing gear. The +Y landing gear is located just to the right of center. The -Z landing gear is located to the extreme left in the photograph, and partially visible -Y footpad is located in the center and behind the descent engine nozzle.

Figure 11 offers a closeup view of the Apollo 11 Lunar Module descent engine nozzle. The +Z landing gear ladder is located on the upper left-hand side in the photograph.



**Figure 11. (NASA Photograph AS11-40-5864) Closeup view of Apollo 11 Lunar Module descent engine nozzle bell and the +Z landing gear.**

Based on photographic data analysis, the clearance between the nozzle exit plane and the lunar surface was estimated to be from 12 to 15 inches. The static clearance resting on a planar rigid surface was about 18.5 inches. The descent engine nozzle did not make contact with the lunar surface during the Apollo 11 landing maneuver.

The nozzle exit plane of the descent engine was close enough to the lunar surface to allow for effective thrust amplification. The descent engine was still thrusting at the time of footpad contact; the thrust level was on the order of 2000 pounds. The analysis indicated that the descent engine nozzle did not make contact with the lunar surface during the landing maneuver.

Views of the +Y, -Z, -Y and -Y, respectively, of the Apollo 11 Lunar Module landing gear footpads are shown in the following photographs (Figures 12, 13, 14, and 15).

Figure 12 is a view of the Apollo 11 Lunar Module +Y landing gear and footpad.



**Figure 12. (NASA Photograph AS11-40-5858) Apollo 11 Lunar Module +Y landing gear and footpad, looking from the area of the +Z footpad location toward the +Y footpad.** The sink speed was 1.8 feet per second and the planar velocity was 2.2 feet per second perpendicular to the shadow and in the -Y direction.

The +Y footpad contact probe shown here is close to horizontal to the plane of the lunar surface. Analysis indicates that the +Y footpad was the first to make lunar surface contact. At the time of contact, the Lunar Module was basically translating along the body Y axis in the -Y direction.

This photograph also shows that the +Y footpad penetration into the lunar surface was shallow—less than 3 inches. A small amount of lunar soil buildup on the leading edge of the footpad indicates that the +Y footpad skid distance was on the order of inches.

Figure 13 is a view of the Apollo 11 Lunar Module  $-Z$  footpad, located in the bottom left-hand corner. The  $+Y$  footpad is located in the top center of the photograph.



**Figure 13. (NASA Photograph AS11-40-5925) Closeup view of Apollo 11 Lunar Module  $-Z$  footpad and the  $+Y$  footpad, located in the top center of the photograph, and looking down a line connecting the  $-Z$  footpad and the  $+Y$  footpad. The sink speed was 1.8 feet per second and the planar velocity was 2.2 feet per second parallel to the  $-Z$  deflected probe and in the  $-Y$  direction.**

In this photograph, the  $-Z$  footpad surface contact probe is rotated upward at about a 20-degree angle from the plane of the lunar surface. The contact probe was designed to buckle without the buckling forces degrading the landing performance during the touchdown maneuver.

At the time of touchdown, the Lunar Module was basically translating from right to left (in the photograph) or parallel to the position of the contact probe. The soil pattern in the area of the trailing edge of the  $-Z$  footpad indicates that skidding did occur—less than 3 inches—after the  $-Z$  footpad made initial contact with the lunar surface.

The  $+Y$  footpad, shown in the top center of the photograph, indicates a similar penetration and skid distance.

Figure 14 offers another view of the Apollo 11 Lunar Module –Y footpad and the contact probe.

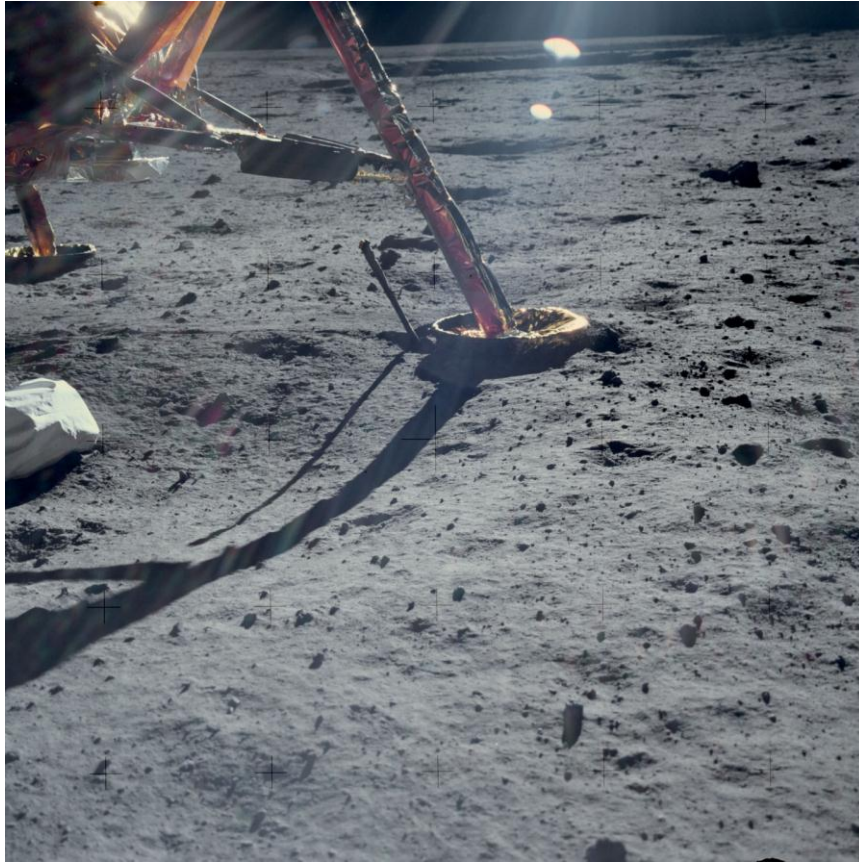


**Figure 14. (NASA Photograph AS11-40-5865) Apollo 11 Lunar Module –Y landing gear and footpad, located in approximately the upper center of the photograph. The -Z footpad is in the extreme upper left.**

This photograph shows the –Y footpad contact probe rotated upward approximately 20 degrees from the plane of the lunar surface. Footpad motion at the time of contact would have been in the direction perpendicular to the landing gear shadow moving from left to right.

The –Y footpad penetration into the lunar surface was very shallow—less than 3 inches—and the skid distance was on the order of inches.

Figure 15 is a view of the Apollo 11 Lunar Module –Y footpad with the contact probe standing very close to vertical with respect to the lunar surface.



**Figure 15. (NASA Photograph AS11-40-5850) Apollo 11 Lunar Module –Y landing gear and footpad, looking at the –Y footpad from the area of the +Z landing gear. The sink speed was 1.8 feet per second and the planar velocity was 2.2 feet per second perpendicular to the shadow and in the –Y direction.**

At the time of footpad contact, the –Y footpad was translating from left to right (in the photograph). The –Y footpad penetration into the lunar surface was less than 3 inches and the skid was on the order of inches.

Photographs of the Apollo 11 landing site show that the site was relatively free of lunar craters and boulders and, as such, presented a relatively flat landing surface.

### **7.1.1 Summary: Apollo 11 Lunar Module Landing**

Lunar dust, blown from the surface by the descent engine plume impingement, was detected at an altitude of about 100 feet. The dust was not detrimental to landing visibility and, as such, did not compromise the safety of the landing.

The Apollo 11 Lunar Module was basically flying perpendicular to the local slope at the time of first footpad contact with the lunar soil. The landing velocities and body rotational rates at the time of touchdown were well within the touchdown design envelopes, and the landing surface slope was well under the 12-degree design limit for the landing system. From the crew point of view, at the time of touchdown, the horizontal velocity vector was about 87 degrees to the left of forward, or primarily translating along the -Y body axis.

Analysis of the photographic data indicates the maximum footpad penetration was less than 3 inches and a skid distance after footpad contact with the lunar surface was less than 3 inches. The photographs also indicate that the Apollo 11 landing site was relatively free of large lunar craters and boulders.

The landing digital simulation and the landing gear photographic analysis indicated that gear energy absorption and landing stability performance were well within the design envelope. The simulation also indicated that the lunar soil absorbed more than 80 percent of the touchdown kinetic and potential energies.

The descent engine nozzle did not make contact with the lunar surface during this landing maneuver.

## **7.2 Apollo 12 Lunar Landing**

The Apollo 12 Lunar Module landed on November 19, 1969, in the Oceanus Procellarum located at 3°, 11', 51.0" S and 23°, 23', 8.0" W, with astronaut Charles Conrad, Jr. as Lunar Module commander, and astronaut Alan L. Bean as pilot. The Lunar Module landed approximately 600 feet from the touchdown site for Surveyor III, which had landed on the moon on April 20, 1967.

Lunar dust appeared at an altitude of about 100 feet during descent. This result was similar to the lunar dust produced during the Apollo 11 landing, and was caused by the interaction of the descent engine plume and the lunar surface. No degradation in visibility was noted above 100 feet. The dust cloud increased in intensity as the descent continued. Below an altitude of 50 feet, the degradation in visibility continued until the landing site surface was completely obscured.

The descent engine thrust termination was initiated at about 1.3 seconds prior to first footpad contact or about the time the landing probe contact light came on—or shortly thereafter. This implies that the descent engine thrust at the time of footpad contact with the lunar surface was negligible.

Analysis of the camera film indicated that the lunar erosion caused by the descent engine plume was greater than that observed on Apollo 11.<sup>14</sup>

The Apollo 12 landing velocities were well with the design touchdown velocity envelope. The sink speed at the time of first footpad contact was 3.3 feet per second with an associated horizontal velocity of 0.4 feet per second in the -Y direction and 1.7 feet per second in the +Z direction. From the crew point of view, the horizontal velocity vector was about 13 degrees to the left of forward. At the time of first footpad contact, the pitch attitude was -3.0 degrees and the roll attitude was -1.4 degrees.

The Apollo 12 Lunar Module pitch, roll, and yaw rate time histories during the touchdown dynamic maneuver are presented in Figures 16, 17, and 18.

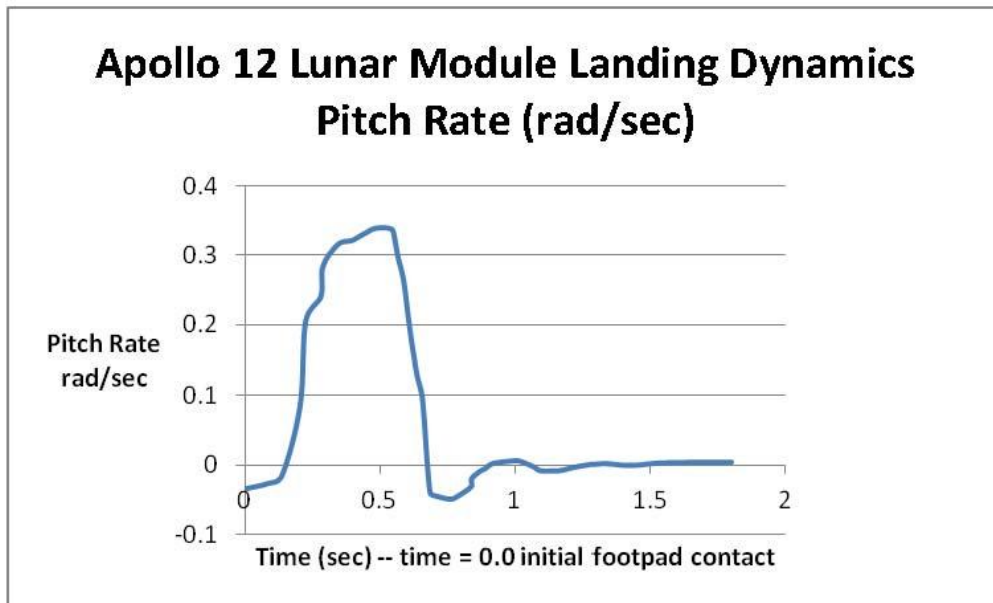


**Figure 16. Apollo 12 Lunar Module pitch rate as a function of time.** The pitch rate data were derived from the Lunar Module on-board guidance computer.

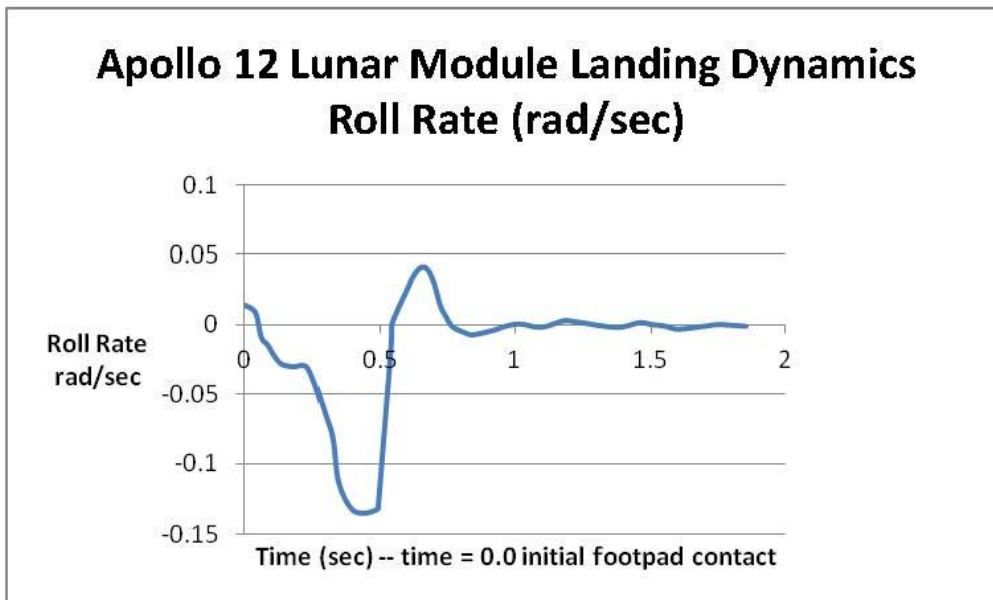


**Figure 17. Apollo 12 Lunar Module roll rate as a function of time.** The roll rate data were derived from the Lunar Module on-board guidance computer.

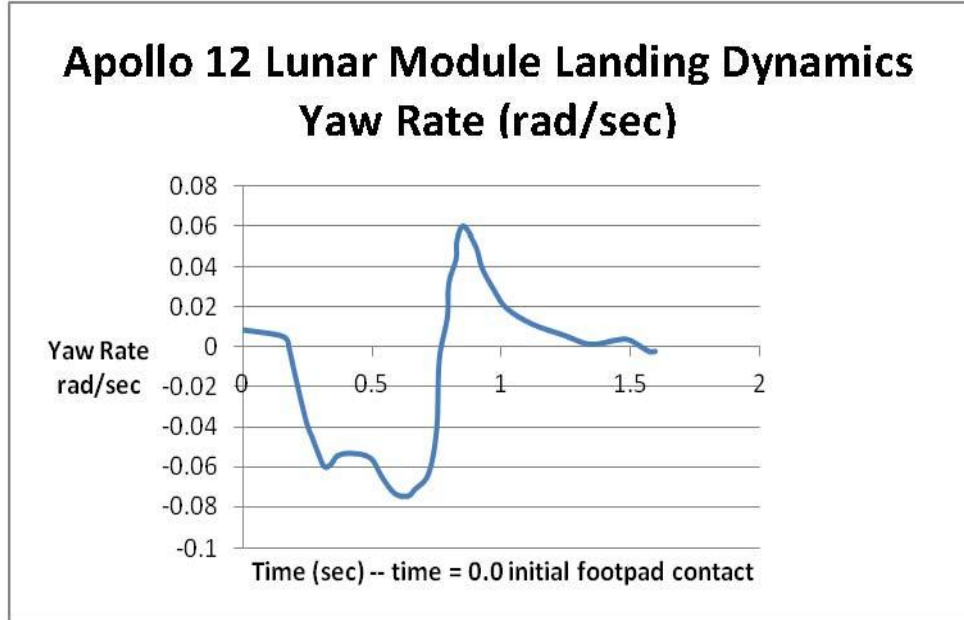


**Figure 18. Apollo 12 Lunar Module yaw rate as a function of time.** The yaw rate data were derived from the Lunar Module on-board guidance computer.

During the landing maneuver, the peak pitch rate was +0.33 radians per second and occurred approximately 0.5 seconds from initial footpad contact. Also, the peak roll rate was -0.13 radians per second and occurred at 0.4 seconds. The peak yaw rate was -0.075 radians per second occurring at 0.6 seconds. The final at-rest attitudes were +3.0 degrees in pitch and -3.8 degrees in roll. The yaw attitude was assumed to be zero. Based on these data, the local landing slope was computed to be 4.8 degrees.

Figures 16, 17, and 18 indicate the Lunar Module predominate rotational motions were in the pitch and roll axes. The yaw rate, by comparison, was smaller.

The touchdown dynamic digital simulation of the Apollo 12 landing indicated that the +Y footpad was the first to make contact with the lunar surface. The Lunar Module came to rest approximately 1.5 seconds after the initial footpad contact with the lunar surface.

The digital simulation indicated that all primary strut strokes were less than 2.5 inches and the secondary strut strokes were less than 4.5 inches.

The landing gear energy absorption and landing stability performance were well within the design envelope.

The analysis also indicated that the descent engine nozzle did not make contact with the lunar surface during the landing maneuver.

Figure 19 is a view of the Apollo 12 Lunar Module—the Intrepid—resting on the lunar surface.



**Figure 19. (NASA Photograph AS12-46-6749) Overall view of Apollo 12 Lunar Module resting on the lunar surface.** The local lunar surface slope was computed to be 4.8 degrees, with the uphill side in the +Z direction. The sink speed was 3.3 feet per second and the planar velocity was 1.7 feet per second perpendicular to the shadow. The +Z landing gear is to the extreme right, within the shadowed area of the Lunar Module.

This photograph shows a view looking down the  $-Y$  body axis. The  $+Y$  landing gear is located in the right center of the photograph and the astronaut is located to the right of the  $+Y$  landing gear. The  $-Z$  landing gear is to the extreme left. The  $+Z$  landing gear is behind the astronaut and in the shadow of the Lunar Module. The  $-Y$  landing gear is located behind the descent engine nozzle bell and is not totally visible.

The flight path would have been just over the crater located to the left  $+Y$  landing gear prior to landing. The horizontal motion at the time of initial footpad contact would have been from left to right (in the photograph) or flying uphill.

The descent engine nozzle clearance was in the range of 11 to 15 inches. This photograph also indicated that the descent engine nozzle did not make contact with the lunar surface during the landing maneuver.

Views of the +Y, +Y, -Y, and -Y, respectively, of the Apollo 12 Lunar Module landing gear footpads are shown in Figures 18, 19, 20, and 21.

Figure 20 is a view of the Apollo 12 Lunar Module +Y landing gear and footpad and descent engine nozzle.



**Figure 20. (NASA Photograph AS12-46-6905) The +Y landing gear and footpad.** The descent engine nozzle is located in the upper left-hand corner. The sink speed was 3.3 feet per second and the planar velocity was 1.7 feet per second approximately parallel to the shadow and in the +Z direction.

The +Y footpad penetration was less than 3 inches; the skid distance during footpad contact was on the order of inches.

The depression to the left of the +Y footpad is a lunar crater with a diameter approximately the same as that of the landing gear footpad. At the time of footpad impact, the Lunar Module was traveling in the direction of the Lunar Module shadow.

Initial speculation was that this crater might have been the initial +Y footpad impact location and subsequently bounced and translated to the current at-rest position. It is noted that the elasticity of the landing gear, structure, and lunar soil mechanical properties would be insufficient to store the energy required to produce a bounce of this magnitude. This would imply that the descent engine was still thrusting during the landing maneuver and, as such, produced a floating effect and gave the appearance of

a bounce of this magnitude. However, the descent engine thrust termination time and the basic direction of the landing maneuver do not support this hypothesis.

It is noted, in this photograph, that an adequate clearance between the descent engine nozzle exit plane and the lunar surface existed, which indicates the descent engine nozzle did not make contact with the lunar surface during the landing maneuver.

Figure 21 is a view of the Apollo 12 Lunar Module +Y landing gear and footpad.



**Figure 21. (NASA Photograph AS12-46-6904) Apollo 12 +Y landing gear and footpad. Also shown: an imprint of the astronaut's space suit boot.**

Analysis indicated that the +Y footpad was the first to make contact with the lunar surface. Based on the lunar soil pattern next to the left of the boot print, +Y footpad translation after initial contact with the lunar surface was on the order of 5 inches.

The footpad penetration and astronaut boot penetration patterns at the Apollo 12 landing site were similar to those of the Apollo 11 landing site in depth of penetration and cohesiveness of the lunar soil (reference boot print photograph in Appendix B, photograph 4B, *NASA Photograph AS11-40-5878*). This implies that the lunar surface mechanical properties at the Apollo12 landing site were approximately the same as those at the Apollo 11 landing site.

Figure 22 is a view of the Apollo 12 Lunar Module -Y landing gear and footpad.



**Figure 22. (NASA Photograph AS12-46-6900) Apollo 12 -Y landing gear and footpad.** The -Z landing gear is located in the upper right-hand corner of the photograph. The sink speed was 3.3 feet per second and the planar velocity was 1.7 feet per second approximately parallel to the shadow and in the +Z direction.

The -Y footpad was moving in the general direction from right to left or primarily forward at the time of lunar surface contact. The footpad translation during during surface contact was minimal to nil. The photographic data indicate that the penetration of the -Y footpad into the lunar surface was on the order of 3 inches.

Figure 23 is a closeup view of the Apollo 12 Lunar Module –Y landing gear and footpad.



**Figure 23. (NASA Photograph AS12-46-6901) Close-in view of Apollo 12 –Y footpad.** (Similar view as in Figure 20.) Descent engine nozzle bell is located in the top left-hand side of photograph.

This photograph indicates the –Y footpad penetration into the lunar soil was less than 3 inches and translational motion of the –Y footpad after lunar surface contact was negligible. The lunar soil buildup around the perimeter of the footpad was fairly uniform, indicating the soil buildup was due primarily to vertical impact velocity of the footpad with a minimal translation after impact.

The photographs indicate the Apollo 12 landing site was relatively free of large lunar craters (10 feet or larger in diameter) and boulders and, as such, presented a relatively flat landing surface.

### **7.2.1 Summary: Apollo 12 Lunar Module Landing**

The pattern of lunar dust detection at an altitude of about 100 feet was similar to that of the Apollo 11 Lunar Module landing. As before, the intensity of dust increased as the descent to the lunar surface continued. Below an altitude of 50 feet, however, the degradation of visibility continued until the landing site surface was completely obscured.

The Apollo 12 landing touchdown velocities and initial body rotational rates were well within the touchdown design envelopes, and the landing surface slope was well under the 12-degree design value for the landing system. From the crew point of view, the horizontal velocity vector would be about 13 degrees to the left of forward or primarily flying uphill.

The photographs of the landing gear and footpads indicate a footpad penetration of less than 3 inches and a skid distance after footpad contact of less than 5 inches.

The photographs also indicate the Apollo 12 landing site was relatively free of large lunar craters and boulders.

The landing digital simulation and photographic analysis indicated the landing gear energy absorption and landing stability performance were well within the design envelope.

The descent engine nozzle did not make contact with the lunar surface during the landing maneuver.

The lunar surface mechanical properties were approximately the same as those at the Apollo 11 landing site.

### **7.3 Apollo 13 Lunar Landing (Aborted)**

Apollo 13 was launched on April 11, 1970, with astronauts James A. Lovell as Lunar Module commander, John L. Swigert as Command Module pilot, and Fred W. Haise as pilot. About halfway to the moon, an oxygen tank in the Service Module exploded, resulting in an aborted mission. The Apollo 13 crew traveled on to swing by the moon and return safely to Earth. The Apollo 13 Lunar Module never landed on the moon.

### **7.4 Apollo 14 Lunar Landing**

The Apollo 14 Lunar Module landed on February 5, 1971, in the Fra Mauro located at 3°, 38', 43.0" S and 17°, 28', 16.9" W, with astronaut Alan B. Shepard Jr. as Lunar Module commander, and astronaut Edgar D. Mitchel as pilot.

During final descent to the lunar surface and at an altitude of less than 1500 feet, it was determined that the designated landing site area was too rough for landing, and that the automatic landing guidance was bringing the Lunar Module in short of the targeted landing site. Manual control was initiated at an altitude of about 360 feet and at a range of 2200 feet from the target site. Subsequently, the Lunar Module was flown to a desirable landing point. The crew noted that it was relatively easy to pick an exact landing spot and fly to it with precise control.

Similar to the Apollo 11 and 12 landings, lunar dust caused by the interaction between the descent engine plume and lunar surface was detected at an altitude of 110 feet. As with the other landings, the presence of lunar dust was not detrimental to landing visibility during the final Apollo 14 descent. Some lunar

surface erosion was noted due to interaction between the descent engine plume and lunar surface. The descent engine thrust was terminated about 2 seconds after the surface probe contact light was activated. This implies that the descent engine was still thrusting at the time the initial landing gear footpad made contact with the lunar surface.<sup>15</sup>

The Apollo 14 landing velocities were well within the design touchdown velocity envelope. The sink speed at the time of first footpad contact was 3.1 feet per second, with an associated horizontal velocity of 1.7 feet per second in the +Y direction and 1.7 feet per second in the +Z direction. From the crew point of view, the horizontal velocity vector would be about 45 degrees to the right of forward. At the time of first footpad contact, the pitch attitude was -1.9 degrees, the roll attitude was -2.0 degrees, and the yaw attitude was +3.2 degrees. The final at-rest attitudes were -1.8 degrees in pitch, -6.9 degrees in roll, and +1.4 degrees in yaw.

Based on the on-board computer data, the local slope was computed to be 7.1 degrees.

The Apollo 14 Lunar Module pitch, roll, and yaw rate time histories during the touchdown dynamic maneuver are presented in Figures 24, 25, and 26.

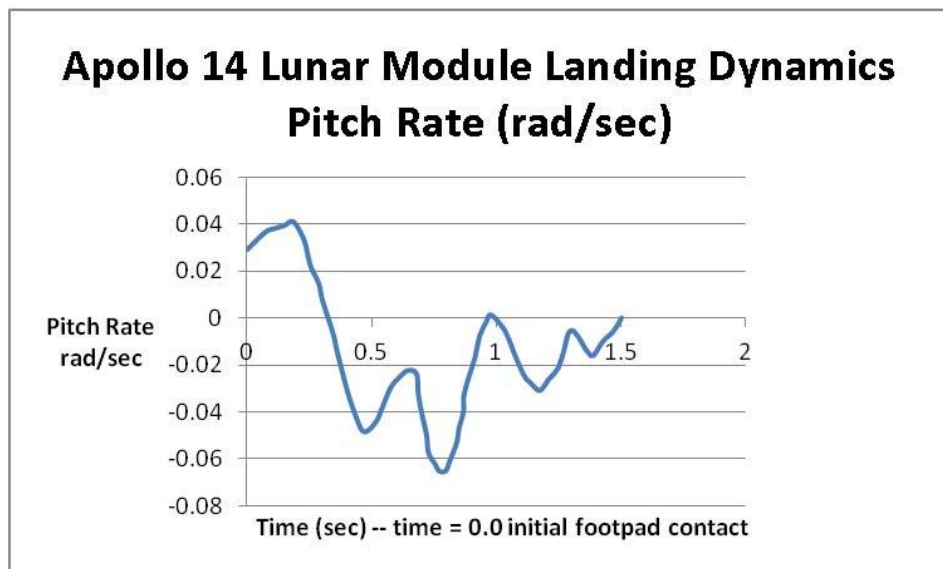


**Figure 24. Apollo 14 Lunar Module pitch rate as a function of time.** The pitch rate data were derived from the Lunar Module on-board guidance computer.

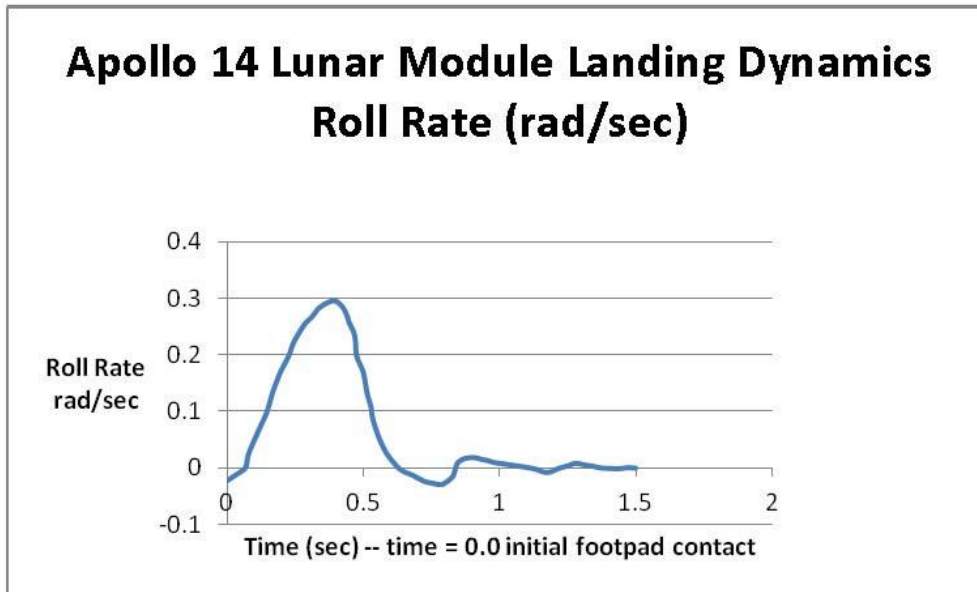


**Figure 25. Apollo 14 Lunar Module roll rate as a function of time.** The roll rate data were derived from the Lunar Module on-board guidance computer.

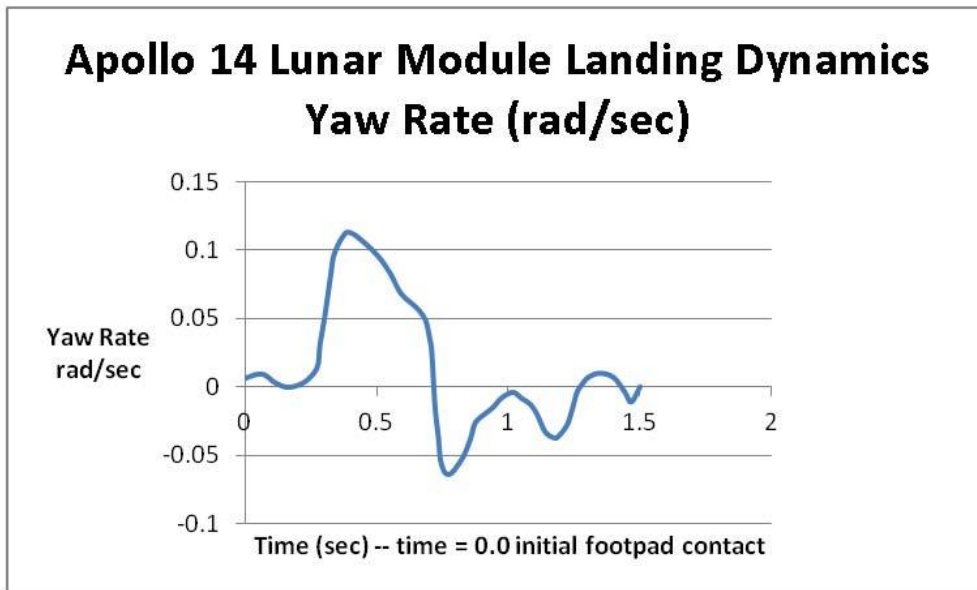


**Figure 26. Apollo 14 Lunar Module yaw rate as a function of time.** The yaw rate data were derived from the Lunar Module on-board guidance computer.

During the landing maneuver, data from the on-board computer indicated the peak pitch rate was  $-0.07$  radians per second and occurred approximately  $0.8$  seconds after initial footpad contact. Also, the peak roll rate was  $+0.3$  radians per second and occurred at  $0.4$  seconds, and the peak yaw rate was  $+0.11$

radians per second and occurred at 0.4 seconds. The entire Apollo 14 touchdown dynamics were arrested in less than 1.5 seconds.

Figures 24, 25, and 26 show that the Lunar Module predominate rotational motions were in the roll and yaw axes. The pitch rate, by comparison, was smaller.

Digital simulations of the Apollo 14 landing indicated that the -Y footpad was the first to make contact with the lunar surface, followed by the -Z footpad approximately 0.4 seconds later. The simulation also revealed that all primary strut strokes and secondary strut strokes were less than 1 inch, which indicated that the touchdown energies of the Lunar Module were absorbed primarily by the lunar surface soil.

The landing gear energy absorption and landing stability performance were well within the design envelope.

Figure 27 is a view of the Apollo 14 Lunar Module -Z landing gear located in the lower right-hand side of the photograph.

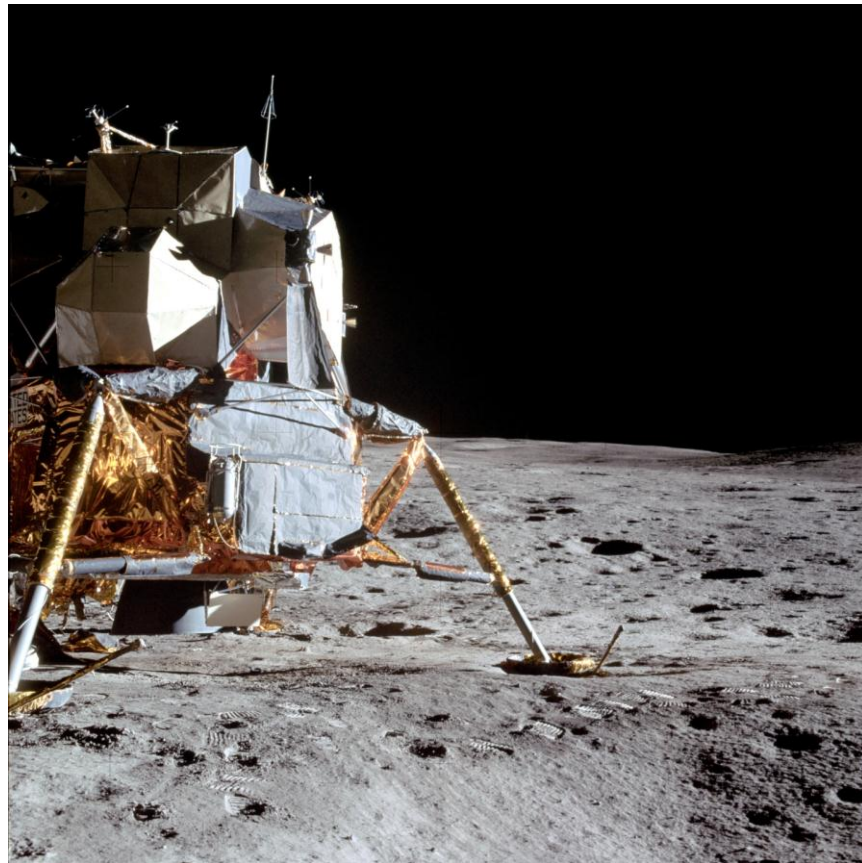


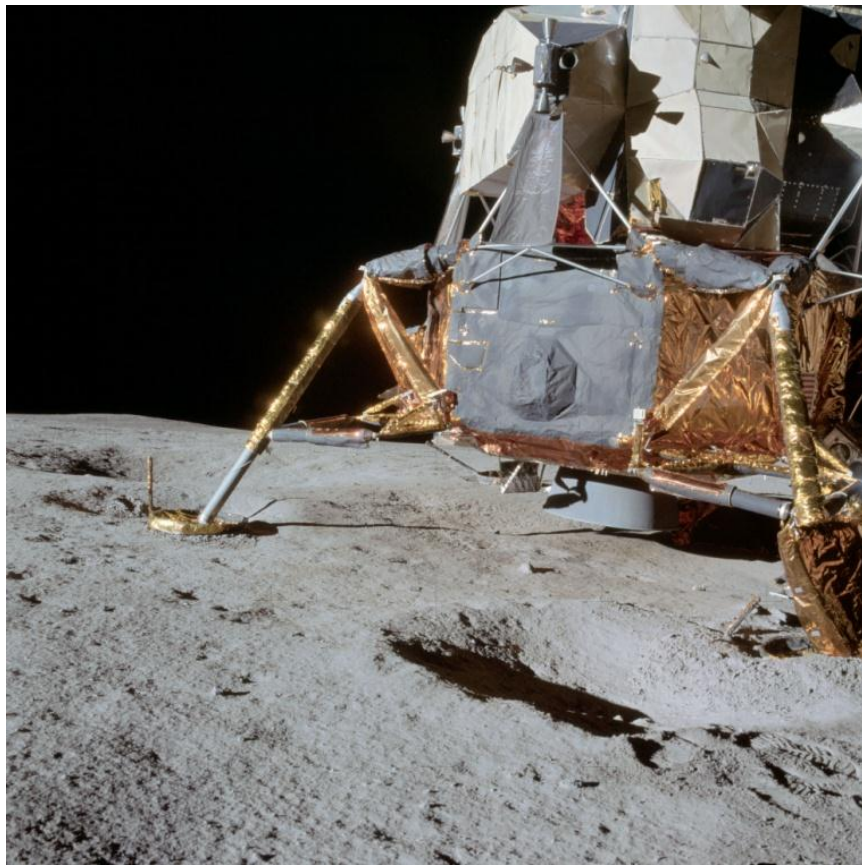
**Figure 27. (NASA Photograph AS14-66-09278) View of -Z landing gear and footpad located to right side of Lunar Module.** The local lunar surface was computed to be 7.1 degrees with the -Y footpad being on the downhill side. The sink speed was 3.1 feet per second and the planar velocity was 2.4 feet per second at 45 degrees in the +Y and +Z axes direction.

This view of the  $-Z$  footpad shows very little footpad penetration into the lunar surface—less than 3 inches. At the time of footpad contact, the  $-Z$  footpad was translating approximately parallel to the line connecting the  $-Z$  footpad and the  $+Y$  footpad (from right to left in the photograph).

The clearance between the descent engine nozzle and the lunar surface was on the order of 14 inches. The descent engine nozzle did not make contact with the lunar surface during the landing maneuver.

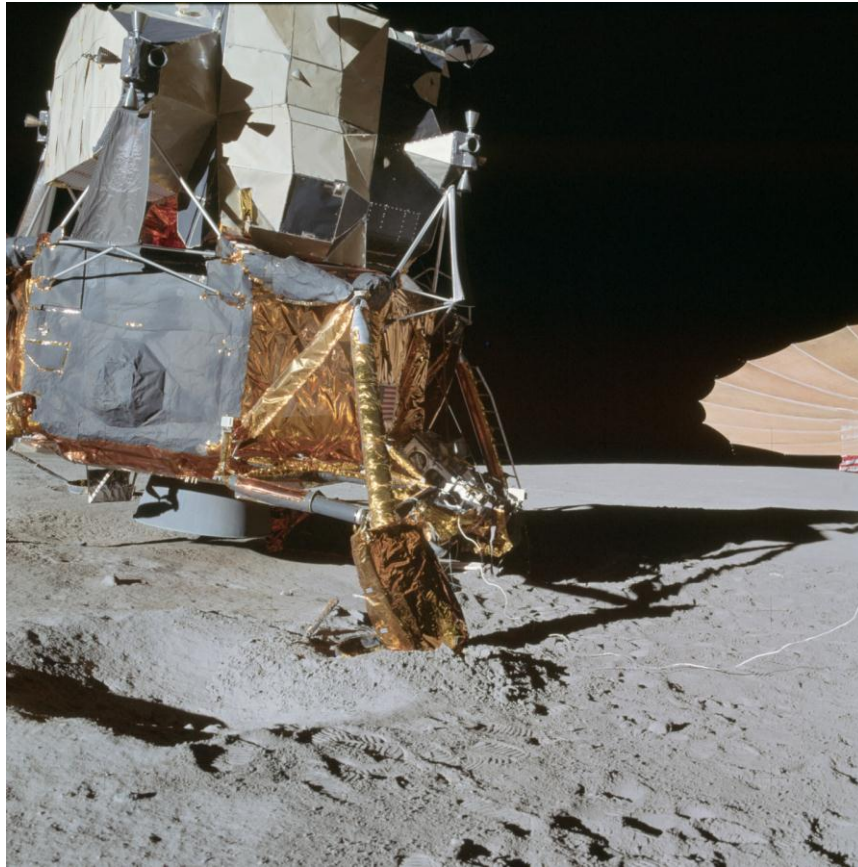
The astronaut boot penetration patterns, located just below the  $-Z$  footpad, are similar to those of the Apollo 11 landing site with regard to depth of penetration and cohesiveness of the lunar soil (reference boot print photograph in Appendix B, photograph 4B, *NASA Photograph AS11-40-5878*). Also, the penetration patterns of the  $-Y$  and  $-Z$  footpads are similar to Apollo 11 footpad imprints. This implies that the lunar surface bearing strength at the Apollo 14 landing site was approximately the same as that at the Apollo 11 landing site.

Figure 28 shows the Apollo 14 Lunar Module—the Antares—resting on the lunar surface. This view is of the  $-Z$ ,  $+Y$  quadrant. The lunar crater, located in the lower right-hand side of the photograph, is estimated to be on the order of 20 feet in diameter, with an associated maximum depth ranging from 2 to 4 feet.



**Figure 28. (*NASA Photograph AS14-66-09254*) View of  $-Z$  landing gear, located in left side of photograph; and the  $+Y$  landing gear, located in lower-right side. This view is looking downhill with respect to the 7.1-degree local slope.**

Figure 29 shows the Apollo 14 Lunar Module resting on the lunar surface with the +Y landing gear located in the lower center. The flight path at the time the initial footpad contact was 45 degrees right of forward.



**Figure 29. (NASA Photograph AS14-66-09255) View of +Y landing gear, located in lower center of photograph; and the +Z landing gear, located in Lunar Module shadow to the right.**

This photograph displays a view of the +Y landing gear. The +Y footpad is obscured by the lunar soil buildup. The + Z landing gear (the primary strut with the ladder) is shown on the right. This photograph also offers a clear view of the descent engine nozzle—the clearance between the nozzle and the lunar surface is visible, and is estimated to be about 14 inches. Again, this indicates that the descent engine nozzle did not make contact with the lunar surface during the landing maneuver.

It is noted that some of these photographs of the Lunar Module **can** give an optical illusion of landing downhill when the local lunar slope is just the opposite, such as in photographs 28 and 29.

Views of the +Y, +Y, -Y, -Y, -Z, -Z, and -Z, respectively, of the Apollo 14 Lunar Module landing gear footpads are shown in the following photographs (Figures 30, 31, 32, 33, 34, 35, and 36).

Figure 30 offers a close-up view of the Apollo 14 Lunar Module +Y footpad.



**Figure 30. (NASA Photograph AS14-66-09234) View of +Y footpad showing footpad penetration and some soil buildup in the direction of motion.**

The +Y footpad is visible in this photograph . The footpad penetration into the lunar soil was more than 6 inches, which is deeper than the footpad penetrations into the lunar soil for either the Apollo 11 or the Apollo 12 landing.

The translation of the +Y footpad during the landing is estimated to be less than 10 inches. Photographic analysis of the +Y footpad penetration pattern indicated more of a “plowing” action than on previous landings. This implies that the simplified soil dynamic model used in the Apollo 11 landing dynamic simulation may not be appropriate for predicting the lunar soil forces acting on the +Y footpad.<sup>‡</sup>

The –Y and –Z footpad penetration patterns are very similar to the penetration patterns of the Apollo 11 and 12 landing gear footpads.

---

<sup>‡</sup> A more sophisticated Lunar Module footpad/soil interactive model might be more appropriate in this landing case, such as the footpad/soil interaction model reported in Reference 6, "Anon. Lunar Module (LM) Soil Mechanics Study. Final Report. Rept. AM-68-1, Energy Controls Division, Bendix Corporation, May 1, 1968."

Figure 31 shows a view of the trailing edge of the Apollo 14 Lunar Module +Y footpad.



**Figure 31. (NASA Photograph AS14-66-09235) View of +Y footpad showing contact probe and trailing edge the footpad.** The sink speed was 3.1 feet per second and the planar velocity was 2.4 feet per second at a 45-degree angle between the +Y and +Z axes.

The +Y footpad and the initial contact point the lunar surface contact probe are shown in this photograph. The probe contact point is located in the upper left-hand corner. The initial contact by the probe was on the order of 50 inches from the final resting position of the +Y footpad.

This photographic view of the +Y footpad also indicates that the footpad penetrated the lunar surface by more than 6 inches.

Figure 32 provides a closeup view of the Apollo 14 Lunar Module -Y footpad.



**Figure 32. (NASA Photograph AS14-66-09269) View of -Y footpad showing initial contact footpad pattern and subsequent footpad translation. Some lunar soil buildup in the direction of the footpad motion is noted.**

At the time of footpad contact, the -Y footpad was translating from left to right (in the photograph), or approximately 45 degrees with respect to the -Y landing gear strut shadow. This photograph indicates that the -Y footpad penetration into the lunar soil was less than 3 inches, and that a skid distance was on the order of 5 to 10 inches.

Figure 33 provides a closeup view of the Apollo 14 Lunar Module -Y footpad.



**Figure 33. (NASA Photograph AS14-66-09270) View of -Y footpad showing lunar soil buildup on footpad in the direction of the footpad translational motion.**

The -Y footpad would have been translating diagonal down (in the photograph), or about 45 degrees rotated to the right of the -Y landing gear strut shadow. This photograph shows some buildup of lunar soil on the leading edge of the footpad, and also indicates that the footpad penetration into the lunar soil was less than 3 inches.

Figure 34 is a closeup view of the Apollo 14 Lunar Module -Z footpad.

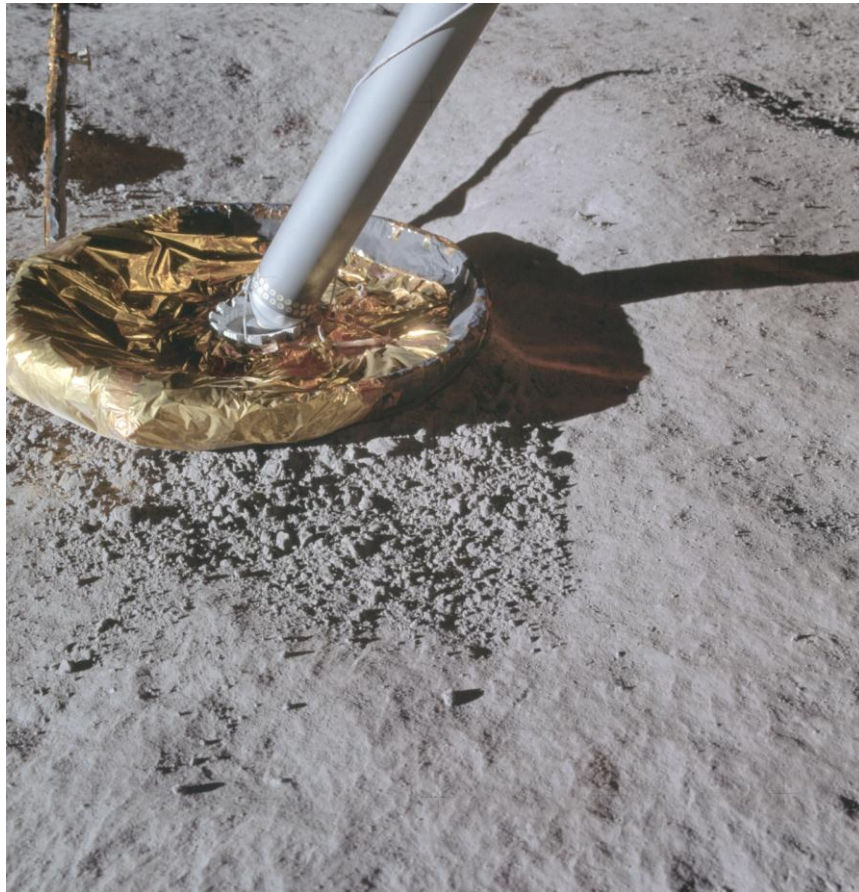


**Figure 34. (NASA Photograph AS14-66-09264) View of -Z footpad showing footpad penetration and some soil buildup in the direction of initial footpad motion.**

Lunar soil buildup along the leading edge of the -Z footpad is visible in this view. The photograph also indicates that the footpad penetration was less than 3 inches.

Figure 35 shows a view of the Apollo 14 Lunar Module  $-Z$  footpad, looking approximately in the  $-Y$  direction.



**Figure 35. (NASA Photograph AS14-66-09265) View of  $-Z$  footpad showing the contact probe.**

This photograph indicates that the initial contact of the contact probe with the lunar surface was close to the center of a small lunar crater, visible in the upper left corner. The distance between the final resting position of the center of the  $-Z$  footpad and the initial probe contact point was approximately 18 inches. This photograph indicates that the footpad penetration into the lunar surface was less than 3 inches.

#### **7.4.1 Summary: Apollo 14 Lunar Module Landing**

Lunar dust was detected at an altitude of 110 feet; however, this was not detrimental to landing visibility during the final descent.

The Apollo 14 landing touchdown velocities—3.1 feet per second sink speed and 2.4 feet per second translational speed—were well within the touchdown design envelope. Also, the rotational rates at touchdown were well within the design envelope. The landing surface slope was computed to be 7.1 degrees—well under the 12-degree slope design condition for the landing system. From the crew point of view at the time of landing gear touchdown, the horizontal velocity vector would be about 45 degrees to the right of forward.

The photographs indicate that footpad penetration was typically less than 3 inches except for the +Y footpad penetration, which was on the order of 6 inches. This footpad penetration depth was greater than the footpad penetrations on Apollo 11 and 12. The skid distances after footpad contact was on the order of 3 inches.

The analysis indicated that the descent engine nozzle did not make contact with the lunar surface during the landing maneuver.

The landing gear energy absorption and landing stability performance were well within the design envelope.

The +Y landing gear footpad showed more “plowing” action than on the Apollo 11 and 12 landings. The simplified lunar soil model used in the Apollo 11 landing dynamic simulation **may not** be appropriate for predicting the lunar soil/footpad interaction forces acting on the +Y landing gear footpad.

Except for the +Y landing footpad, the landing gear footpad penetration patterns were similar to those at the Apollo 11 landing site. It is inferred that the static bearing strength of the lunar soil was approximately the same as that of the Apollo 11 landing site.

### **7.5 Apollo 15 Lunar Landing**

The Apollo 15 Lunar Module landed on July 30, 1971, at the Hadley Rille located at 26°, 7', 56.0" N and 3°, 38', 1.9" E, with astronaut David R. Scott as Lunar Module commander, and astronaut James B. Irwin as pilot.

During final descent, several mid-course corrections essentially re-designated the desired landing point. The final landing site was approximately 1100 feet from the initial targeted point. Interaction between the descent engine plume and the lunar surface that would have produced lunar dust was not noted.

The Apollo 15 touchdown was the most dynamic of all prior landings. Touchdown kinetic energy was 70 percent higher than Apollo 14 and approximately 6 times the touchdown kinetic energy of Apollo 11 landing. Apollo 15 was the first landing to have the 10-inch extended descent engine nozzle and the first Lunar Module to carry a Lunar Rover Vehicle on board.

During the landing maneuver, the descent engine nozzle buckled. The buckling was attributed to a buildup pressure in the nozzle due to thrusting in close proximity of the lunar surface, and was **not due to the nozzle making contact with the lunar surface**. The clearance between the nozzle exit plane and the lunar surface remained positive during the landing maneuver.<sup>16</sup>

The Apollo 15 lunar landing was, by far, the most dynamic of the Apollo landings up until now. The Apollo 15 Lunar Module had the highest touchdown kinetic energy of Apollo 11, 12, and 14. Also, the Apollo 15 landing occurred on the steepest lunar slope, which in this case was 11 degrees.

Figure 36 shows a view of the Apollo 15 Lunar Module descent engine buckled nozzle.

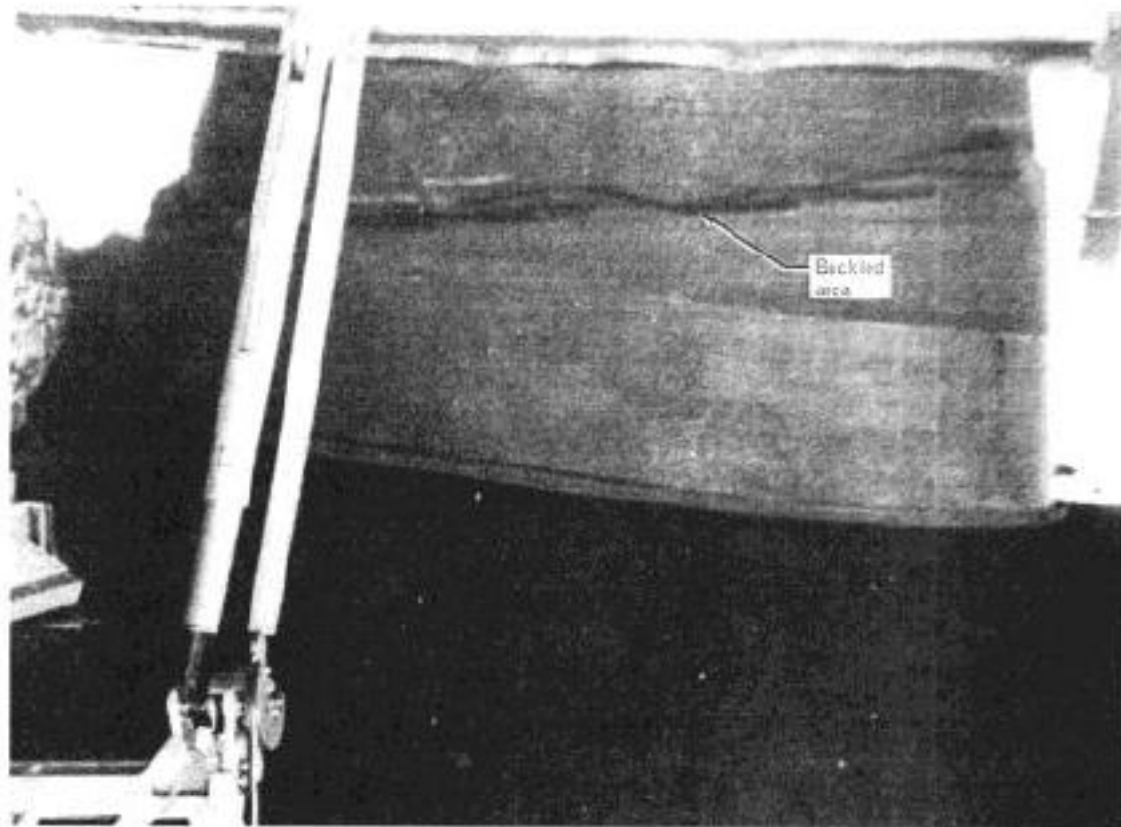


**Figure 36. Apollo 15 Lunar Module descent engine buckled nozzle.**<sup>16</sup>

The introduction of the Lunar Rover Vehicle greatly improved the range of lunar exploration of the astronauts on the lunar surface. The rover weighed about 1200 pounds (Earth) and had a range on the order of 20 miles. The longest single trip for the Apollo 15 astronauts in the rover was about 8 miles.

The Apollo 15 landing was within the design touchdown velocity envelope. The sink speed at the time of first footpad contact was 6.8 feet per second, with an associated horizontal velocity of 1.2 feet per second in the +Y direction and 0.6 feet per second in the +Z direction. From the crew point of view, the horizontal velocity vector would be about 63 degrees to the right of forward.

The Apollo 15 Lunar Module pitch, roll, and yaw rate time histories during the touchdown dynamic maneuver are presented in Figures 37, 38, and 39, respectively. Composite body rates as a function of time are shown in Figure 40.

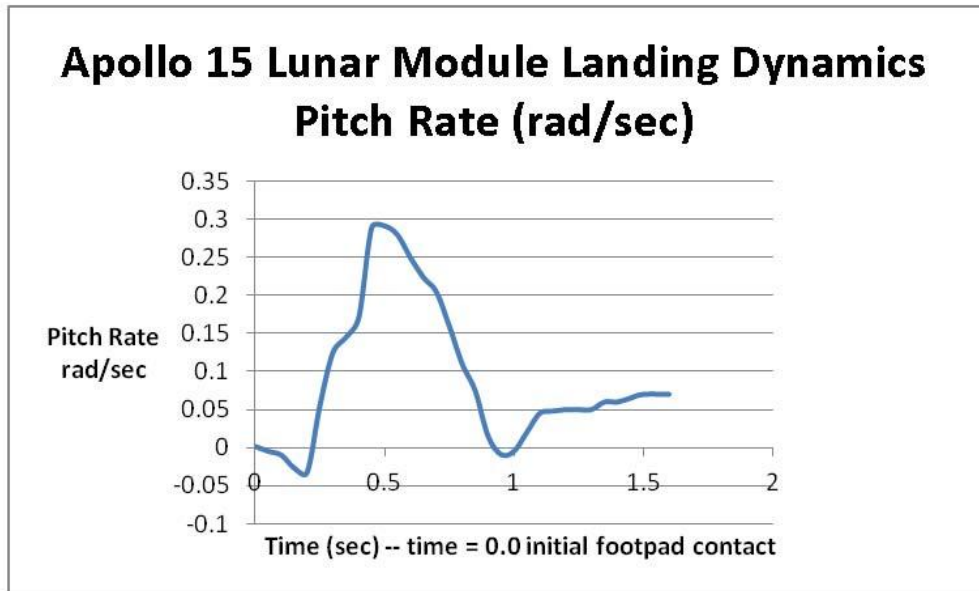


**Figure 37. Apollo 15 Lunar Module pitch rate as a function of time.** The pitch rate data were derived from the Lunar Module on-board guidance computer.

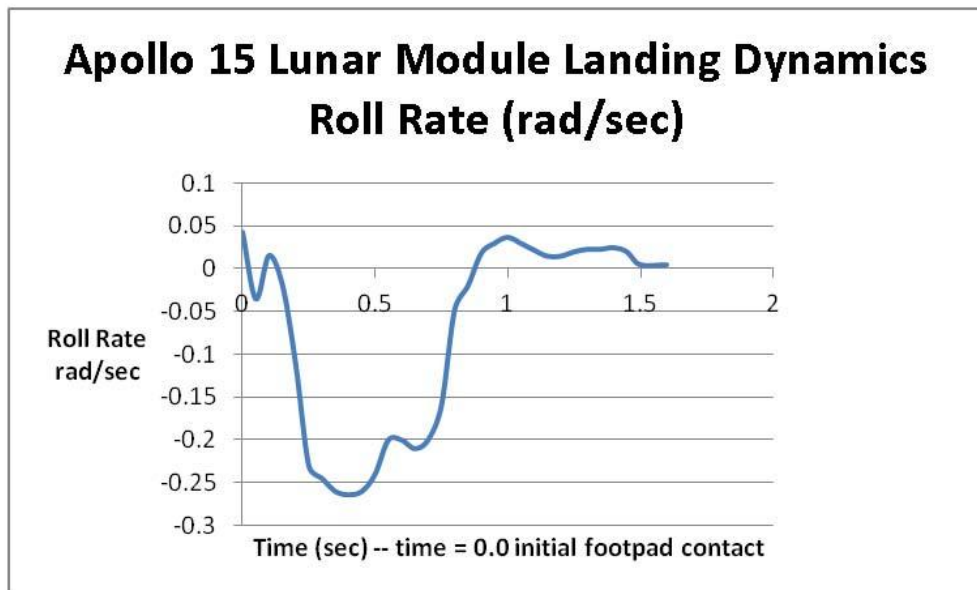


**Figure 38. Apollo 15 Lunar Module roll rate as a function of time.** The roll rate data were derived from the LM on-board guidance computer.

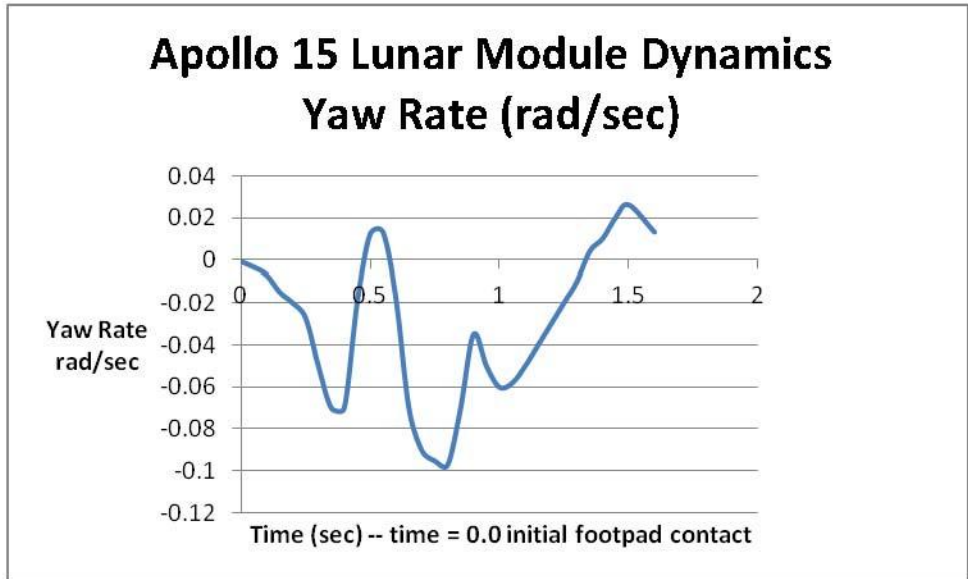


**Figure 39. Apollo 15 Lunar Module yaw rate as a function of time.** The yaw rate data were derived from the Lunar Module on-board guidance computer.

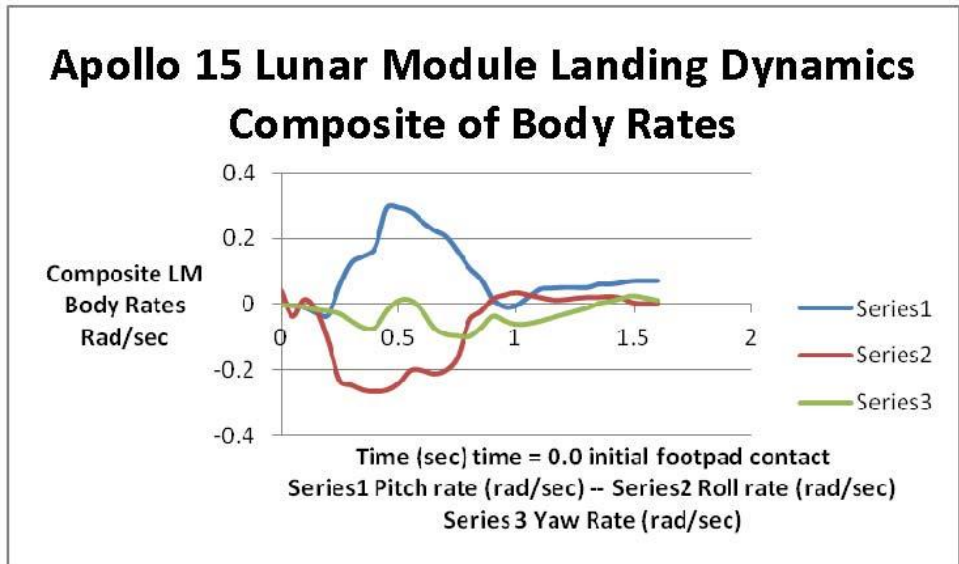


**Figure 40. Apollo 15 Lunar Module composite body rates as a function of time.** (Note: LM = Lunar Module)

During the landing maneuver, data from the on-board computer indicated that the peak pitch rate was  $+0.29$  radians per second and occurred approximately 0.5 seconds after initial footpad contact. Also, the peak roll rate was  $-0.26$  radians per second and occurred at 0.4 seconds, and the peak yaw rate was  $-0.10$  radians per second and occurred at 0.8 seconds. The final at-rest attitudes were 6.9 degrees in pitch up and 8.6 degrees in roll down. The yaw attitude was assumed to be zero. Based on these data, the local landing slope was computed to be 11 degrees. The landing gear system was designed to land on slopes up to 12 degrees.

Digital simulations of the Apollo 15 landing indicated that the landing gear +Y footpad and the +Z footpad made lunar surface contact nearly simultaneously. The digital simulation also indicated that each of the landing gear primary struts stroked 1.0 inch except for the +Z primary strut, which stroked 3.0 inches, and that the +Z landing gear footpad was off the landing surface in the final at-rest position. The astronauts reported that the Lunar Module did not teeter while they ascended or descended the +Z landing gear ladder or during on-board internal activities, and also reported that the +Z landing gear footpad could be rotated about the footpad attachment ball joint.

The landing gear energy absorption and landing stability performance were within the design envelope.

Figure 41 is a view of the Apollo 15 Lunar Module—the Falcon—resting on the lunar surface.



**Figure 41. (NASA Photograph AS15-86-11600) The +Y, +Z quadrant of Apollo 15 Lunar Module resting on lunar surface.** The sink speed was 6.8 feet per second and the planar velocity was 1.3 feet per second at a 67-degree angle to the right of the +Z axis.

This photograph shows the inclination of the Z axis with respect to the lunar surface. The lunar slope was computed to be 11 degrees, with the  $-Y$  and  $-Z$  footpads located on the downhill side.

Figure 42 is a view of the Apollo 15 Lunar Module resting on the lunar surface, and shows the  $+Y$ ,  $-Z$  quadrant.



**Figure 42. (NASA Photograph AS15-87-11818) The  $+Y$ ,  $-Z$  quadrant of Lunar Module resting on lunar surface.**

In this photograph, the  $+Y$  landing gear is situated to the extreme right. The landing gear  $+Z$  footpad is positioned to the right of  $+Y$  landing gear footpad and is not visible. This photograph also illustrates the steepness of the 11-degree lunar slope.

Figure 43 is a view of the  $-Y$ ,  $-Z$  quadrant of Apollo 15 Lunar Module resting on the lunar surface.

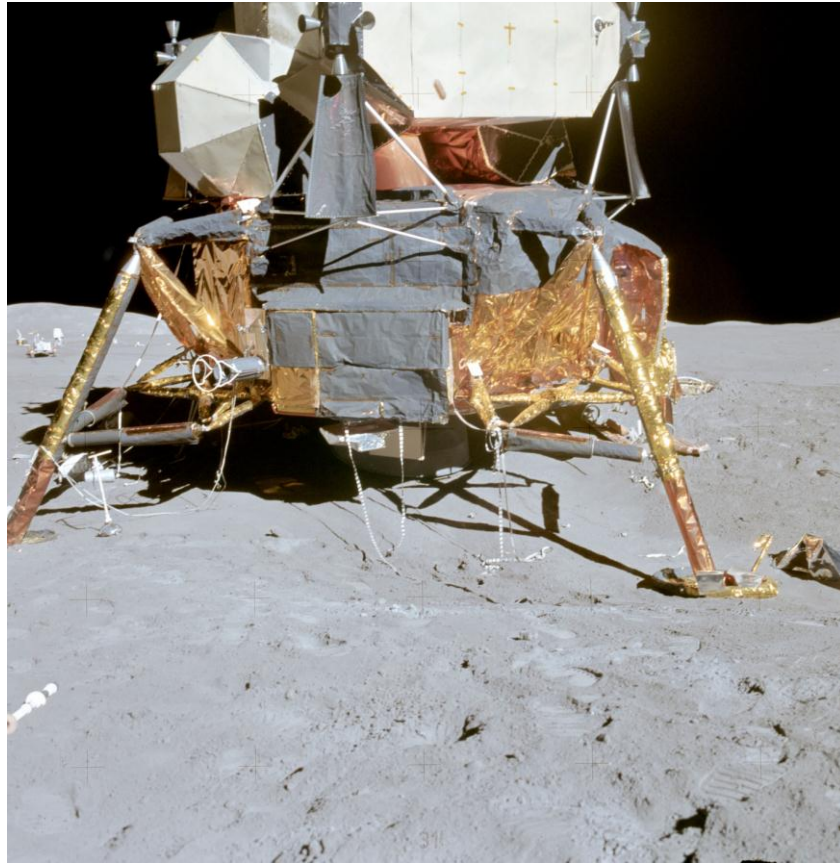


**Figure 43. (NASA Photograph AS15-87-11839) The  $-Y$ ,  $-Z$  quadrant of Lunar Module resting on lunar surface. The  $-Z$  landing gear and footpad is located in the lower right-hand corner.**

This photograph shows the  $-Z$  footpad resting on the lunar surface. The  $-Z$  footpad penetration into the lunar surface was estimated to be less than 3 inches.

Descent engine nozzle clearance was estimated to be approximately 6 inches. The descent engine nozzle did not make contact with the lunar surface during the landing maneuver; however, the nozzle did buckle due to the increase in nozzle pressure caused by the engine thrust in close proximity to the lunar surface.

Figure 44 offers a view of the of the Apollo 15 Lunar Module and the Lunar Rover Vehicle (located in the right-hand side of the photograph).



**Figure 44. (NASA Photograph AS15-82-11601) Lunar Module and Lunar Rover Vehicle resting on lunar surface.**

The Lunar Rover Vehicle allowed the astronauts considerable increase in range of exploration. The four-wheeled vehicle could carry two astronauts a range on the order of 20 miles, and had a weight on the moon of about 200 pounds.

Figure 45 is a view of an Apollo 15 astronaut boot print in the lunar soil.

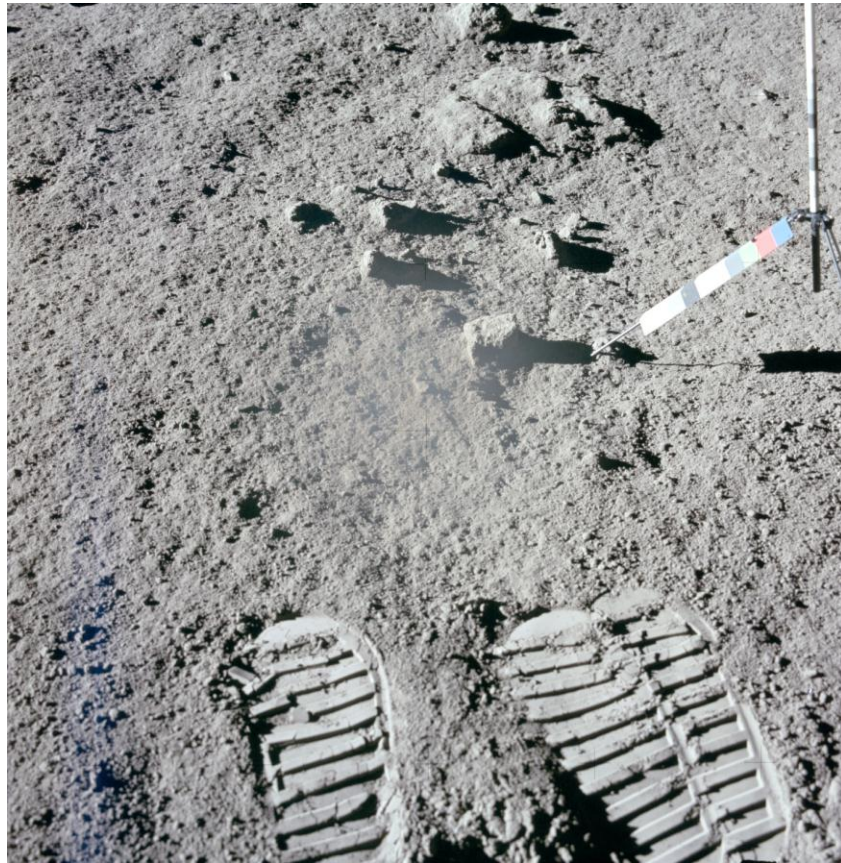


**Figure 45. (NASA Photograph AS15-82-11534) Apollo 15 astronaut boot print.**

It is noted that the footpad penetration and astronaut boot penetration patterns at the Apollo 15 landing site were similar to that of the Apollo 11 landing site with regard to depth of penetration and cohesiveness of the lunar soil (reference boot print photograph in Appendix B, photograph 4B, *NASA Photograph AS11-40-5878*). This implies that the lunar surface mechanical properties at the Apollo 15 landing site were approximately the same as those at the Apollo 11 landing site.

### **7.5.1 Summary: Apollo 15 Lunar Module Landing**

No lunar dust was reported during descent. Therefore, the visibility of the landing site was not seriously degraded.

Apollo 15 Lunar Module landing proved to be the most dynamic of all of the previous landings. The touchdown kinetic energy was the highest of any previous landings by 70 percent. The landing touchdown velocities—6.8 feet per second sink speed and 1.3 feet per second translational speed—were within the touchdown design envelope. The landing lunar surface slope was 11 degrees, which was within the design envelope of 12 degrees. The rotational rates at touchdown were well within the design envelope.

From the crew point of view, at the time of landing gear touchdown, the horizontal velocity vector would be about 67 degrees to the right of forward.

The photographs indicate that footpad penetration was less than 3 inches, and that a skid distance after footpad contacts points was on the order of inches.

The landing gear energy absorption and landing stability performance were well within the design envelope.

Although the descent engine nozzle did buckle, the cause was not due to contact with the lunar surface during the touchdown maneuver, but rather to an increase in nozzle pressure from the descent engine thrusting in close proximity of the lunar surface.

The lunar surface mechanical properties were approximately the same as those at the Apollo 11 landing site.

## **7.6 Apollo 16 Lunar Landing**

The Apollo 16 Lunar Module landed on April 21, 1972, in the Descartes Highlands located at 8°, 52', 22.8" S and 15°, 30', 0.7" E, with astronaut John W. Young as commander, and astronaut Charles M. Duke, Jr. as pilot.

The Lunar Module landed about 900 feet from the original lunar surface target point. Small traces of lunar dust were noted during final descent at an altitude of about 80 feet. The intensity of dust increased until final touchdown; however, this increase did not jeopardize landing safety. Visibility was sufficient to avoid small craters and boulders at the targeted landing site.

The sink speed at the time of first footpad contact was 5.6 feet per second. The horizontal velocity was negligible. The descent engine thrust was terminated approximately 1.0 second after the surface probe contact light was activated.<sup>17</sup>

The final resting attitude was + 2.5 degrees in pitch, and negligible roll and yaw angles. The lunar landing site slope was derived from on-board computer data, which indicated that the local surface slope was 2.5 degrees. The astronauts stated that it was difficult to estimate the magnitude of local slopes in the area. However, they did state that when landing in any area 80 feet from the actual landing site, the local slopes could range in the area of 6 to 10 degrees.

The touchdown velocities and landing slope were well within the landing gear design envelope.

Figure 46 offers a view of the Apollo 16 Lunar Module—the Orion—resting on the lunar surface. The Lunar Rover Vehicle is shown on the right.

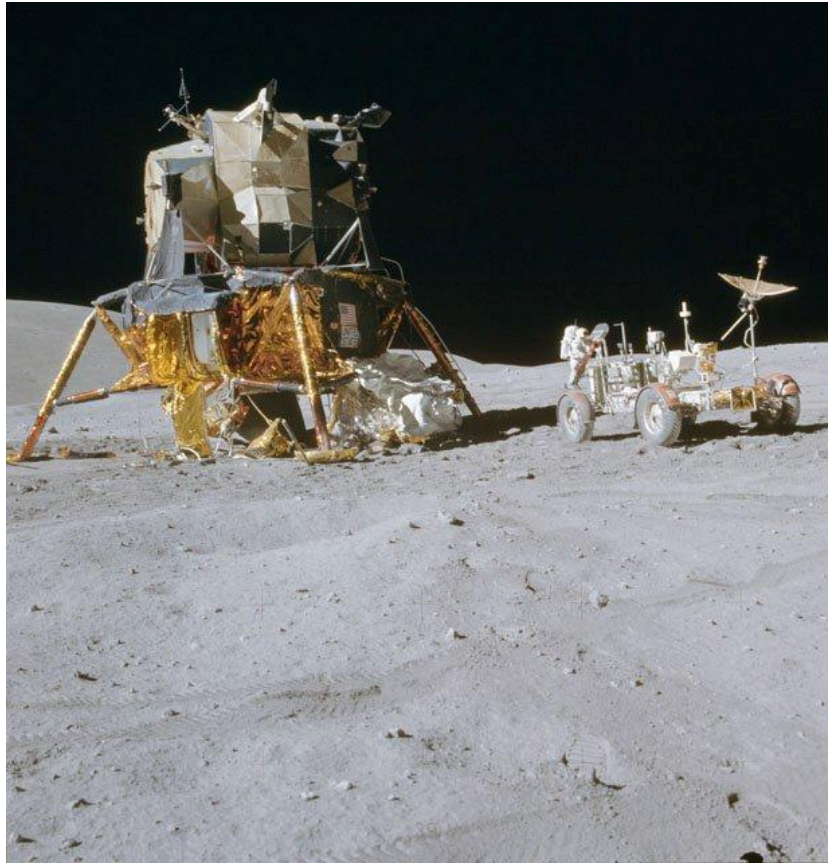


**Figure 46. (NASA Photograph AS16-107-17437) Apollo 16 Lunar Module and Lunar Rover Vehicle resting on lunar surface.** The sink speed was 5.6 feet per second; the planar velocity was negligible. The local slope was computed to be 2.5 degrees with the +Z footpad located on the uphill side.

This photograph shows a view of the Lunar Module looking down the  $-Y$  axis. The  $+Y$  landing gear is located in the center of the Lunar Module, the  $+Z$  landing gear is located to the right of the Lunar Module, and the  $-Z$  landing gear is located to the left.

Apollo 16 was the second mission to carry a Lunar Rover Vehicle, which gave astronauts a considerable increase in range of lunar surface exploration.

Figure 47 offers a similar view of the Apollo 16 Lunar Module resting on the lunar surface.



**Figure 47. (NASA Photograph AS16-107-17435) View of Apollo 16 Lunar Module showing the descent engine nozzle clearance between nozzle exit plane and lunar surface.**

An amplification of this photograph shows the descent engine nozzle clearance to be less than 6 inches. No nozzle buckling during the landing maneuver was noted. Static clearance for the undeformed landing system between the nozzle exit plane and the bottom of the landing gear footpads was 8.5 inches.

During the landing maneuver, the descent engine nozzle did not make contact with the lunar surface. There was no evidence of the descent engine nozzle buckling during the landing maneuver.

Figure 48 provides a closeup view of the Apollo 16 Lunar Module –Y footpad and landing gear struts.

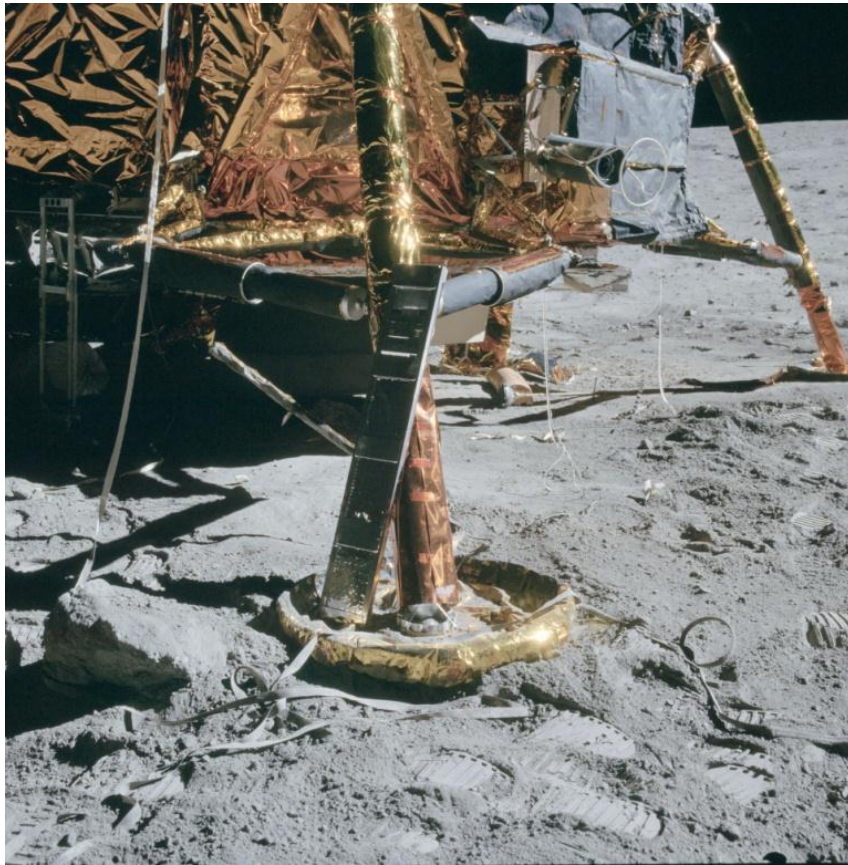


**Figure 48. (NASA Photograph AS16-107-17441) The –Y footpad and landing gear strut.** The –Z landing gear is shown in the right center. The sink speed was 5.6 feet per second; planar velocity was negligible.

A boulder, located adjacent to the –Y footpad, measured approximately 36 inches across and less than a foot in height above the lunar surface. The landing gear footpad was connected to the primary strut via a ball joint, which was surrounded by honeycomb energy-absorbing material. It was judged that if the footpad landed on top of the boulder, the landing gear system would have sufficient mobility and energy-absorbing capability to prevent any damage to the structure.

The –Y footpad penetration into the lunar soil was less than 3 inches. The skid distance of the footpads after lunar surface contact was negligible.

Figure 49 offers a view of the Apollo 16 Lunar Module  $-Y$  landing gear facing the  $-Z$  directions.

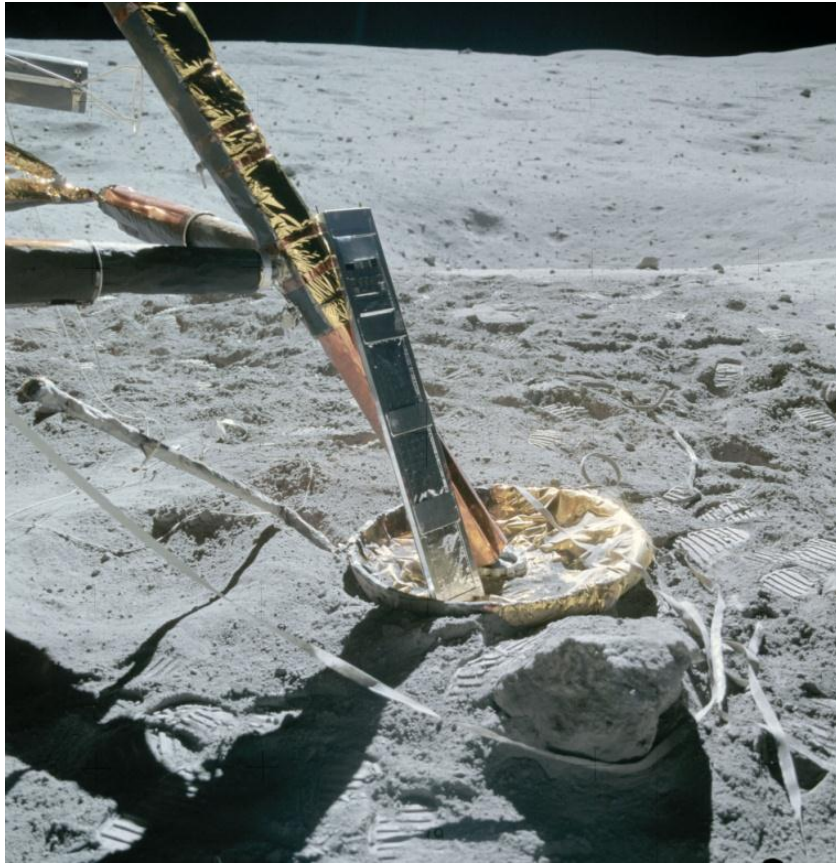


**Figure 49. (NASA Photograph AS16-107-17442) The  $-Y$  landing gear struts and footpad.**

This photograph shows the absence of soil buildup around the perimeter of the footpad, indicative of a vertical landing with little or no horizontal velocity.

Photographic analysis of the post-landing configuration and the on-board instrumentation indicated that during the touchdown maneuver, the landing gear stroking was negligible in absorbing the touchdown kinetic and potential energies. From a standpoint of landing stability and landing gear energy absorption, landing dynamics were well within the design envelope.

Figure 50 is a view of a lunar rock and an Apollo 16 astronaut boot print.



**Figure 50. (NASA Photograph AS16-107-17451) View of lunar rock and an astronaut boot print in the lunar soil.**

It is noted that the footpad penetrations and astronaut boot print pattern at the Apollo 16 landing site are similar to those of the Apollo 11 landing site with regard to depth of penetration and cohesiveness of the lunar soil (reference boot print photograph in Appendix B, photograph 4B, *NASA Photograph AS11-40-5878*). This implies that the lunar surface mechanical properties at the Apollo 16 landing site were approximately the same as those at the Apollo 11 landing site.

### **7.6.1 Summary: Apollo 16 Lunar Module Landing**

No lunar dust was reported during final descent. Therefore, landing site visibility was not compromised.

Apollo 16 Lunar Module touchdown dynamics were very benign. Landing touchdown velocities were 5.6 feet per second sink speed, and the translational speed was negligible. Landing velocities were well within the design envelope. The landing lunar surface slope was 2.5 degrees, which was within the design envelope of 12 degrees. The rotational rates at touchdown were also well within the design envelope.

From the crew point of view, at the time of landing gear touchdown, the horizontal velocity was negligible.

The photographs indicate that footpad penetrations were less than 3 inches, and that the footpad skid distances were negligible.

The landing gear energy absorption and landing stability performance were well within the design envelope.

The lunar surface mechanical properties were approximately the same as those at the Apollo 11 landing site.

## **7.7 Apollo 17 Lunar Landing**

The Apollo 17 Lunar Module landed on December 11, 1972, at the Taurus Littrow located at 20°, 1', 26.9" N and 30°, 46', 18.7" E, with astronaut Eugene A. Cernan as Lunar Module commander and astronaut Harrison H. Schmitt as pilot.

During final descent, it was determined that the targeted landing site was not the ideal place to land. The re-designated landing site was about 1000 feet from the initial targeted site. The Lunar Module went into manual control at an altitude of about 300 feet. Lunar dust, caused by the descent engine plume and lunar surface interaction, was encountered at an altitude of about 70 feet; however, this was not a detrimental factor in landing visibility.

The touchdown sink speed was 3.0 feet per second, and the lateral or planar velocities were negligible. The final at-rest attitudes were +5.3 degrees in pitch, -2.6 degrees in roll, and negligible in yaw. Based on the at-rest attitude, the effective lunar landing site slope was 5.9 degrees, which would include any local landing gear footpad depression, such as being in a crater, plus the local slope.<sup>18</sup>

The Apollo 17 landing velocities were within the design touchdown velocity envelope. The amount of the touchdown kinetic and potential energies absorbed by the landing gear system was negligible and well within the landing gear design envelope. The landing dynamics were benign and within the design touchdown stability envelope.

Figure 51 is a view of the Apollo 17 Lunar Module—the Challenger—resting on the lunar surface.

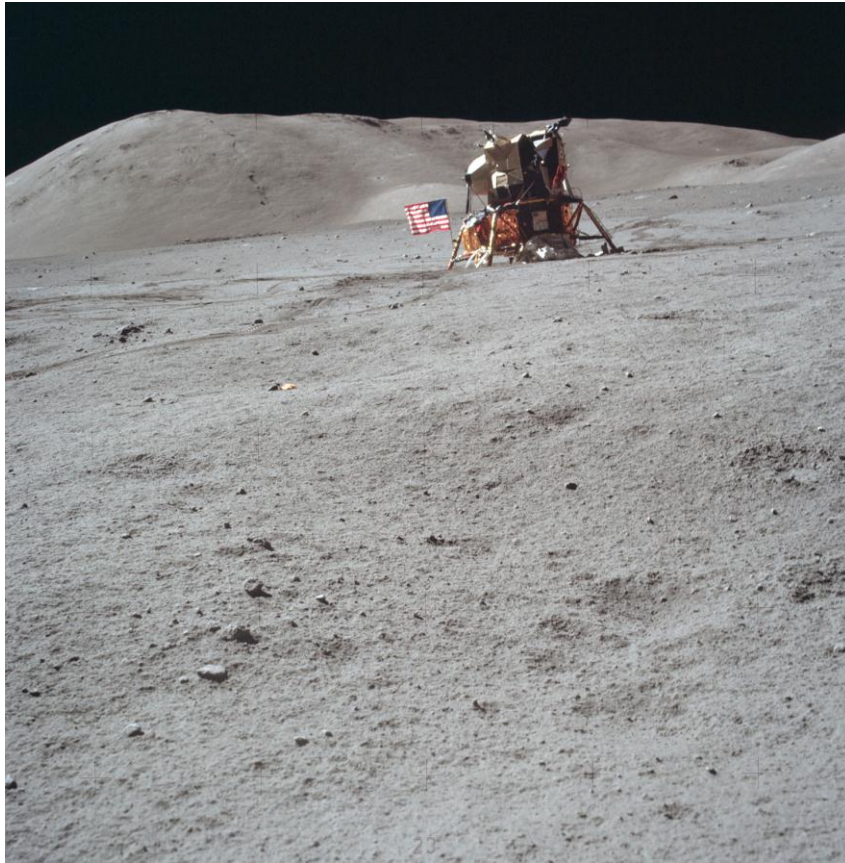


**Figure 51. (NASA Photograph AS17-134-20511) Lunar Module resting on lunar surface.** The local effective slope was computed to 5.9 degrees with the +Z landing gear footpad resting on the uphill side.

The Apollo 17 Lunar Module +Z landing gear is located to the right and "uphill" in the photograph. The –Z landing gear and the US flag are located to the left.

Figure 52 offers a close-in view of the Apollo 17 Lunar Module resting on the lunar surface.

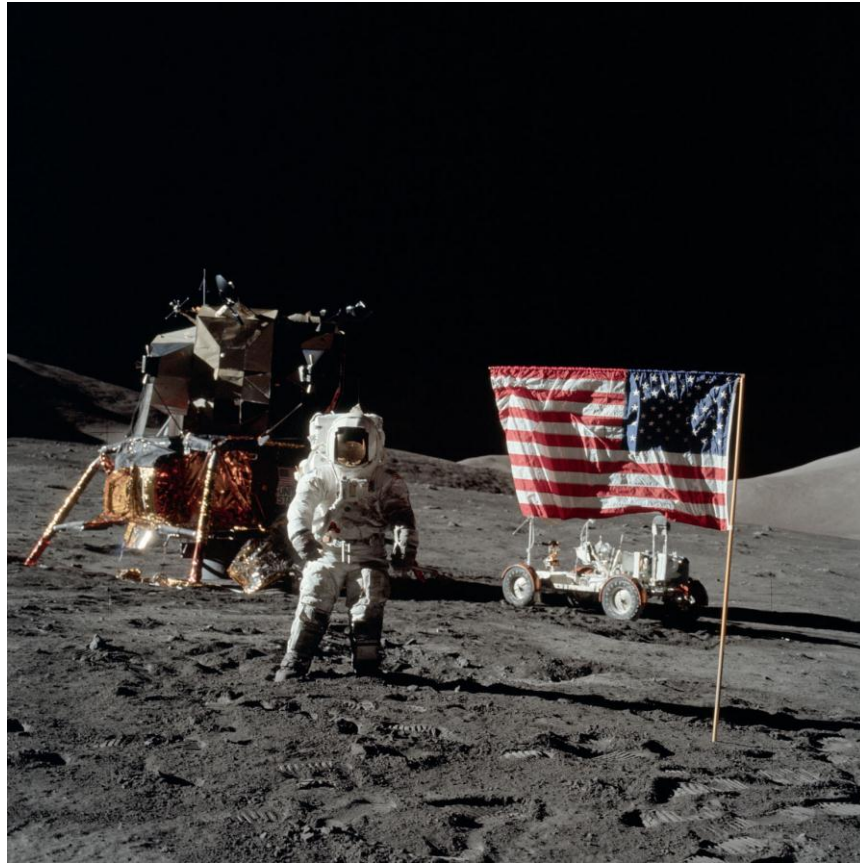


**Figure 52. (NASA Photograph AS17-134-20382) Lunar Module resting on lunar surface.** The +Y landing gear is located to the left of the astronaut. The +Z landing gear footpad is resting on the uphill side.

The US flag and the Lunar Rover Vehicle (pictured beneath the flag) are visible in this photograph. The descent engine nozzle is located behind the +Y landing gear. The clearance between the lunar surface and the engine nozzle exit plane is about 6 inches. There was no evidence of the buckling of the descent engine nozzle.

Figure 53 is a view of the Apollo 17 Lunar Module –Z landing gear with the –Z landing gear footpad resting at the bottom of a small lunar crater.



**Figure 53. (NASA Photograph AS17-134-20388) The –Z landing gear struts and footpad.**

The –Z landing gear footpad is resting at the bottom of a lunar crater that is estimated to be 5 feet in diameter, approximately 10 inches in depth, and would have contributed to about a 2- to 3-degree increase in the effective landing site slope. Correcting for this, the local lunar slope at the landing site would be about 3 degrees.

The footpad penetration into the lunar soil was less than 3 inches. Another sizable crater can be seen in the upper right-hand corner of the photograph. That crater was estimated to be 15 feet in diameter. A smaller crater and some rocks were also in the vicinity of the –Z footpad.

Photographic analysis of the Apollo 15 configuration and the on-board instrumentation indicated the landing gear stroking was negligible during the touchdown maneuver. From a touchdown dynamics standpoint, the landing stability and landing gear energy absorption were well within the design envelope.

Figure 54 is a view of the Apollo 17 astronaut boot print in the lunar soil.



**Figure 54. (NASA Photograph AS17-134-20432) Astronaut's boot print in lunar soil.**

It is noted that the footpad penetration and astronaut boot penetration patterns at the Apollo 17 landing site were similar to those at the Apollo 11 landing site with regard to depth of penetration and cohesiveness of the lunar soil (reference the Apollo 11 astronaut boot print photograph in Appendix B, photograph 4B, *NASA Photograph AS11-40-5878*). This implies the lunar surface mechanical properties at the Apollo 17 landing site were approximately the same as those at the Apollo 11 landing site.

### **7.7.1 Summary: Apollo 17 Lunar Module Landing**

Lunar dust was first observed at an altitude of 60 to 70 feet during final descent, with no report of degradation in landing visibility.

Apollo 17 Lunar Module touchdown dynamics were benign. The touchdown velocities were low, with a sink speed of 3.0 feet per second, and the translational velocities were negligible. The landing velocities were well within the design envelope. The effective landing lunar surface slope was computed from the on-board guidance computer data to be 5.9 degrees, which accounts for the fact that the  $-Z$  footpad was at the bottom of a lunar crater that measured approximately 10 inches in depth. The local lunar slope was computed to be about 3 degrees—within the design envelope of the 12-degree slope. The rotational rates at touchdown were well within the design envelope.

The photographs indicate that footpad penetration was less than 3 inches and skid distances of the landing gear footpads were nil.

The landing gear energy absorption and landing stability performance were well within the design envelope.

The lunar surface mechanical properties at the Apollo 17 landing site were approximately the same as those at the Apollo 11 landing site.

## **8.0 Author's Annotation — Apollo 16 and 17 Landings**

The author, who worked in the Structures and Mechanics Division of the Engineering Directorate at Johnson Space Center, was responsible for all post-flight digital simulations of the Apollo Lunar Module touchdown dynamics. However, Apollo landings 16 and 17 touchdown dynamics analyses were restricted to evaluating the touchdown conditions such as velocity, lunar surface landing slope, and post-landing photographs of the landing gear systems in determining structural landing loads, landing dynamic stability, landing gear energy absorption, and landing surface slope. The Apollo 16 and 17 landings were considered benign landings, which were very stable and well within the touchdown energy capability of the landing gear system. At the time the landing dynamics assessments were made, the time histories of the Apollo 16 and 17 Lunar Module rotational rates were not available. A minimal effort was made, on the author's part, to provide a time domain simulation of these landings.

## 9.0 Conclusions

During final descent and landing, all but one Apollo Lunar Module landing detected some level of intensity of lunar dust due to the interaction between the descent engine plume and the lunar surface. Apollo 16 did not report the present of dust during final descent. The lunar dust was most severe for the Apollo 12 landing, during which the dust masked the lunar surface in the final seconds of the landing maneuver. However, landing visibility for all other Apollo landings was acceptable.

Analysis of the Apollo 11 touchdown dynamics was the most comprehensive of all Apollo landings. These touchdown dynamics were used to develop the lunar surface soil mechanical properties. The touchdown analysis indicated that the nominal lunar surface bearing strength was 1.88 psi per inch of penetration for a normalized landing gear footpad surface of 1071 square inches.

The nominal friction coefficient between the footpads and the lunar surface was 0.33 at the Apollo 11 landing site. The lunar surface soil and footpad interaction model used in determining the soil mechanical properties were appropriate for all Apollo landing simulations except for the Apollo 14 landing.

The Apollo 14 +Y landing gear footpad had a more severe “plowing” effect than any other landing. The simplified soil model did have a plowing term in the equation, but the coefficient was calibrated using Apollo 11 touchdown data. For this reason, the simplified lunar soil model may not be appropriate for predicting the interaction forces between the +Y landing gear footpad and lunar soil during the landing dynamics maneuver.

Photographic analysis of all of the Apollo landing sites of the footpad patterns and astronaut boot print patterns in the lunar soil indicated that the other Apollo landing sites possessed similar soil mechanical properties to that of the Apollo 11 landing site.

All Apollo landings were within the design envelope for the landing gears system from the standpoint of landing stability, landing gear energy absorption, landing surface slope, and lunar surface bearing strength. The most dynamic landing was Apollo 15, with a sink speed of 6.8 feet per second and a translation speed of 1.3 feet per second flying uphill into an 11-degree sloped surface.

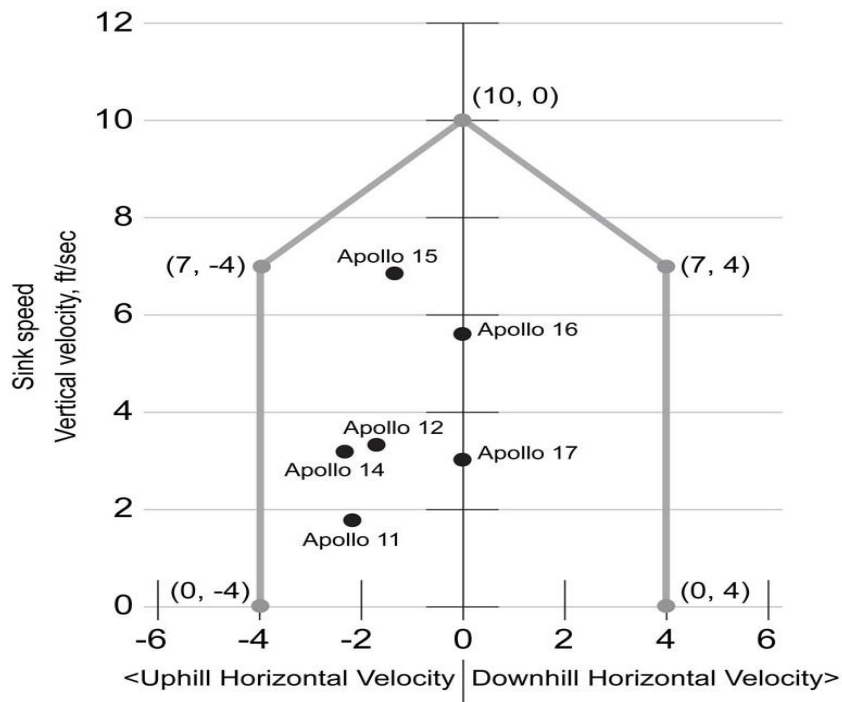
For most Apollo landings, the footpad penetration was less than 3 inches into the lunar soil. The Apollo 14 landing was the exception, with a landing gear footpad penetration of more than 6 inches. All of the landing sites had approximately the same lunar soil mechanical properties.

Table 1 provides a summary of the touchdown conditions for all Apollo Lunar Module landings.

**Table 1. Summary of Apollo Lunar Module Landing Conditions**

Apollo Mission	Date of Landing	Sink Speed (ft/sec)	Translational Velocity (ft/sec)	Local Landing Surface Slope (degrees) and Comment
11	July 20, 1969	1.8	2.2	4.5 – landing translating from right to left across the slope; visibility was <b>not</b> degraded by lunar dust.
12	Nov. 19, 1969	3.3	1.7	4.8 – landing translating uphill; visibility was degraded by lunar dust.
13	Launched April 11, 1970	Mission aborted	N/A	N/A
14	Feb. 5, 1971	3.1	2.4	7.1 – landing translating uphill; visibility <b>not</b> degraded by lunar dust.
15*	July 30, 1971	6.8	1.3	11.0 – landing translating uphill; visibility was <b>not</b> degraded by lunar dust; added 10 inches to the descent engine nozzle skirt
16	April 21, 1972	5.6	Negligible	2.5 – vertical landing; visibility <b>not</b> degraded by lunar dust; added 10 inches to the descent engine nozzle skirt
17	Dec. 11, 1972	3.0	Negligible	2.5 – vertical landing; visibility <b>not</b> degraded by lunar dust; added 10 inches to the descent engine nozzle skirt

\* Apollo 15 was, by far, the most dynamic of all Apollo Lunar Module landings. The Apollo 15 Lunar Module landed with the highest kinetic energy and on the steepest lunar slope of all the Apollo Lunar Module landings.



**Figure 55. Apollo Lunar Module landing velocities with respect to the touchdown velocity envelope (or Doghouse).**

## 10.0 References

- <sup>1</sup> Mantus, M, Lerner E, and Elkins W. Landing Dynamics of the Lunar Excursion Module (Method of Analysis). Rept. LED-520-6, Grumman Aircraft Engineering Corp., March 6, 1964.
- <sup>2</sup> Doiron, HH. Lunar Landing Dynamics Studies. Paper presented at Eleventh Manned Spacecraft Center Technical Symposium, Houston, Texas, Jan. 25, 1965, pp. 1-19.
- <sup>3</sup> Walton, WC, Jr., Herr, RW, and Leonard, HW. Studies of Touchdown Stability for Lunar Landing Vehicles. J. Spacecraft Rockets, vol. 1, no. 5, Sept. Oct. 1964, pp. 552-556.
- <sup>4</sup> Walton, WC, Jr.; and Durling, BJ. A Procedure for Computing the Motion of a Lunar-Landing Vehicle During the Landing Impact. NASA TN D-4216, Oct. 1967.
- <sup>5</sup> Herr, RW, and Leonard, HW. Dynamic Model Investigation of Touchdown Stability of Lunar-Landing Vehicles. NASA TN D-4215, Oct. 1967.
- <sup>6</sup> Anon. Lunar Module (LM) Soil Mechanics Study. Final Report. Rept. AM-68-1, Energy Controls Division, Bendix Corporation, May 1, 1968.
- <sup>7</sup> Blanchard, UJ. Full-scale Dynamic Landing-Impact Investigation of a Prototype Lunar Module Landing Gear. NASA TN **D-5029**, Mar. 1969.
- <sup>8</sup> Zupp, GA, Doiron H H. A Mathematical Procedure for Predicting the Touchdown Dynamics of a Soft Landing Vehicle. NASA TN D-7045 February 1971.
- <sup>9</sup> Zupp, GA, Hewlett, M. Lunar Module 1/6 Scale Model Correlation Study, MSC-IN-67-1, Manned Spacecraft Center, Houston, Texas, November 15, 1966.
- <sup>10</sup> Rogers, WF. Apollo Experience Report – Lunar Module Landing Gear Subsystem, NASA TN D-6850 June 1972.
- <sup>11</sup> Terzaghi, K. Theoretical Soil Mechanics. John Wiley and Sons, Inc., 1943.
- <sup>12</sup> Nelson, JD, and Vey, E. Bearing Capacity of Lunar Soil. Paper presented at the American Society of Mechanical Engineers Winter Annual Meeting, New York, New York, Nov. 29-Dec. 4, 1964, Paper no. 64-WA/AV/13.
- <sup>13</sup> MSC-00171 Apollo 11 Mission Report, December 1971, Mission Evaluation Team, Houston, TX.
- <sup>14</sup> MSC-01855 Apollo 12 Mission Report, March 1970, Mission Evaluation Team, Houston, TX.
- <sup>15</sup> MSC-04112 Apollo 14 Mission Report, May 1971, Mission Evaluation Team, Houston, TX.
- <sup>16</sup> MSC- 05161 Apollo 15 Mission Report, December 1971, Mission Evaluation Team, Houston, TX.
- <sup>17</sup> MSC-07230 Apollo 16 Mission Report, August 1972, Mission Evaluation Team, Houston, TX.
- <sup>18</sup> JSC-07904 Apollo 17 Mission Report, March 1972, Mission Evaluation Team, Houston, TX.
- <sup>19</sup> Jones, EM, Glover, K. “The First Lunar Landing,” *Apollo Lunar Surface Journal*, Oct. 4, 2011.

## Appendix A: Apollo 11 Lunar Module Touchdown Dynamics

Results of the Apollo 11 Lunar Module touchdown simulations are presented in this appendix. The primary objectives of the simulations were to identify the lunar surface soil mechanical properties and the local surface slope, and to evaluate landing gear performance for the Apollo 11 landing. The identification process was iterative, and started with an initial estimate of the soil parameters: surface bearing strength, surface/footpad friction coefficient, plowing coefficient, and local surface slope with respect to the horizontal velocity vector. The lunar soil/footpad interaction model is presented in Appendix B: Lunar Soil Mechanical Properties Model. Based on the initial estimate of the soil parameters and touchdown initial conditions, a time domain solution was developed and comparisons were made between the predicted and measured body rotational rates and the landing gear strut strokes. Based on the “goodness” of the comparison, the lunar soil parameters were updated and the simulation was repeated. This process was repeated until “convergence” (in the judgment of the author) was obtained.

The mass properties used in the Apollo 11 touchdown simulation are defined in Appendix C: Apollo 11 Lunar Module Mass Properties at Touchdown. The landing gear energy absorption properties are presented in Appendix D: The Apollo 11 Landing Gear Load Stroke Characteristics. The descent engine thrust tail-off characteristics are presented in Appendix E: The Apollo 11 Lunar Module descent Engine Thrust Tail-off Characteristics. The theoretical analysis used in the Apollo 11 landing dynamic simulation is documented in Reference 8.

The touchdown conditions—such as velocity vector, angular orientation, and associated body rotational rates as defined by the on-board computer—were fixed parameters in the iteration process.

In the touchdown simulation, the pitch (a rotation about the body Y axis), roll (rotation about the body Z axis), and yaw (rotation about the body X axis) angles were assumed to be equivalent to the Euler angles with the associated rotation sequence of pitch, roll, and yaw, respectively. At the time of touchdown, the body coordinate system was approximately aligned with the inertial coordinate system.

The Apollo 11 Lunar Module state vectors, at the time of footpad contact, were derived from the on-board guidance computer and are shown in Tables, 1A, 2A, and 3A.

**Table 1A. Lunar Module Landing Orientation, Pitch, Roll, and Yaw**

Orientation with Respect to the Body Coordinate System	Initially at Touchdown Time = 102:45:39.8	Final Orientation Time = 102:48:44
Pitch ( $\theta_Y$ ) (degrees)	0.8240	4.3726
Roll ( $\theta_Z$ ) (degrees)	2.6038	0.3296
Yaw ( $\theta_X$ ) (degrees)	15.3259	12.9858

**Table 2A. Lunar Module Touchdown Rotational Rates**

Rotational kinetic energy at touchdown was 6.5 foot-pounds.

Pitch rate (rad/sec)	0.0100	0.0000
Roll rate (rad/sec)	-0.0280	0.0000
Yaw rate (rad/sec)	-0.0108	0.0000

**Table 3A. Apollo 11 Lunar Module Touchdown Velocities Expressed in the Inertial Coordinate System**

Translational kinetic energy at touchdown was 1957.8 foot-pounds.

$V_x$ (ft/sec)	-1.80	0.0000
$V_y$ (ft/sec)	-2.20	0.0000
$V_z$ (ft/sec)	-0.10	0.0000

The data in Table 1A, 2A, and 3A indicate that the Lunar Module was primarily translating along the inertial -Y axis or to the pilot's left at about a right angle to the local surface slope. The sink speed at the time of footpad contact with the lunar surface was 1.8 feet per second, with an associated horizontal velocity of 2.2 feet per second. The touchdown velocities were well within the touchdown design velocity envelope, and the body rotational rates were less than the design allowable of 0.035 rad/sec at the time of touchdown.

Again, in the evaluation of the lunar surface parameters and landing gear strut strokes, the criteria for convergence in the iteration process was the measure of "goodness" in the correlation between the measured and predicted pitch, roll, and yaw rates, and measured and predicted maximum landing gear strut strokes.

A comparison between the measured and predicted Apollo 11 Lunar Module pitch, roll, and yaw rate time histories, respectively, with time equal zero at the initial footpad contact, are presented in Figures 1A, 2A, and 3A. A comparison between the predicted and measured pitch rate during the touchdown landing maneuver is shown in Figure 1A.

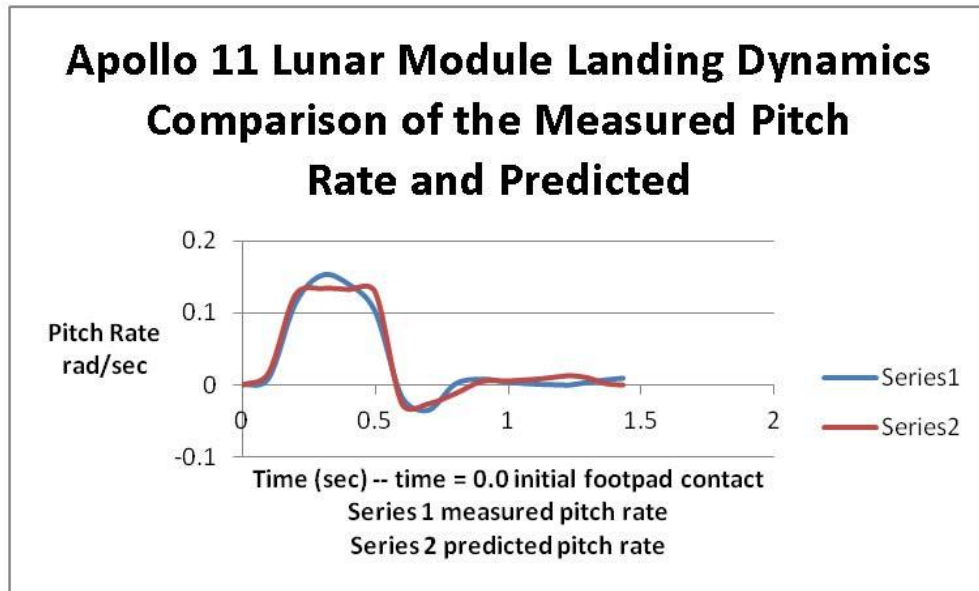


Figure 1A. Comparison between the measured and predicted pitch rate during Apollo 11 Lunar Module touchdown maneuver.

The pitch rate, both measured and predicted, indicated that the significant pitch motion started approximately 0.1 seconds after initial footpad contact. The pitch rate peaked out at about 0.15 rad/sec and started to decay around 0.5 seconds, and going negative at around 0.65 second with a maximum negative rate of 0.05 rad/sec. The pitch rate correlation was judged excellent.

Figure 2A shows a comparison between the predicted and measured roll rate during the touchdown landing maneuver.

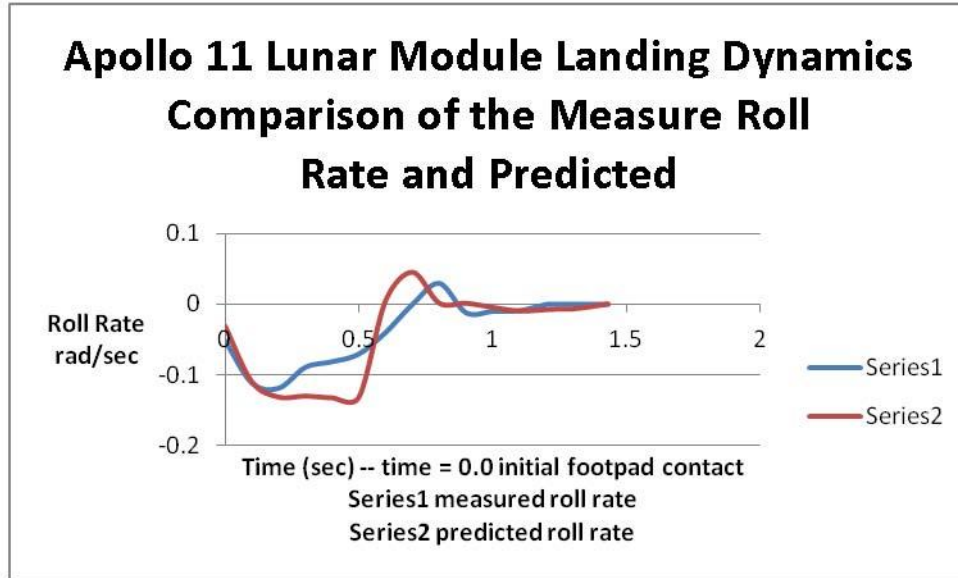


Figure 2A. Comparison between the measured and predicted roll rate during Apollo 11 Lunar Module touchdown maneuver.

The roll rate history is also indicative that the +Y footpad was the first to make contact with the lunar surface. The measured peak roll rate was -0.11 rad/sec and the peak predicted roll rate was approximately the same. These peaks occurred approximately 0.1 seconds after initial footpad contact. The measured roll rate started to decay after peaking. The predicted roll rate was approximately constant up until 0.5 seconds into the landing whereas the measured roll rate started to decay just after peaking. The areas under the roll rate curves were nearly the same. The correlation between the predicted and measured roll rates were judged to be good.

Figure 3A shows a comparison between the predicted and measured yaw rate during the touchdown landing maneuver.

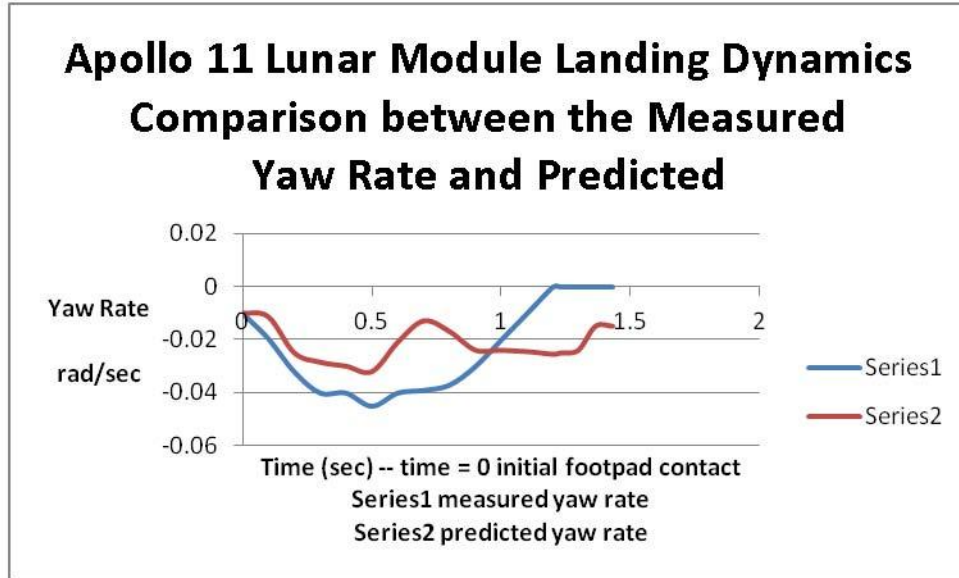


Figure 3A. Comparison between the measured and predicted yaw rate during Apollo 11 Lunar Module touchdown maneuver.

The yaw rate was small in comparison to the pitch and roll rate; however, the measured yaw did not indicate that the Lunar Module had come to rest until about 1.2 seconds after the initial footpad contact with the lunar surface. The maximum measured yaw rate was -0.041 rad/sec occurring at 0.5 seconds into the landing. The maximum predicted yaw rate was -0.032 rad/sec occurring at about 0.5 seconds into the landing. The comparison between the measured and predicted yaw rates was judged to be fair.

Based on this simulation, the initial contact with the lunar surface was the +Y footpad followed by the +Z footpad about 0.1 seconds later. The measured pitch rate peaked at about 0.3 seconds into the landing, with an associated pitch rate of slightly less than 0.15 rad/sec. The maximum predicted pitch rate was 0.14 rad/sec. The pitch rate also indicated a slight negative rate that peaked about 0.6 seconds into the landing. This negative pitch rate indicated that the -Z footpad was in contact with the lunar surface, and that the subsequent rebound was due to the elasticity of the landing gear structure. After the initial landing gear footpad contact, the resulting dynamics motion was arrested in less than 1.5 seconds. Overall, the comparison between the measured and predicted pitch rate history was judged to be very good, matching both pitch rate magnitude and shape.

Table 4A shows a comparison between measured and predicted landing gear strut strokes. The measured strut strokes were derived from various photographs, taken at different angles, of the Lunar Module resting on the lunar surface. The measurement strut stroke tolerance was about 1 inch.

**Table 4A. Comparison Between the Measured and Predicted Maximum Lunar Module Landing Gear Strut Strokes for Apollo 11 Landing.** Total energy absorbed by the landing gears was 537.5 foot-pounds measured and 366.7 foot-pounds predicted. Notes: a) all strut strokes are in inches; b) the measured strut strokes are derived from photographs taken at the Apollo 11 landing site post touchdown; c) N/D stands for “No Data.”

<b>Landing Gear Strut Strokes (strut strokes are in inches)</b>	<b>+Y</b>	<b>+Z</b>	<b>-Y</b>	<b>-Z</b>
Primary Strut Stroke – Measured	0.0	0.0	0.0	0.0
Predicted	0.0	0.0	0.0	0.0
Right Secondary Strut Stroke Compression – Measured	0.0	N/D	0.0	0.0
Predicted	0.0	0.0	0.0	0.0
Right Secondary. Strut Stroke Tension – Measured	2.7	N/D	3.2	2.5
Predicted	1.8	0.0	1.0	1.5
Left Secondary Strut Stroke Compression – Measured	0.0	0.0	0.0	0.0
Predicted	0.0	0.0	0.0	0.0
Left Secondary. Strut Stroke Tension – Measured	0.5	4.0	0.0	N/D
Predicted	0.7	1.8	1.2	0.0

The landing gear data presented on Table 4A are indicative that all of the landing gear strut stroking was in the secondary struts and was restricted to tension stroking only. This would indicate that the landing was on a “low” friction surface with all footpads translating “outward” from the static Lunar Module configuration. The primary struts stroking was essentially elastic, with the magnitude of primary strut stroking being negligible. The measured strut strokes were derived from photographic analysis and tended to indicate more secondary tension stroking than the predicted values. It should be noted that the landing gear strut stroke analysis using the post-landing configuration photographs would not reflect any secondary strut compression stroking. The landing dynamic digital simulation did not indicate any secondary strut compression stroking. In this case, the overall correlation between the predicted and measured strut strokes was considered good.

The Apollo 11 landing was well within the energy absorption capability of the landing gear system and well within the design envelope for the touchdown velocity and surface slope. The touchdown kinetic energy was about 1960 foot-pounds and the predicted energy absorption by the landing gear system was about 370 foot-pounds. This implies that about 80 percent of the landing kinetic and potential energies were absorbed by the interaction between the footpads and the lunar surface soil.

The converged lunar soil mechanical properties that produced the final correlations are presented in Table 5A, along with an estimate of the maximum parameter dispersion.

**Table 5A. Lunar Soil Mechanical Properties and Dispersions at Apollo 11 Lunar Module Landing Site as Determined by the Iterative Process from the Lunar Module Landing Simulations.** The normalized area (1071 in<sup>2</sup>) of the Lunar Module footpad was based on 80 percent of the footpad diameter in contact with the lunar surface. The diameter of a Lunar Module footpad is approximately 36 inches. The footpad depth is approximately 6 inches.

Mechanical Property	Best Estimate	Dispersions
Friction coefficient between the lunar surface and the LM footpad, $\mu$	0.33	0.25 to 0.40
Bearing strength, $K_v$ (lb/in)	2000 lb/inch	1750 lb/inch to 2250 lb/inch
Bearing Strength normalized to 1071 in <sup>2</sup> footpad area, (lb/in <sup>3</sup> )	1.88 psi/inch	1.6 psi/inch to 2.1 psi/inch
Plowing coefficient, $K_p$ (lb/in)	8.3 lb/inch	6.2 lb/inch to 10.5 lb/inch
Landing surface slope (degrees)	4.5 <sup>0</sup>	4.2 <sup>0</sup> to 4.8 <sup>0</sup>

The lunar surface mechanical properties were well within the assumed design values. The design condition for the landing site was an equivalent surface slope of 12 degrees. The Apollo 11 landing site slope was a maximum of 4.8 degrees, with the best estimate being 4.5 degrees. The lunar surface bearing strength was well within the design value. The design specification for the landing gear footpad assumed a lunar surface bearing strength of 1.0 psi at a penetration depth of 4 inches. Assuming a linear model, the design bearing strength coefficient,  $K_v$ , would be 0.25 psi/inch, which is well within the nominal measured value of 1.88 psi/inch predicted at the landing site.

The design specification of friction coefficient between the lunar surface and the Lunar Module footpad was assumed to be 0.40 or greater. The measured nominal friction coefficient was 0.33 or slightly less than the design specification value. However, accounting for the effects of footpad plowing would lead to an effective friction coefficient of about 0.36, which, for all practical purposes, was within the range of the design specification value. Landing dynamic simulations indicated that the landing gear system had an adequate energy absorption margin and landing stability margins when the coefficient of friction between the landing gear footpad and the surface was less than 0.40.

The touchdown dynamic simulation indicated that the landing gear footpad penetration of the lunar soil ranged from 2.0 to 3.5 inches. The simulation indicated that the slide-out distance for the footpad range from 1.0 to 3.5 inches from the initial point of lunar surface contact. The simulation also indicated that during the touchdown maneuver, the “rock-up” angle was about 2 degrees. The crew reported no sensation of rock-up during the touchdown phase.

Overall, the correlation between the analytically predicted and measured pitch, roll, and yaw rates and the landing gear strut strokes for the Apollo 11 landing indicated that the simplified footpad/soil interaction model was more than adequate to accurately determine the mechanical properties of the lunar surface and the landing gear performance. The lunar surface bearing strength was well above the footpad design value of 0.25 psi/inch. The surface-to-footpad friction coefficient was slightly less than the design value of 0.4; however, this did not present a threat to the safety of the landing.

The landing gear energy absorption and landing stability was well within the design values. The total energy absorption capability of all four landing gear systems was about 162,000 foot-pounds. The landing gear secondary strut energy absorption capability in tension stroking is 5167 foot-pounds per strut. The Apollo 11 touchdown kinetic energy was about 1960 foot-pounds, based on touchdown mass of 484 slugs. For the Apollo 11 landing, the energy absorption capability of the landing system was orders of magnitude greater than the touchdown kinetic energies of the Apollo 11 Lunar Module.

## Appendix B: Lunar Soil Mechanical Properties Model

Prior to the Apollo 11 landing, several lunar soil model studies were conducted with the primary objective of developing Lunar Module footpad/soil interaction models.<sup>6</sup> The deviation of these footpad/soil interaction models relied heavily on experimental data and was very comprehensive and complex. The Bendix model was incorporated into the Manned Spacecraft Center landing dynamics code, and was subsequently used in predicting the Lunar Module model touchdown dynamics on simulated lunar soils.

A review of the Apollo 11 photographic coverage of the footpads indicated that the translational motion of the footpads was less than a quarter of the footpad diameter, and the footpad penetrations into the lunar surface was on the order of inches. The Apollo 11 landing gear footpad photographs suggest that a simplified soil/footpad model might be appropriate. The simplified soil/footpad model would account for first-order effects of the soil forces acting on the footpads.

The on-board computer indicated that, at the time of footpad contact, the Lunar Module was translating primarily in the  $-Y$  direction at about 2.2 feet per second. Figures 1B, 2B, 3B, and 4B provide views of the landing gear  $+Y$  and  $-Z$  footpads.

Figure 1B is a view of the Lunar Module  $+Y$  landing gear and footpad.

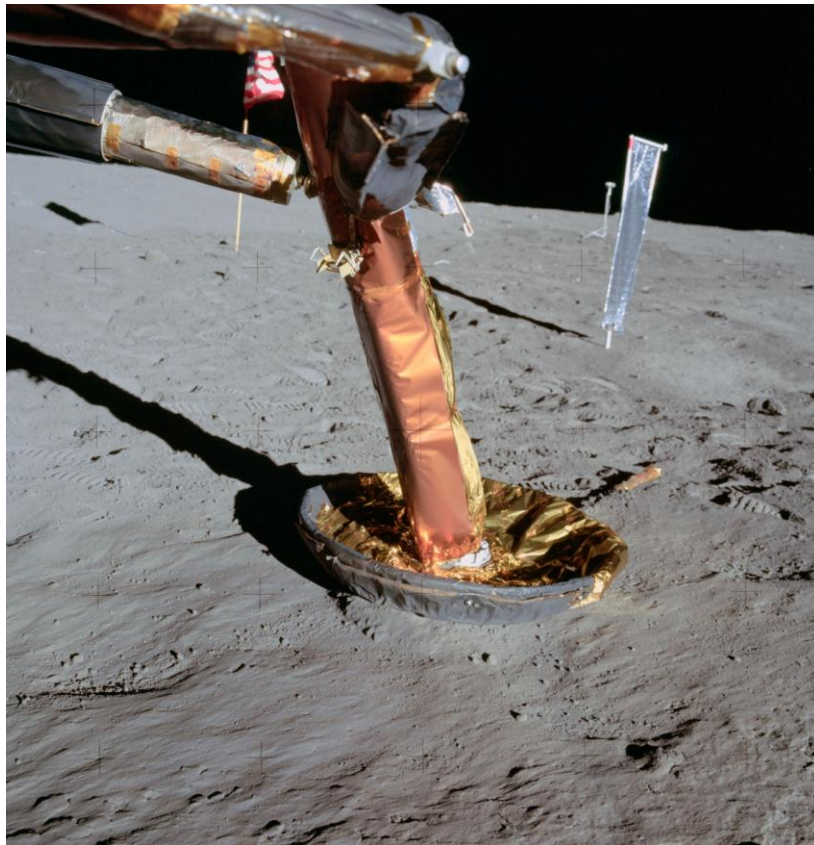


**Figure 1B. (NASA Photograph AS11-40-5920)** The  $+Y$  footpad looking down the  $+Y$  Lunar Module body axis. The  $+Y$  axis is approximately parallel to the contact probe, which is embedded into the lunar soil.

The +Y footpad shows some lunar soil buildup in the direction of motion, and would have some contribution to the horizontal force between the footpad and landing surface.

Figure 2B shows a closeup view of the +Y footpad and contact probe.



**Figure 2B. (NASA Photograph AS11-40-5917) The +Y footpad showing approximately 2/3 of the contact probe embedded into the lunar soil and situated about parallel to the surface. Evidence of +Y footpad skidding is also revealed.**

Figure 3B shows a view of the -Z footpad and the shadow of the contact probe.



**Figure 3B. (NASA Photograph AS11-40-5926) The -Z landing gear footpad.**  
The +Y footpad is located in the top portion of the photograph.

This photograph shows a buildup of lunar soil to the left of the -Z footpad. The -Z footpad penetration into the lunar surface was shallow. Based on this photograph, the penetration is estimated to be less than 3 inches. This photograph and the photograph in Figure 1B indicate that the +Y footpad has lunar soil buildup similar to the -Z footpad. The contact probe on the -Z footpad is bent upward at an estimated angle of about 20 degrees. The translation after -Z footpad contact is estimated to be in the range of 3 to 5 inches.

Figure 4B is a view of the astronaut's boot print.



**Figure 4B. (NASA Photograph AS11-40-5878) Astronaut's boot print, indicating sufficient bearing strength to support human mobility on lunar surface.**

This photograph indicates that the lunar soil is more than sufficient to support astronaut activities on the lunar surface. Also in evidence is the “high” lunar soil shear stress friction angle or angle of internal friction and soil cohesion factor.

Based on these data, a simplified version of the Bendix footpad/soil interaction model was used in the Apollo 11 landing dynamic simulations. The simplified model incorporated the first-order effect of the footpad/soil forces. These simplifications assumed that the footpad was rigidly attached to the ball joint of the landing gear primary strut. This assumption allowed the footpad to have three translational degrees of freedom, and eliminated the rotational degrees of freedom of the footpad. The primary forces acting on the footpad would then be a vertical force that was a function of the vertical penetration of the footpad into the lunar surface, and a horizontal force governed by the surface/footpad friction plus a horizontal resistance force as a function of the translational distance of the footpad.

In summary, the photographs of the Apollo 11 Lunar Module indicate that the penetration of the footpads into the lunar surface were shallow, estimated to be less than 3.5 inches, which is indicative of a “high” bearing strength of the lunar surface. The footpad sliding distance after initial footpad contact was somewhat less than a foot, with a “small” buildup of lunar soil on the footpad in the direction of lateral motion or the footpad leading edge.

Based on the photographic analysis of the landing gear footpads, the lunar surface/footpad force interaction model was idealized to have a vertical force component that was a linear function of the footpad vertical penetration (bearing strength parameter). The horizontal lunar surface force component was a function of the vertical force (sliding friction parameter) and the horizontal sliding distance (plowing parameter).

The vertical lunar soil force,  $F_V$ , acting on the footpad is give by Equation 1B or

$$F_V = K_V * A * Z_P \tag{1B}$$

where  $K_V$  -- bearing strength coefficient (psi/inch)

$A$  -- Footpad reference area was 1071 in<sup>2</sup>, which was based on an effective diameter of about 29 inches.

$Z_P$  -- Footpad vertical penetration (inch)

It is noted that, in this analysis, the footpad bearing area is constant with soil penetration. In reality, the footpad does not have a flat contact area, but it does have some curvature. For “shallow” footpad penetrations, the flat contact area assumption was considered acceptable.

The horizontal lunar soil force,  $F_H$ , is given by Equation 2B or

$$F_H = \mu F_V + K_P S_D \tag{2B}$$

where  $\mu$  -- coefficient of friction between the lunar surface and footpad

$F_V$  -- vertical lunar force acting on the footpad (pounds)

$K_P$  --- plowing force coefficient ( $\frac{\text{pounds}}{\text{in}}$ )

$S_D$  --- skid distance (in)

It is estimated from the photographic data that the frontal area of the footpad in contact with the lunar surface was approximately 30 in<sup>2</sup>.

Equations 1B and 2B represent the simplified Bendix footpad/soil interaction model that was used in the iterative process to identify the lunar soil mechanical properties for the Apollo landing site. The parameters,  $K_v$ , the lunar surface bearing strength coefficient,  $\mu$  the friction coefficient between the footpad and the lunar surface and,  $K_p$ , the plowing or skid force coefficient were the variables in the iteration process, along with surface slope.

Equations 1B and 2B represent the characterization of the simplified model of the lunar soil/footpad interaction. The parameters,  $K_v$ , bearing strength coefficient,  $\mu$ , sliding friction coefficient, and,  $K_p$ , the plowing coefficient represent the lunar surface mechanical properties.

**NOTE: It is important to emphasize that the simplified lunar soil model is very restrictive to the bounds of the motion and displacements of the footpads observed in the Apollo 11 landing. Applications of this lunar soil/Lunar Module model outside of these bounds should be used with caution. The Bendix model, as reported in Reference 6, should be considered in cases that were outside the boundary of motion that the footpads experienced on the Apollo 11 landing.**

## Appendix C: Apollo 11 Lunar Module Mass Properties at Touchdown

The Apollo 11 Lunar Module mass properties used in the touchdown simulation are given in Table 1C. The mass properties were derived from the descent trajectory data and may not be the exact Lunar Module mass properties at the time of footpad contact; however, these data were judged to be adequate in accurately predicting the Apollo 11 touchdown dynamics.

**Table 1C. Lunar Module Mass Properties at the Time of Footpad Contact with Lunar Surface.**

Note: all units are in pound-feet-seconds. The cross-products in the inertia matrix were assumed negligible.

Mass (slugs)	484
$I_{XX}$ (slug-ft <sup>2</sup> )	12,164
$I_{YY}$ (slug-ft <sup>2</sup> )	12,840
$I_{ZZ}$ (slug-ft <sup>2</sup> )	15,347
Primary Strut Bearing Friction Coefficient	0.23
Center of Mass Height Above Landing Gear Footpad, $h_{cg}$ (ft)	11.868

These Lunar Module mass properties are probably on the high side, due to the fact that there were less than 20 seconds of propellant left in the descent stage tanks at the time of footpad contact. This lighter condition would have resulted in a slightly higher center of mass,  $h_{cg}$ , but due to the soft landing conditions, the “rock-up” after touchdown was nil or less than 2 degrees. Therefore, the difference in center of mass location in the touchdown analysis correlation was of a higher order effect or negligible.

## Appendix D: Apollo 11 Lunar Module Landing Gear Load Stroke Characteristics

The Lunar Module landing gear system had one primary strut and two secondary struts in the Cantilever design. The primary strut had a total stroke capability of 32 inches in compression only. The primary struts had two levels of honeycomb energy absorption load. Secondary struts could absorb landing energies in both compression and tension stroking. The secondary strut compression side was of one level only, whereas the tension side had two stages of honeycomb energy absorption loads. Specific energy absorption characteristics of the Apollo 11 landing gear system are shown in Figure 1D.

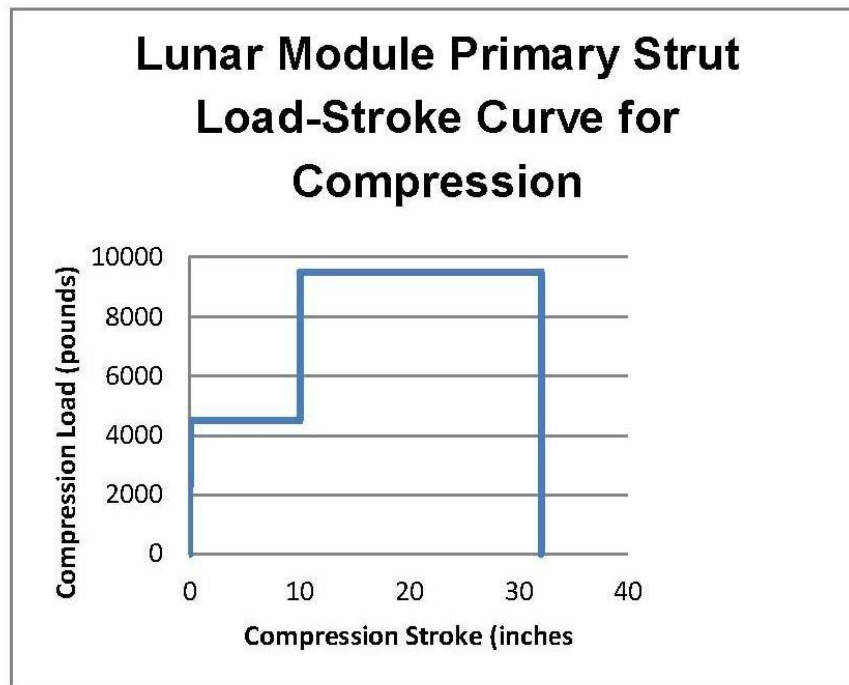


**Figure 1D. Primary strut load-stroke curve.** The primary strut had two stages of honeycomb crush levels—the initial level load of 4500 pounds for about 10 inches of stroke, followed by a honeycomb crush level 9500 pounds for a crush distance of 22 inches. The primary struts were designed for honeycomb compression energy absorption only. Total energy absorption capability was 21,167 foot-pounds per primary strut in compression stroking. This did not include the energy absorbed by the primary strut bearing friction.

The Cantilever design of the primary struts of the landing gear system had two primary components: a stroking-type “ram” or piston, and the fixed cylinder that housed the honeycomb cartridge. These two components were supported by two bearings. When the secondary strut was loaded and the primary strut underwent compression stroking, the bearing loads produced additional compression loading in the primary strut and, as such, provided additional energy absorption capability. The magnitude of the additional compression loading was governed by the bearing friction coefficient, which was nominally 0.23 (see Appendix C), as measured from ground testing.<sup>8,10</sup>

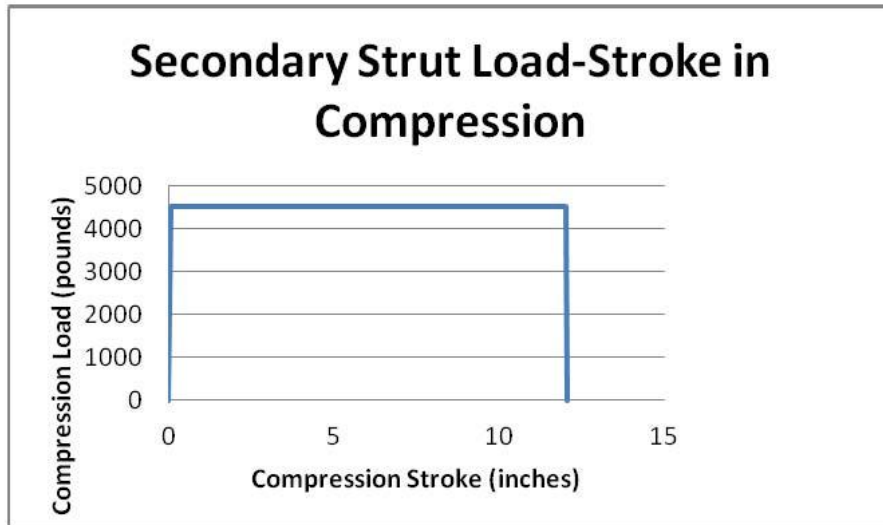


**Figure 2D. Secondary strut load-stroke in compression.** Secondary strut had the capability of absorbing touchdown energies in both tension and compression stroking. The above load-stroke curve is for compression energy absorption in the secondary strut. The initial level of the honeycomb energy absorption load was 4500 pounds for about 12 inches of stroke. Total energy absorption capability was 4500 foot-pounds in compression stroking per strut.

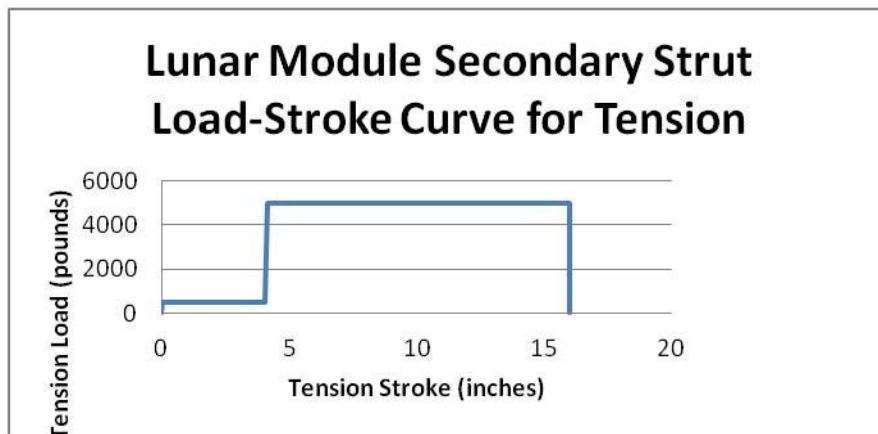


**Figure 3D. Secondary strut tension load-stroke curve.** The load-stroke curve for tension energy absorption for the secondary strut was in two stages. The initial level of the honeycomb energy absorption load was 500 pounds for about 4 inches of stroke, followed by honeycomb energy absorption load of 5000 pounds for 12 inches of stroke. Total energy absorption capability was 5167 foot-pounds per strut in tension stroking.

The total energy absorption capability for each landing gear system was 40,500 foot-pounds, giving the landing gear system a total of 162,000 foot-pounds of energy absorption capability.

## Appendix E: Apollo 11 Lunar Module Descent Engine Thrust Tail-off Characteristics

The descent engine thrust tail-off time history was constructed from Apollo 11 flight data and ground test data. The reconstructed descent engine thrust time history, starting at initial footpad contact, is shown in Figure 1E. Although the thrust time history is reconstructed, it was judged adequate for predicting the Apollo 11 touchdown dynamics.

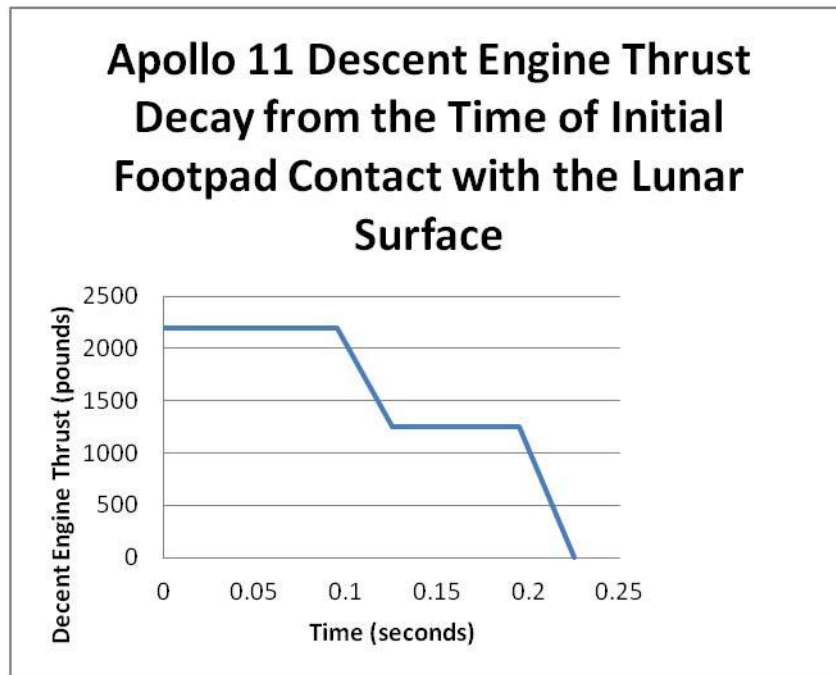


**Figure 1E. Descent engine thrust time history starting with initial Lunar Module landing gear footpad contact and terminating 0.225 seconds later.**

At the time of initial footpad contact, the engine thrust was approximately 2200 pounds. Note that the engine thrust may have been amplified due to the descent engine thrusting in close proximity of the lunar surface. The final clearance between the descent engine nozzle and the lunar surface was determined to be approximately 15 inches, as derived from post-landing photographic analysis.



REPORT DOCUMENTATION PAGE			Form Approved OMB No. 0704-0188	
Public reporting burden for this collection of information is estimated to average 1 hour per response, including the time for reviewing instructions, searching existing data sources, gathering and maintaining the data needed, and completing and reviewing the collection of information. Send comments regarding this burden estimate or any other aspect of this collection of information, including suggestions for reducing this burden, to Washington Headquarters Services, Directorate for Information Operations and Reports, 1215 Jefferson Davis Highway, Suite 1204, Arlington, VA 22202-4302, and to the Office of Management and Budget, Paperwork Reduction Project (0704-0188), Washington, DC 20503.				
1. AGENCY USE ONLY (Leave Blank)	2. REPORT DATE January 2013	3. REPORT TYPE AND DATES COVERED Special Publication		
4. TITLE AND SUBTITLE An Analysis and a Historical Review of the Apollo Program Lunar Module Touchdown Dynamics			5. FUNDING NUMBERS	
6. AUTHOR(S) George A. Zupp, Engineering Directorate, Retired, Structural Engineering Division, NASA Johnson Space Center, Houston, TX 77058				
7. PERFORMING ORGANIZATION NAME(S) AND ADDRESS(ES) Lyndon B. Johnson Space Center Houston, Texas 77058			8. PERFORMING ORGANIZATION REPORT NUMBERS S-1138	
9. SPONSORING/MONITORING AGENCY NAME(S) AND ADDRESS(ES) National Aeronautics and Space Administration Washington, DC 20546-0001			10. SPONSORING/MONITORING AGENCY REPORT NUMBER SP-2013-605	
11. SUPPLEMENTARY NOTES				
12a. DISTRIBUTION/AVAILABILITY STATEMENT Unclassified/Unlimited Available from the NASA Center for AeroSpace Information (CASI) 7115 Standard Hanover, MD 21076-1320 Category: 18			12b. DISTRIBUTION CODE	
13. ABSTRACT (Maximum 200 words) The primary objective of this paper is to present an analysis and a historical review of the Apollo Lunar Module landing dynamics from the standpoint of touchdown dynamic stability, landing system energy absorption performance, and evaluation of the first-order terms of lunar soil mechanical properties at the Apollo 11 landing site. The first-order terms of lunar surface mechanical properties consisted primarily of the surface bearing strength and sliding friction coefficient. The landing dynamic sequence started at first footpad contact. The flight dynamics data used to assess the Apollo 11 landing system performance and the lunar soil mechanical properties included the body axis pitch, roll, and yaw rate time histories as measured by the on-board guidance computer during the Apollo 11 Lunar Module touchdown maneuver, and the landing gear stroke data derived from post-landing photographs. The conclusions drawn from these studies were that the landing gear system performance was more than adequate from a stability and energy absorption standpoint for all Apollo lunar landings, and the lunar soil parameters were well within the limits of the design assumptions for all Apollo landing sites.				
14. SUBJECT TERMS Apollo lunar module; lunar landing; landing gear; touchdown; lunar soil; lunar surface			15. NUMBER OF PAGES 98	16. PRICE CODE
17. SECURITY CLASSIFICATION OF REPORT Unclassified	18. SECURITY CLASSIFICATION OF THIS PAGE Unclassified	19. SECURITY CLASSIFICATION OF ABSTRACT Unclassified	20. LIMITATION OF ABSTRACT Unlimited	



---